AN EXPERIMENTAL INVESTGATION OF THE EFFECT OF REINFORCEMENT PATTERN ON THE BEHAVIOR OF A DEEP REINFORCED CONCRETE BEAM

A Thesis

Presented to

the Faculty of the Department of Civil Engineering

The University of Manitoba

In Partial Fulfillment

of the Requirements for the Degree

Master of Science in Civil Engineering

---

by

Brian Ross Wood

September 1970

ACKNOWLEDGEMENTS

The thesis presented herein was performed in the Department of Civil Engineering, at the University of Manitoba.

The author wishes to acknowledge gratefully the advice and encouragement of Dr. A.M. Lansdown, in the development of the research in this thesis.

The author also wishes to acknowledge the aid, both technical and physical, and the patience offered by the technical staff of the Civil Engineering lab.

SYNOPSIS

Simply supported deep reinforced concrete beams, span to depth of approximately 2, were investigated. The aim was to study behavior and strain distribution and suggest patterns of reinforcement to provide ductility.

Three patterns of reinforcement were studied in two test series. The first series of tests were used to study load deflection characteristics and cracking patterns. The behavior of the first tests was then used to establish the criteria for the procedure of the second test series.

The second test series involved strain readings on the face of the concrete. These readings were taken using Demec gauges. The final two beams of this series were instrumented also with rosettes of Demec gauges and the web reinforcement was instrumented with electric resistance strain gauges.

Test results are presented, the tied-arch analogy discussed and a pattern of reinforcement is suggested.

TABLE OF CONTENTS

LIST OF FIGURES

LIST OF TABLES.

1. INTRODUCTION

1.1 THE DEEP BEAM PROBLEM

Throughout the history of modern design and analysis of reinforced concrete members in bending one of the basic assumptions has been a linear distribution of strain throughout the depth of the member. Analytical methods based on this assumption such as the "Working Stress Method" or more recently the "Ultimate Strength Method" have proved to be satisfactory as long as the depth of the beam has been small in relation to the span. As the span to depth ratio decreases however the strain distribution does not remain linear with depth. This change from almost linear to a noticeably non-linear strain distribution takes place between span to depth ratios of 6 to 2.

This non-linearity of strain complicates an elastic analysis of a homogeneous isotropic beam. Thus the analysis of a non-homogeneous, non-isotropic material such as concrete, which also has a non-linear stress-strain relationship, becomes more complex.

The deep beam, however, has been used more often recently as shear walls in wind, earthquake and blast resistant buildings. Foundation and bearing walls in buildings, short span beams in grillages, bins and hoppers also behave as deep beams. Thus there is a practical need for an understanding of the behavior of deep beams of reinforced concrete.

1.2 DUCTILITY AND THE DEEP BEAM

Often a structure can be subjected to a sudden overloading over a short period of time. Such an overload can be in the form of natural phenomena such as earthquakes, tornados or even hurricanes. Man-made blast loads such as nuclear bombs, dynamite blasts or natural gas explosions have the same effect. If a structure does not have the ability to absorb the large amounts

of energy associated with this type of loading, disastrous collapses can take place.

A structure that possesses the ability to deform greatly without loss of load carrying ability, that is a structure that posses ductility can absorb a great deal of energy. Recent earthquakes[1,2,3], have shown that even if members do not carry enough load to cause collapse of a structure their fracture causes falling debris that takes a large toll of lives.

Even more frightening is the prospect of the results of a small blast load such as a Rownan Point[4], where the sudden overload and brittle failure of supporting members caused loss of life and considerable damage.

With a great deal of care a reinforced concrete structure can be designed to possess enough ductility to prevent failure due to sudden overloading. Deep beams have shown a tendency to fail in shear and usually in a brittle manner when reinforced using conventional practice. A better understanding of deep beam behavior could lead to an unconventional reinforcing to force a ductile type of failure.

1.3 REVIEW OF RESEARCH ON DEEP BEAMS

A great deal of research has been carried out both analytically and experimentally on deep beams. In the current work only that research which is of direct interest to this study will be reviewed.

a) ANALYTICAL

To date most analytical studies have involved elastic studies of homogeneous deep beams. The first major analysis by Dischinger[8] of continuous deep beams showed the non linear strain distribution and led to the Portland Cement Association report on "The Design of Deep Girders"[9].

Since then the researchers have continued elastic studies to find the stress distributions of different types of loading in Deep Beam. These references are reviewed by Malus[5], Geir[6] and Austin[7]. Unfortunately the tools have not been available to shed light on the actual stress distribution in deep reinforced concrete members, particularly after cracking has taken place. With the advent of computer analysis and the finite element technique hopefully such studies will be forthcoming.

b) EXPERIMENTAL - ANALYTICAL

Some experimental studies have confirmed these analytical studies on strain distribution in deep beams. Coker and Filon used photoelastic methods to study strain in deep beams [10]. Karr used small scale aluminum and steel models instrumented with electric resistance strain gauges to study strain distribution[11]. Saad and Hendry used photoelastic methods to study strain distribution[12].

Early tests on reinforced concrete deep beams were performed by Klingroth[13] and by Nylander and Holst[14] in 1942. More insight was given in tests by Benjamin and Williams in 1959[15]. These tests involved full sized, plain and reinforced concrete shear walls subjected to shear forces applied in the plane of the wa-l. Attempts to study stra-ns in these tests were hamepred by the cracks formed in testing.

Further studies were carried out at the University Illinois by Untrauer[16], Dill[17] and de Paiva[18]. These studies along with later studies by Crist[19] and by Ramakrishnan and Ananthanarayana[20] were mainly concerned with predicting the ultimate load of deep re-

inforced concrete beams and do not study the post yielding behavior closely enough to give insight into ductile behavior.

These studies did bring forth a number of interesting points:

i. The presence of vertical reinforcing does not have a significant effect on ultimate load although the deflection is affected.

ii. The studies at Illinois point out the tied arch behavior of a deep beam after cracking. The beam appears to become an arch of concrete tied by the main reinforcing bars.*

These studies have at least in part led to an attempt to recognize more rationally deep beam behavior in the Proposed Revision in the ACI 318 - 63 Building Code[21]. These proposals mainly involve shear provisions for deep beams.

Since shear is an integral part of the problem of deep beams the series of papers by Kani shed some light on the problem. The first of the series describes in detail not only the tied arch analogy but also describes a theory of the cracking mechanisms in diagonal tension[22]. The second is an extension of ideas on shear failure[23]. The third sheds more light on the problem of beams of greater depth. Kani's findings showed considerable loss of safety factor with increase in depth[24].

1.4 APPRAISAL OF EXISTING RESEARCH

The efforts of those involved in analytical approaches have established the basic nature of the problem. These studies have established non-linear

---

* This analogy is described in more detail in section 5.1.

strain distribution as well as a shear strain that is maximum in the compressive zone and not at the neutral axis. These approaches found solutions that apply only to ideal materials and these results cannot be directly applied to concrete which is far from ideal.

Experimental research has involved mainly the study of the ultimate load carrying capacity of various deep beams. A number of methods were developed for predicting cracking loads, ultimate loads and other behavior. Very little effort has been given to the thought of trying to change the behavior or failure mode by changing the reinforcing pattern.

1.5 AIM OF THE INVESTIGATION

This study is a part of a continuing investigation carried out at the University of Manitoba. The aim of this investigation is to find out if a deep reinforced concrete beam can be forced to fail in a more ductile manner than one containing a conventional reinforcing pattern.

Two previous studies have been performed. The first, a preliminary investigation to evaluate beam size, test procedure and give some insight into the type of failure expected [25]. The object of the second investigation was to develop a reinforcing pattern that would provide a maximum range of ductile behavior[5].

The results of Malus' work[5] showed that it is possible to establish a ductile mode of failure by changing the reinforcing pattern. More information must be obtained to understand the basic behavior of deep beams and changes in behavior affected by changes in the pattern of reinforcing.

1.6 THE SCOPE OF THIS STUDY

Malus[5] found there was reason to believe a ductile mode can be established. The scope of this present study is to investigate in more

detail the most successful of Malus' reinforcing patterns and try to establish by more detailed investigation if the reinforcing pattern caused this ductile failure. Unfortunately, Malus[5] did not study more cases of standard types of reinforcing to compare to the unorthodox reinforcing he used.

This study will compare the web reinforcing patterns which produced the best results to a standard reinforced beam (vertical web reinforcing) with the same percentage of tensile reinforcing. In this series, strain measurements were taken for both concrete and reinforcing steel in an attempt to evaluate the performance of the different reinforcing patterns. At the same time the experiments will be used in an attempt to gain a greater understanding of the failure mechanisms.

2. EXPERIMENTAL DETAILS

2.1 INTRODUCTORY REMARKS

As this study is part of a continuing investigation, the size and shape of the beam, the mix proportions of concrete and the loading apparatus were kept similar to those used in previous studies [25,5]. Drawing from the experience of these studies small changes have been made to improve the performance of the testing without affecting any comparisons to the previous studies.

2.2 SELECTION OF BEAM SIZE AND FORMS

The criteria for the selection of the beam size are as follows:

1. Length of the machine bed.
2. Horizontal distance between loading screws.
3. The vertical distance between loading head and test bed taking into account supporting apparatus and deflections.
4. Capacity and stiffness of the test machine.

Based on these criteria, the final specimen had the following dimensions:

Overall length - 74 inches

depth - 22 inches

width - 4 inches

At each end and at the midpoint columns or pilasters were formed by increasing the thickness to 10 inches (See Figure 1). These pilasters were added to provide bearing for the load and reactions, and to reduce stability problems. For this test series the length of the outside of the centre pilaster was reduced to 6 inches to reduce the effect of sharp corners at the pilaster.

The size of the test beam approximates to quarter scale a one story wall panel when each 22-inch panel of the test beam is considered.

The forms used were those built by Malus[5] with a fresh ¼ inch thick masonite hardboard lining. Prior to each casting the forms were coated with shellac then lightly oiled.

2.3 REINFORCEMENT

In order to study the effects of reinforcing arrangement on the behavior of deep reinforced concrete beams in more detail, only the patterns found by Malus' study[5] were used. These patterns were compared to a beam with standard vertical web reinforcing and the same percentage of main steel.

This "standard beam" was tested in series #1 and is shown in Figure 1. The best results previously attained contained 2 #3 bars for main tensile reinforcement. This practice was followed for all the tests in this series. The web reinforcement conformed with the design requirements for minimum shear reinforcement for a standard beam in section 1703 of the 1963 ACI Code Requirements[26]. There were 2 #3 bars used for compressive reinforcing.

From the two previously mentioned studies, two reinforcing patterns with some potential have been found. The most favorable was a criss-cross web reinforcing used by Malus in Beam A3 of his test series. The #2 test series was based on this arrangement (See Figure 2). The main tensile reinforcement was 2 #3 bars. The compression zone was designed as a column. The web reinforcing was a number of 3/16 inch stirrups placed at 45°. The extent of these bars was reduced since some of the bars appeared to affect the cracking pattern adversly, if placed in the direction of the cracking. The percentage of web reinforcing was kept approximately the same. A horizontal bar near the neutral axis was left out to examine its effectiveness. The central pilaster was designed as a column to prevent it from disintegrating under high loads.

The second promising pattern of web reinforcing took the shape of

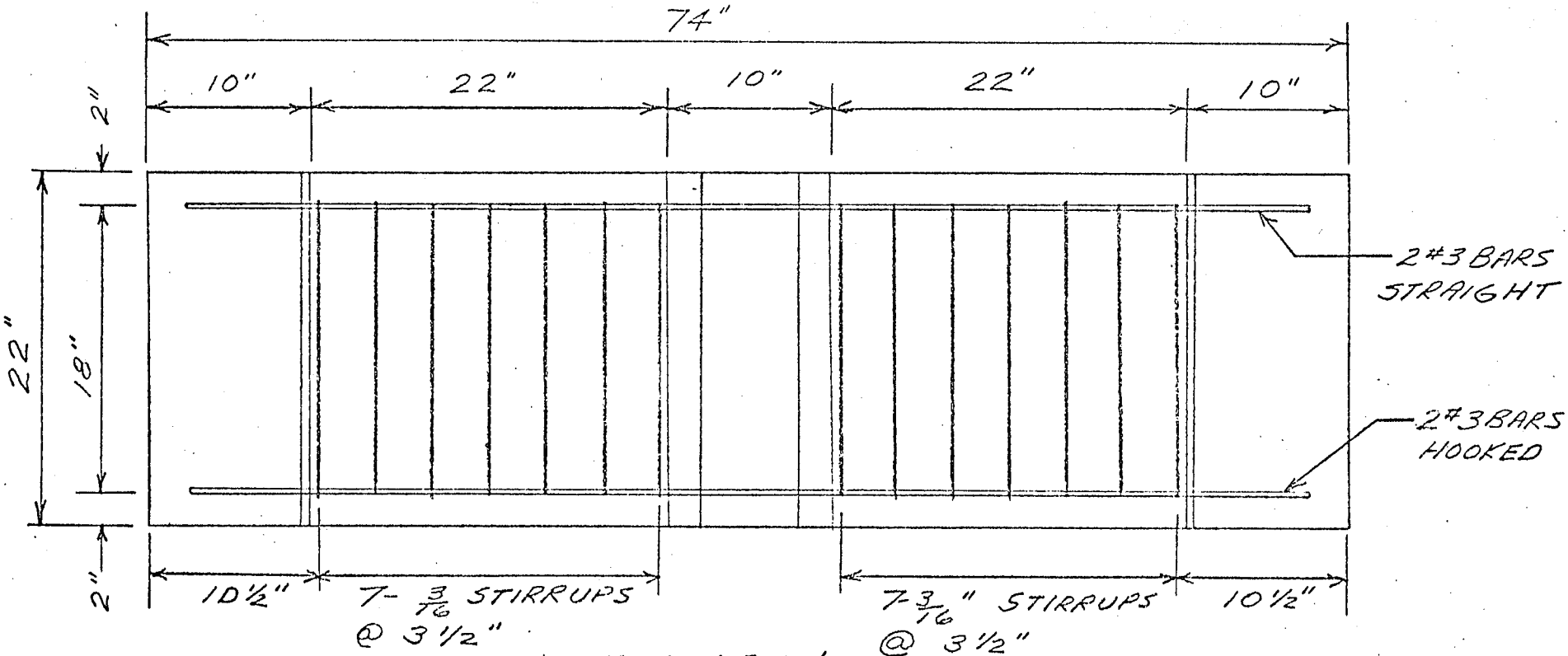

ELEVATION

REINFORCING SERIES #1

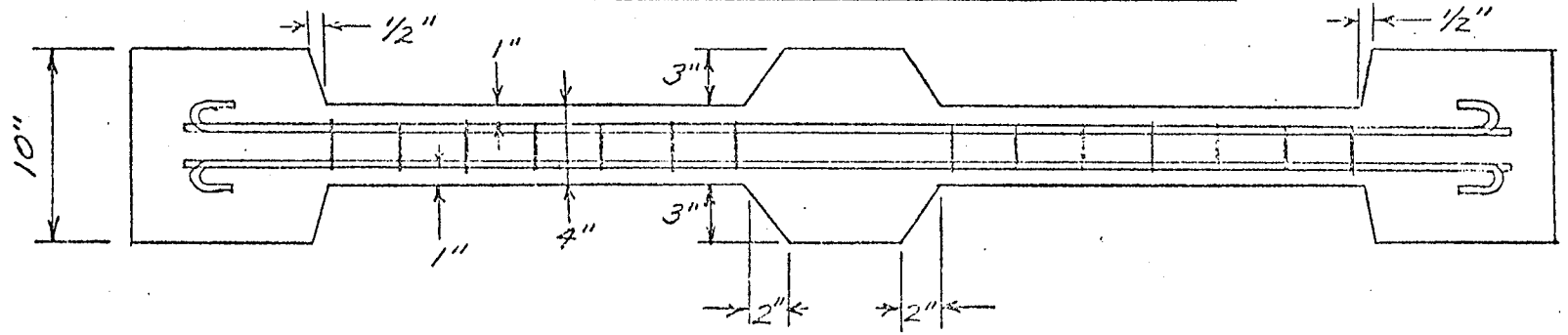

PLAN

FIGURE 1

REINFORCEMENT FOR SERIES #1

Scale:1" = 10"

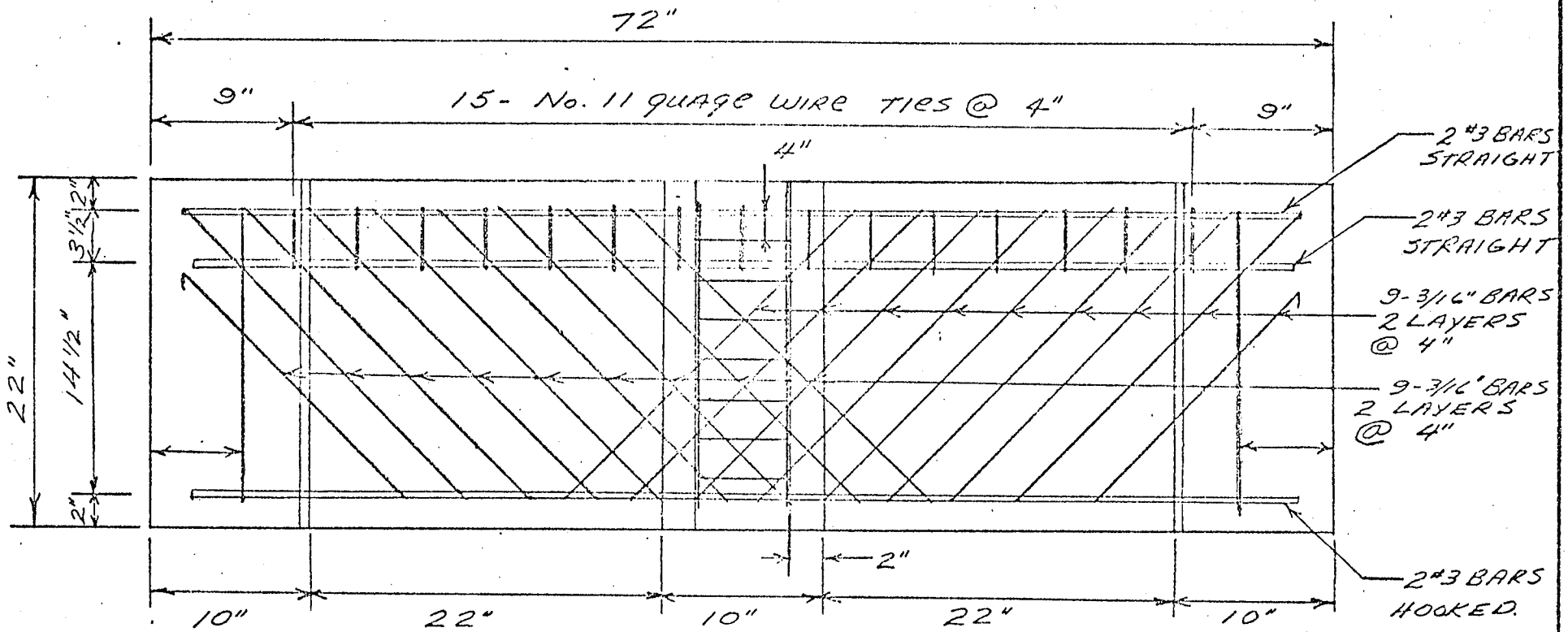

ELEVATION

REINFORCING SERIES #2

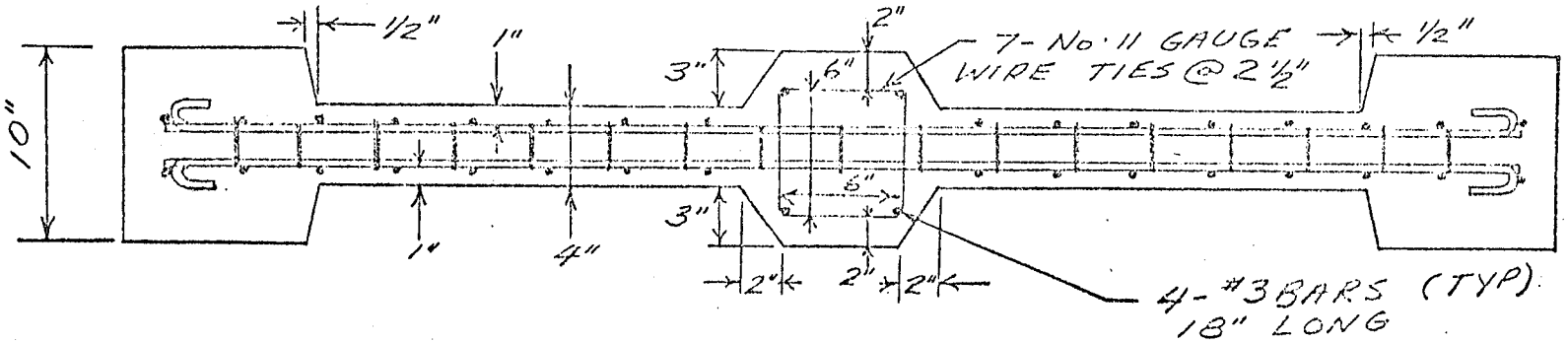

PLAN

FIGURE 2
REINFORCEMENT FOR SERIES #2
Scale : 1" = 10"

parabolic strands of steel as in Malus' beams C2 and C3. The #3 test series was based on this pattern (See Figure 3). Again 2 #3 bars were used for main tensile reinforcement and 4 #3 bars were tied to form a column for the compressive zone. In order to find a more ductile material for the parabolas, ¼ inch hot rolled bars were used. A nominal vertical reinforcing was used to reduce vertical movement. As in series #2, the horizontal bars at the neutral axis were left out and the pilaster was designed as a column.

Test coupons from each test series were sampled from the reinforcing used. Each coupon was tested for yield point, ultimate load and percent elongation per 8 inch length. The results of these tests are shown in Table 1.

2.4 MIX DESIGN, CASTING AND CURING OF CONCRETE

In order to be consistent with the previous tests in this series, the concrete mix design was that used in these previous studies[25, 5]. High -- early -- strength Portland Cement was used to speed the curing of the test specimens.

Owing to the narrow beam width and tight bar spacing (often less than 1 inch clear), a 3/8 inch maximum coarse aggregate was used. This coarse aggregate was crushed granite passing a 3/8 inch sieve but retained by a #4 sieve.

The fine aggregate was well graded with a fineness modulus of about 2.95 and 100% passing a #4 sieve.

The mix was designed to yield a compressive strength of 3000 pounds per square inch at 18 days. The batch proportions were:

High-Early-Strength Portland Cement	Aggregates		Water
	Fine	Coarse	
43.7 lbs.	185 lbs.	64.4 lbs.	30.8 lbs. (dry basis)

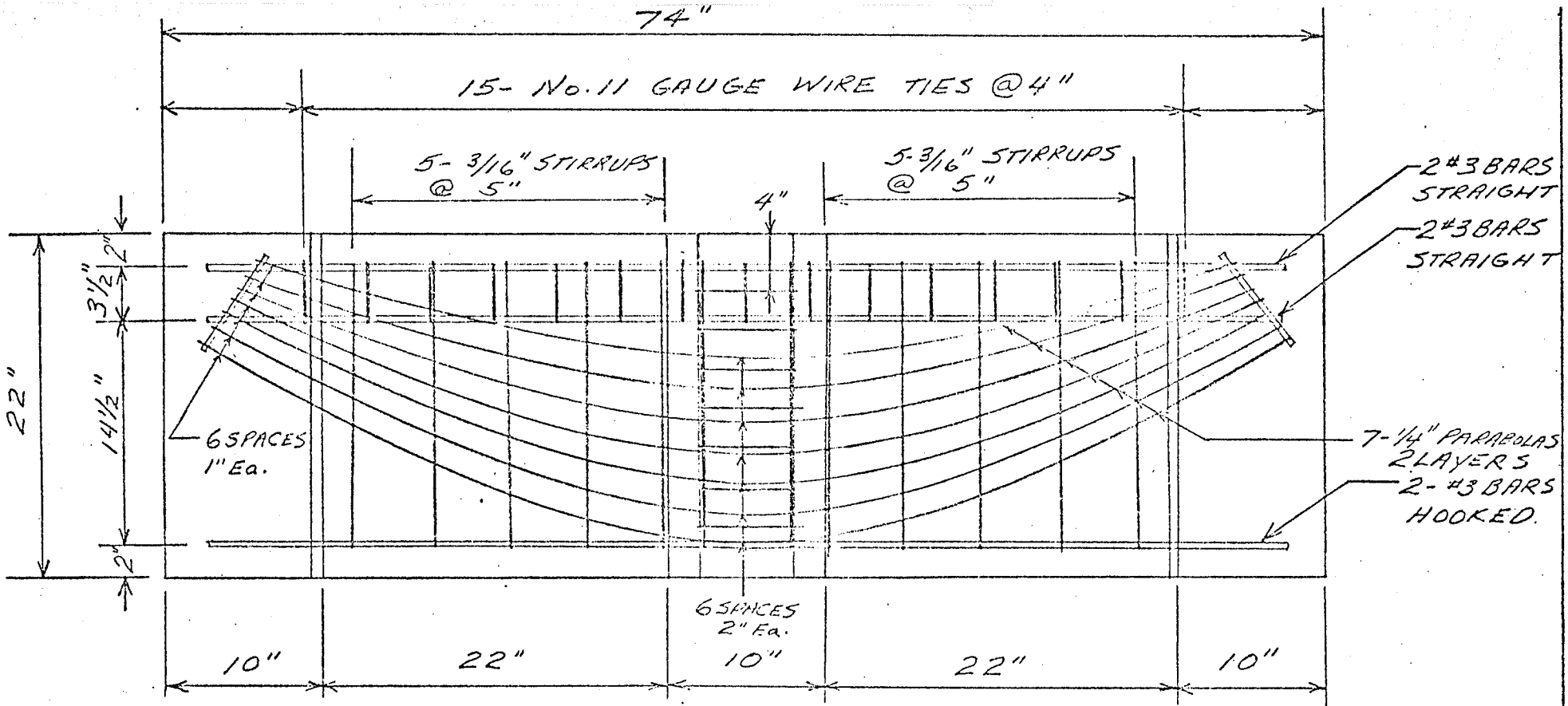

ELEVATION
REINFORCING SERIES #3

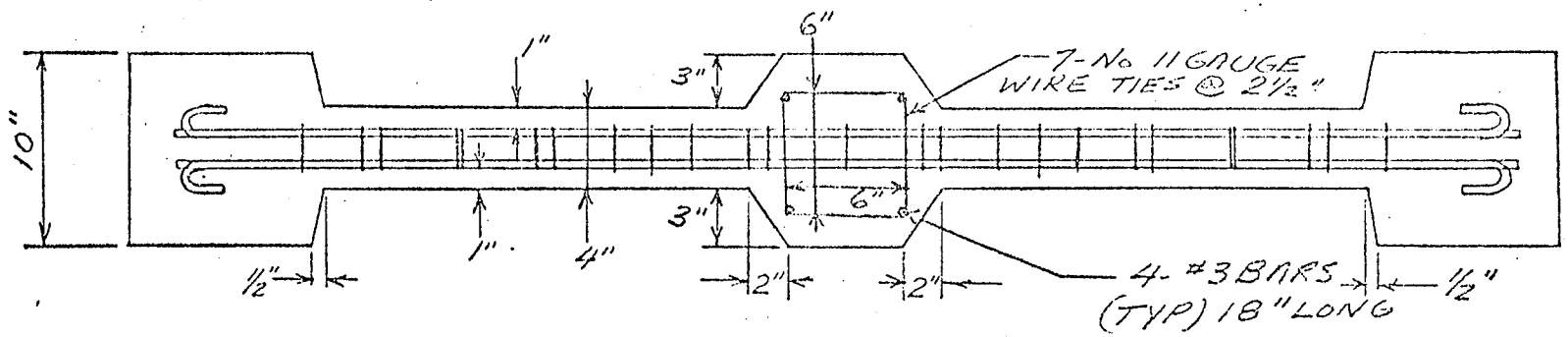

PLAN

FIGURE 3

REINFORCEMENT FOR SERIES #3

Scale : 1" = 10"

TABLE 1

STEEL REINFORCEMENT TENSILE TEST DATA

Beam Sampled	Type of Bar	Diameter (inches)	Sectional Area (sq. ins.)	Ultimate Load (pounds)	Average Tensile (psi)	Yield Load (pounds)	Average Yield Point (psi)	Average Elongation in 8 inch Length (per cent)
1A & 1B	#3 deformed	.375 nominal	.11 .11 .11	8775 8750 8750	78,800	6250 6100 6150	56,100	19.7
1A & 1B	#6 guage wire (stirrups)	.186 .187 .185	.0272 .0275 .0269	2490 2450 2400	90,000	--	--	4.0
2A & 2B	#3 deformed	.375 nominal	.11 .11 .11	8750 8700 8750	79,300	6150 6200 6250	56,400	19.0
2A & 2B	#6 guage wire	.185 .187 .187	.0269 .0275 .0275	2500 2475 2475	91,000	--	--	2.3
2A & 2B	#10 guage wire	.129 .130 .129	.0130 .0133 .0130	685 690 680	52,300	460 490 450	35,600	22.6
3A & 3B	#3 deformed	.375 nominal	.11 .11 .11	8750 8760 8780	79,600	6150 6200 6250	56,300	20.6
3A & 3B	¼" plain round	.259 .256 .250	.0526 .0513 .0490	4050 4150 4100	80,500	3250 3200 3250	63,500	22.7

TABLE 1 (continued)

Beam Sampled	Type of Bar	Diameter (inches)	Sectional Area (sq. ins.)	Ultimate Load (pounds)	Average Tensile (psi)	Yield Load (pounds)	Average Yield Point (psi)	Average Elongation in 8 inch Length (per cent
		.187	.0275	2450				
3A & 3B	#6 guage wire	.186	.0272	2500	91,600	--	--	3.3
		.187	.0275	2550				
		.130	.0133	670		450		
3A & 3B	#10 guage wire	.130	.0133	665	51,300	465	34,700	22.0
		.129	.0130	690		460		

This batch yielded 2¼ cubic feet of concrete. Usually three batches per beam were required, using a mixing time of approximately 10 minutes in a rotating horizontal-tub Eirich machine. (See Figure 4). The slump was measured for each batch and varied from 4½ inches to 6½ inches.

The concrete was placed by hand and each lift was vibrated using a high-frequency internal vibrator with a 3/4 inch head to consolidate placement.

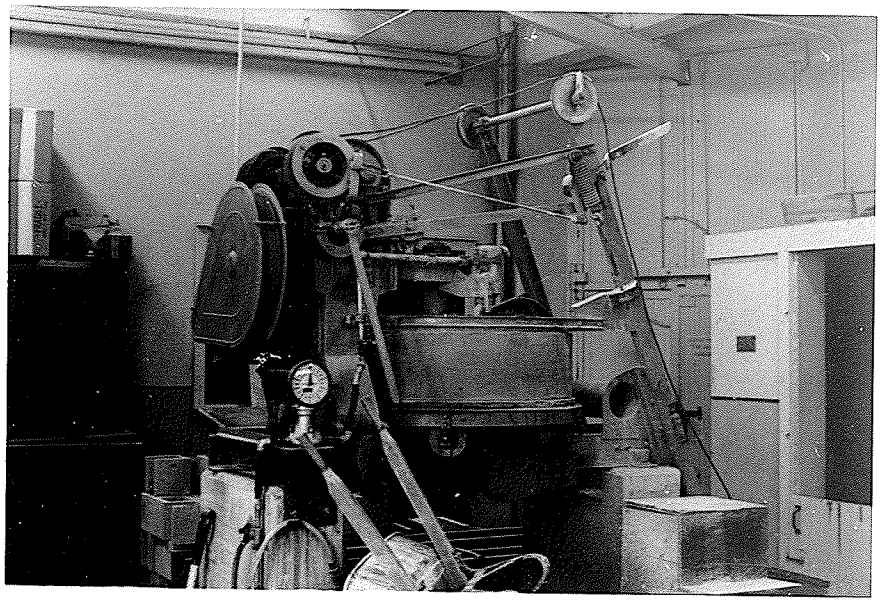

FIGURE 4

EIRICH CONCRETE MIXER USED FOR CASTING THE BEAMS

The concrete was cured for seven days by covering with wet burlap sacks then polyethylene sheets. The forms were stripped and cleaned after one day. After seven days the beams were stored dry up to test date. From each beam cast three compressive test cylinders 6 inches in diameter and12 inches long were taken. In addition, two 4-inch diameter by 4-inch long cylinders for

splitting tensile tests were taken. The compressive tests were performed in accordance with ASTM specifications C 39-64 for "Compressive Strengths of Molded Concrete Cylinders"[27]. The tensile tests were performed in accordance with ASTM designation C 496-64T for "Splitting Tensile Strength of Molded Concrete Cylinders"[28]. The results of these tests are shown in Tables 2 and 3.

2.5 BEAM TESTING ARRANGEMENT AND PROCEDURE

a.) "A" SERIES

For each type of reinforcing a preliminary test was performed to study the behavior and load-deflection characteristics. Particular attention was placed on the downward portion of the load-deflection curve. The information gathered from this test series was

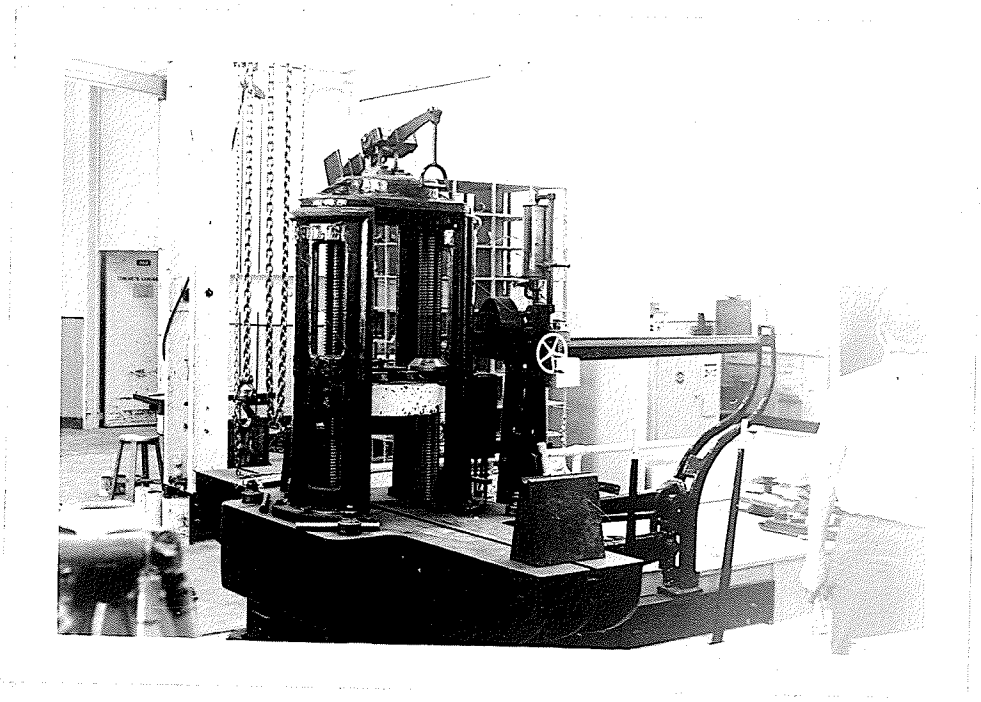

FIGURE 5

RIEHLE TEST MACHINE

TABLE 2

CONCRETE COMPRESSION TEST DATA

Beam Sampled	Cylinder Number	Average Diameter (inches)	Cross-Sectional Area (square inches)	Maximum Load (pounds)	Compressive Strength (psi)	Average Compressive Strength (psi)	Age (days)
1A	1	6	28.3	135,000	4,750	4,633	46
	2	6	28.3	129,000	4,560		
	3	6	28.3	130,000	4,600		
1B	1	6	28.3	130,000	4,600	4,960	63
	2	6	28.3	148,000	5,230		
	3	6	28.3	142,000	5,050		
2A	1	6	28.3	126,000	4,450	4,466	50
	2	6	28.3	123,000	4,350		
	3	6	28.3	130,000	4,600		
2B	1	6	28.3	127,000	4,500	4,290	70
	2	6	28.3	119,000	4,200		
	3	6	28.3	118,000	4,170		
3A	1	6	28.3	124,000	4,380	4,536	36
	2	6	28.3	138,000	4,880		
	3	6	28.3	123,000	4,350		
3B	1	6	28.3	135,000	4,750	4,986	69
	2	6	28.3	141,000	4,980		
	3	6	28.3	148,000	5,230		

TABLE 3

CONCRETE SPLITTING TENSILE TEST DATA

Beam Sampled	Mould Number	Size of Specimen		Splitting Load (rounds)	Tensile Strength (psi)	Average Tensile Strength (psi)	Age (days)
		Diameter (inches)	Length (inches)				
	1	3.98	4.11	14,100	865		
1A	2	4.00	4.00	11,000	688	776	46
	1	3.99	4.02	13,900	867		
1B	2	4.02	4.02	11,000	624	746	63
	1	4.01	4.10	14,700	898		
2A	2	4.03	4.01	14,500	903	900	50
	1	4.01	4.03	15,000	930		
2B	2	3.99	3.99	14,900	935	933	70
	1	4.00	3.99	12,500	783		
3A	2	4.05	4.02	13,100	812	798	36
3B	1	4.00	4.10	15,200	930	930	69

used to plan the closer study in the "B" series of tests.

The machine used to test the beams was a 200,000 pound capacity, screw loading, gear driven, balance beam Riehle testing machine as shown in Figure 5.

Before testing each beam was lightly coated with a white flat latex to improve crack detection. Then a one inch grid was drawn to locate cracking.

The beam was placed in the test machine and "Mercer" dial gauges were attached as shown in Figures 6 and 7. The beam was then given initial load of 1 kip. All dial gauges were set and read. In this test series only gauges 1 to 5 inclusive were used.

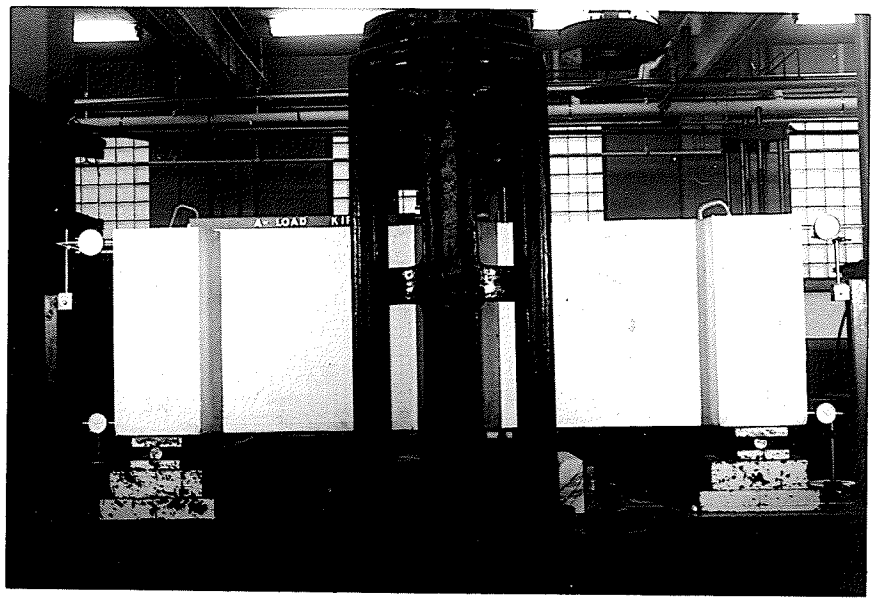

FIGURE 6

TEST SET UP FOR BEAM 1A

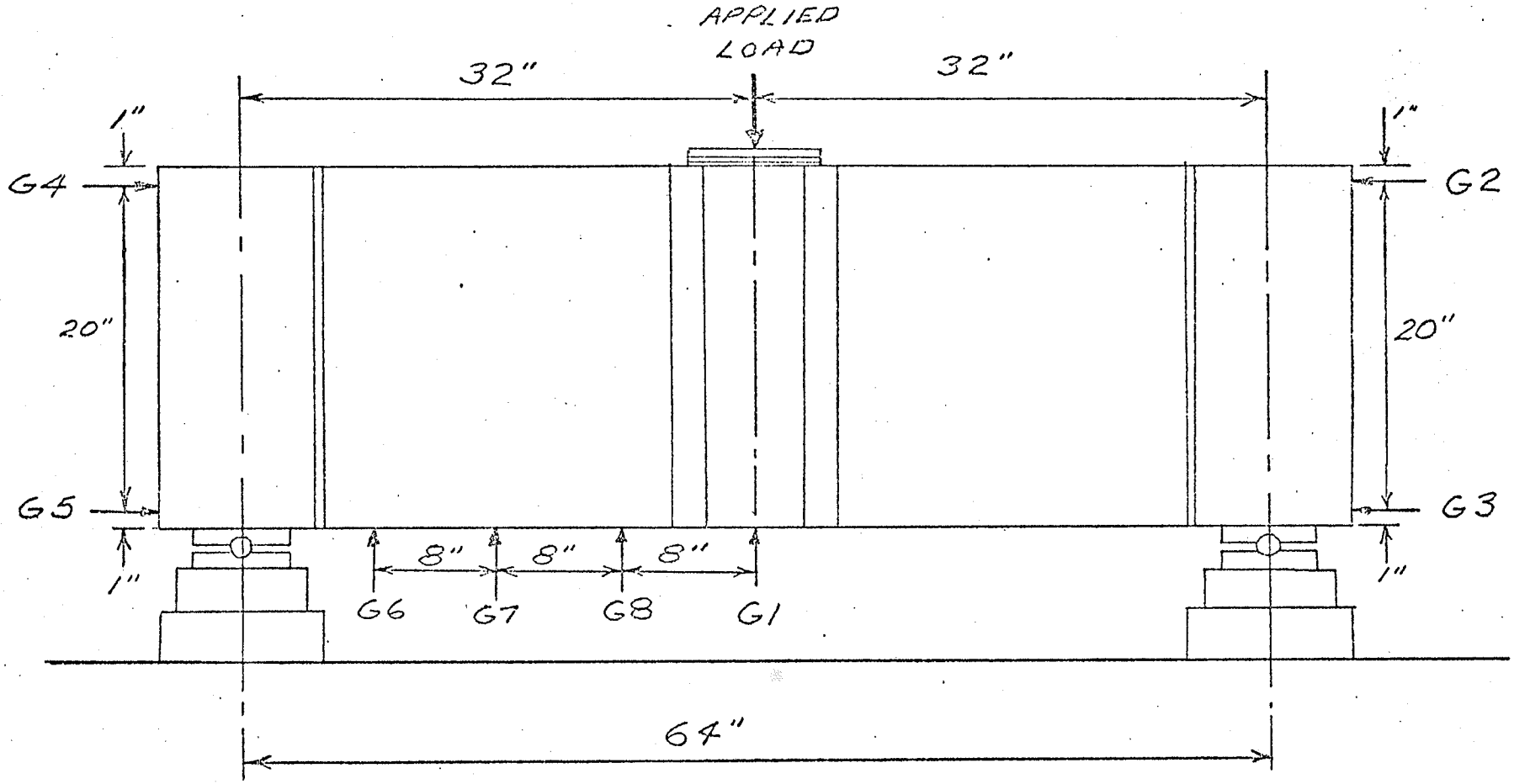

FIGURE 7

LOADING ARRANGEMENT USED FOR TESTS

Scale : 1" = 10"

The beam was then loaded at 5 kip intervals until initial cracking took place. After this initial cracking the load interval was often smaller to facilitate study of the crack pattern. At the end of each increment all gauges were read, cracks were studied and often photographs were taken.

In the yielding and plastic ranges the increments were taken by equal deflections of approximately 0.1 inch. During this period the machine's balance beam was kept balanced at all times.

For these tests in an attempt to further study the characteristics of the beams motion pictures were taken of one of the panels, often at very slow shutter speed.

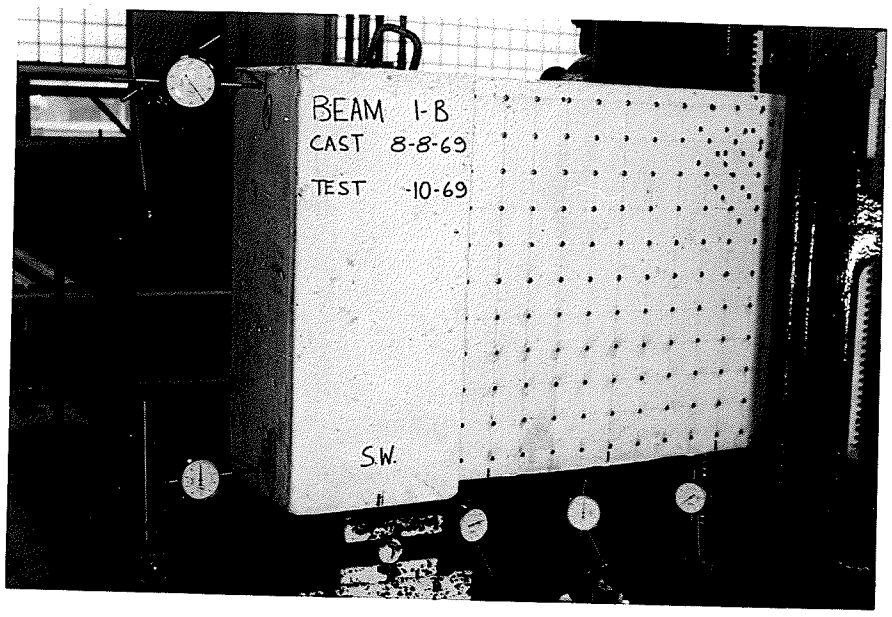

FIGURE 8

DEMEC GRID
FOR BEAM 1B

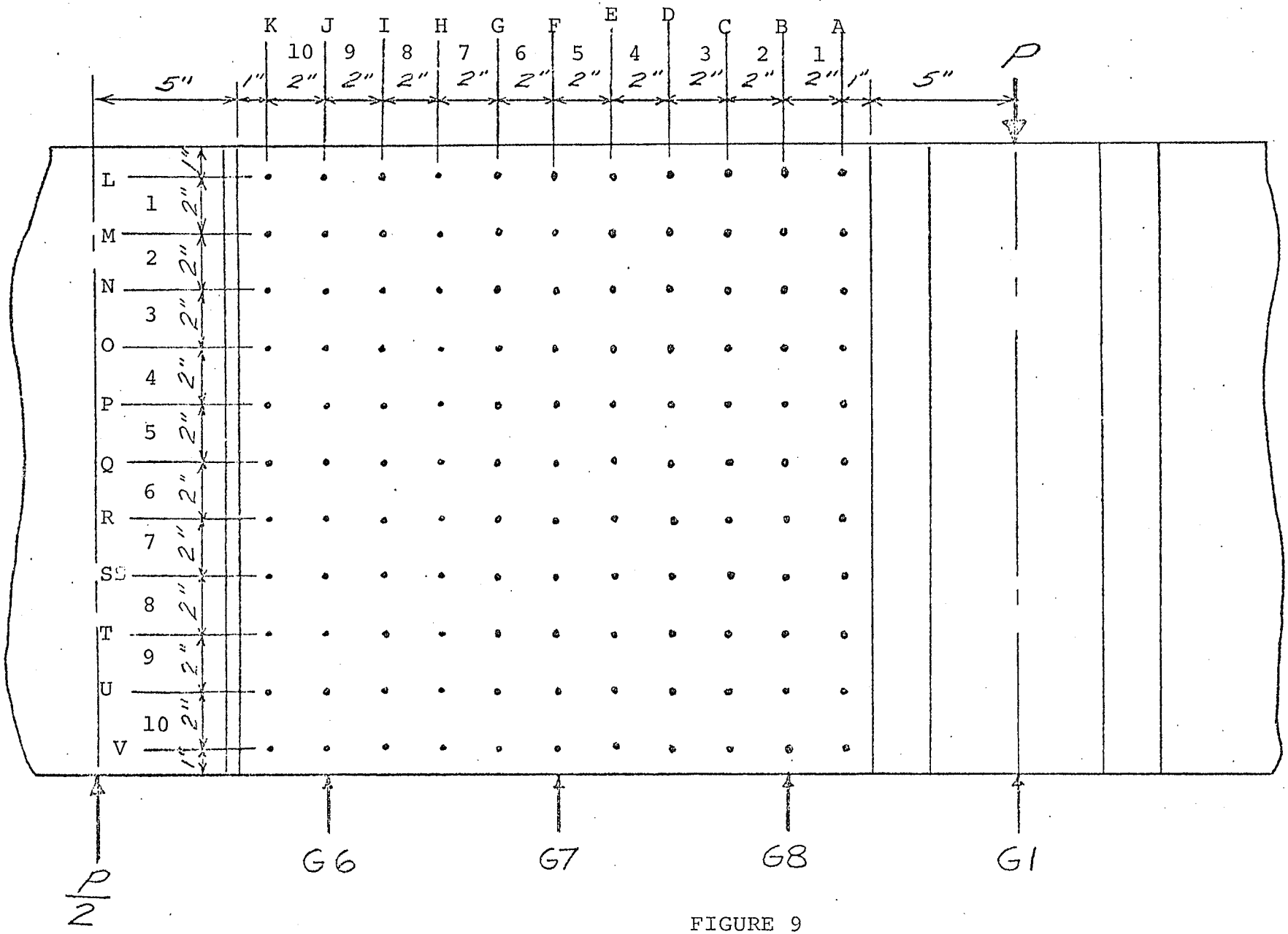

FIGURE 9

DEMEC POINT LAYOUT FOR BEAM 1B

Scale : 1" = 5"

b.) "B" SERIES

A specimen of each type of reinforcing was retested in this series with close attention to strain and deformation characteristics.

For beam 1B a 2 inch grid of Demec points was placed on one panel as shown in Figure 8 and Figure 9. Points were affixed with a fast drying epoxy, "Hysol Epoxi Patch Kit". Using the calibrating bar they were placed as close as possible to the middle reading of the 2 inch Demec gauge shown in Figure 10.

The beam was set in the test machine as shown in Figure 11 and 12. Additional dial gauges 6, 7 and 8 were used to study the movement of the panel.

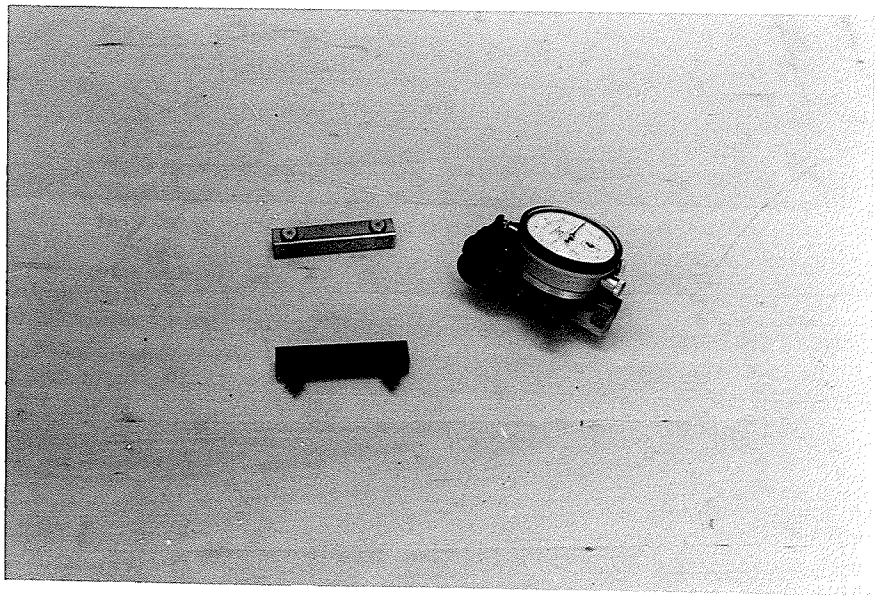

FIGURE 10

DEMEC GAUGE AND
CALIBRATION BARS

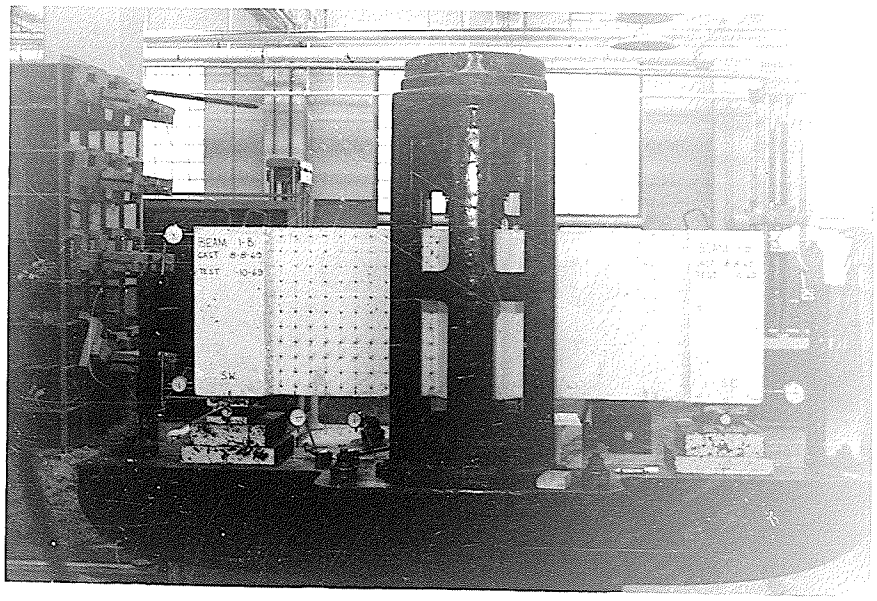

FIGURE 11

BEAM 1B TEST SET UP

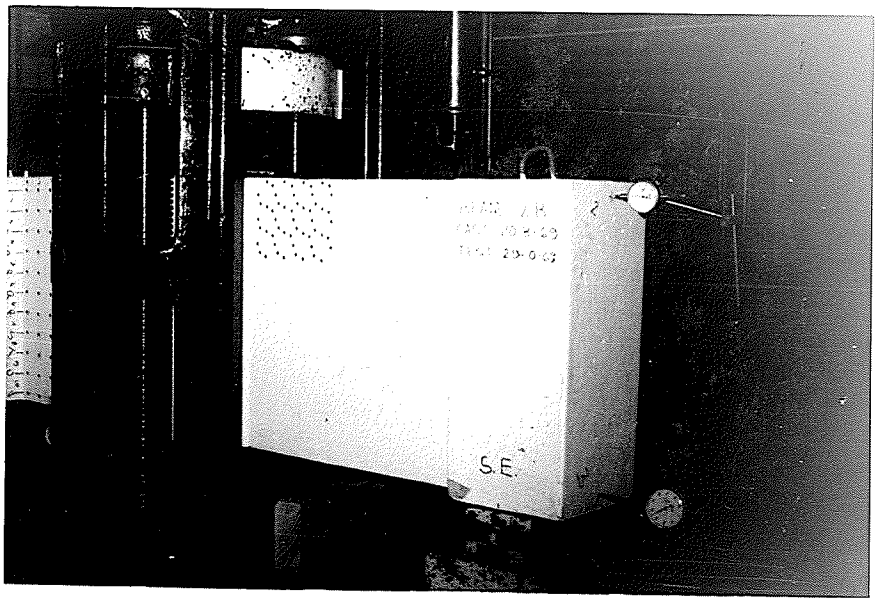

FIGURE 12

BEAM 2B TEST SET UP

An initial load of one kip was placed on the beam and all Demec and dial gauges were read.

Drawing on the experience of beam 1B, beams 2B and 3B not only had a grid of Demec points on one panel but also a number of rosettes of Demec points were placed in the compression zone to find principal strains and their directions. See Figures 13, 14 and 15.

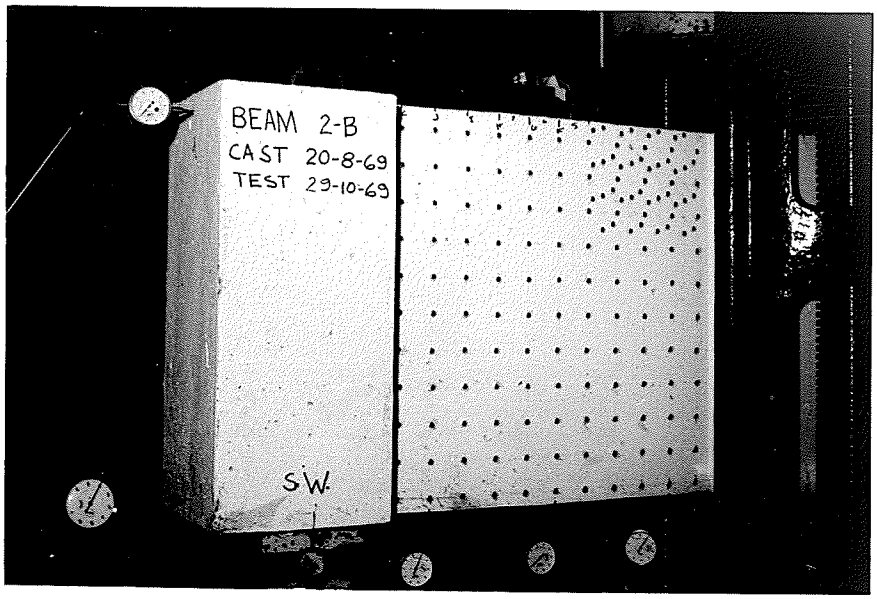

FIGURE 13
DEMEC LOCATION
ON BEAM 2B

In addition Intertechnology "Micro-Measurement" EA-06-125 BB-120 electrical resistance strain gauges were placed on some of the web reinforcing of Beams 2B and 3B to study the effectiveness of these reinforcement patterns as shown in Figure 16. The strain gauges were affixed to a smooth location on the bar and water-proofed with Gagekote #5 silicone coating and protected

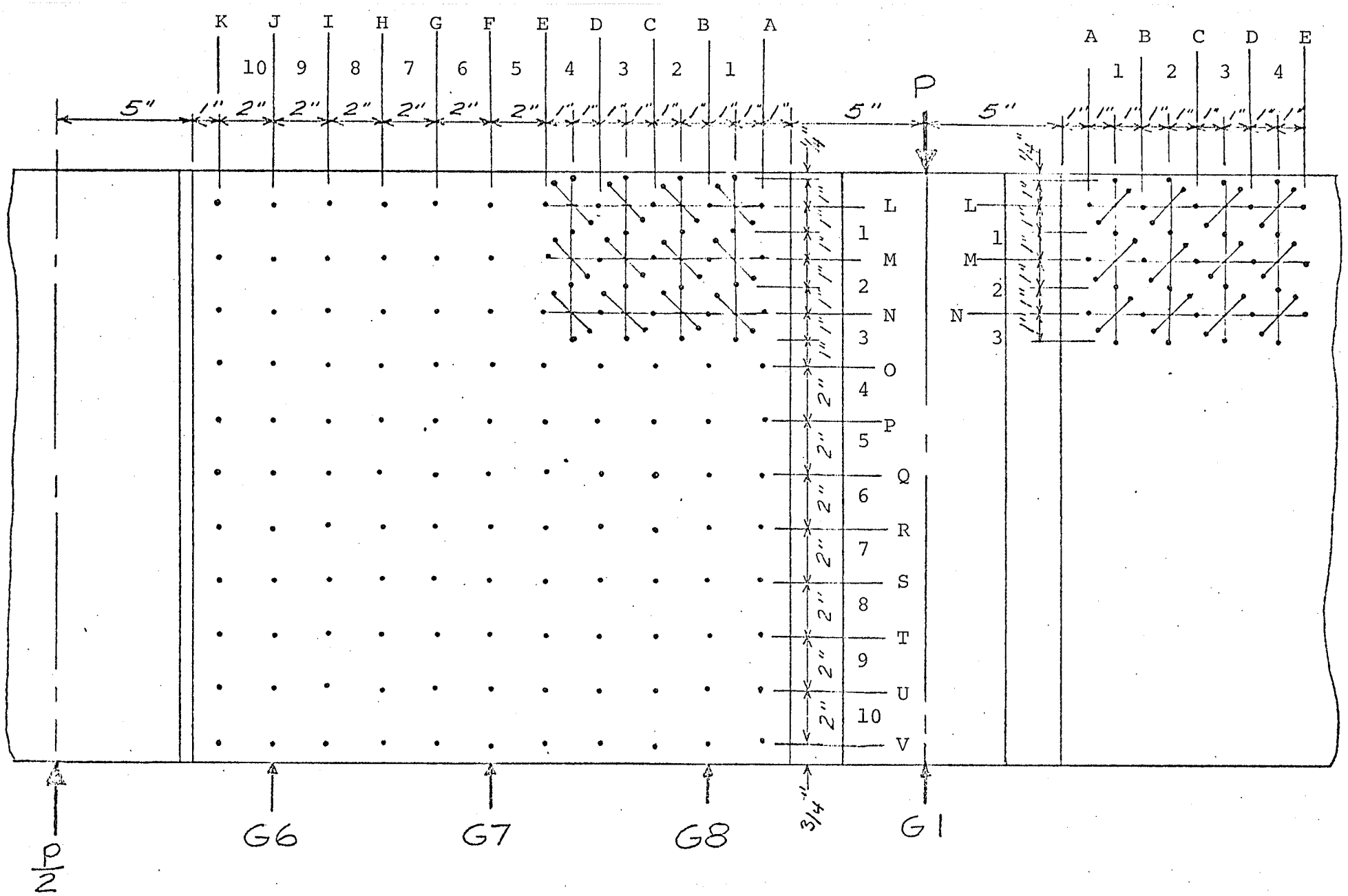

FIGURE 14

DEMEC POINT LAYOUT FOR BEAM 2B

Scale : 1" = 5"

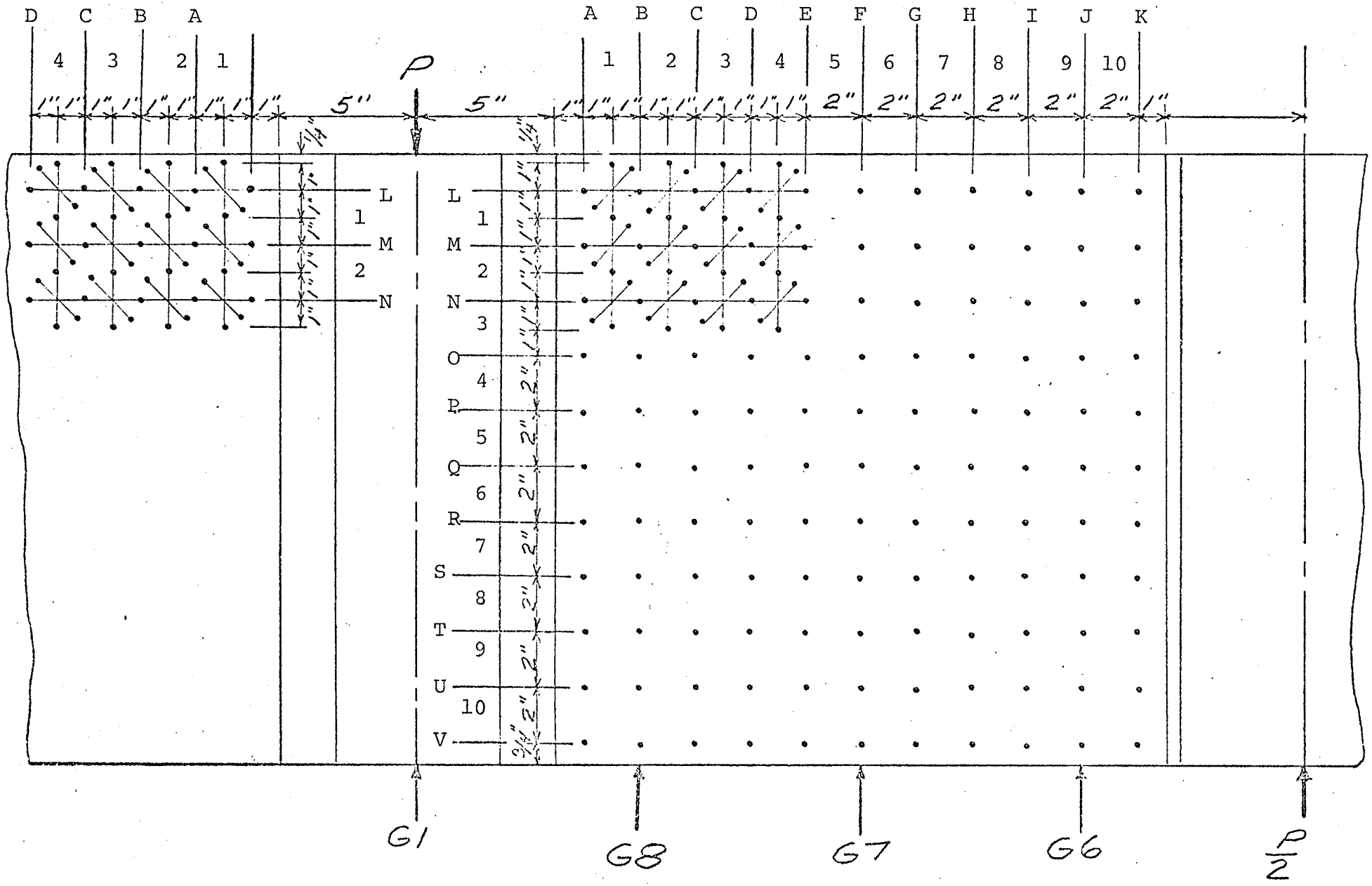

FIGURE 15

DEMEC POINT LAYOUT FOR BEAM 3B

Scale : 1" - 5"

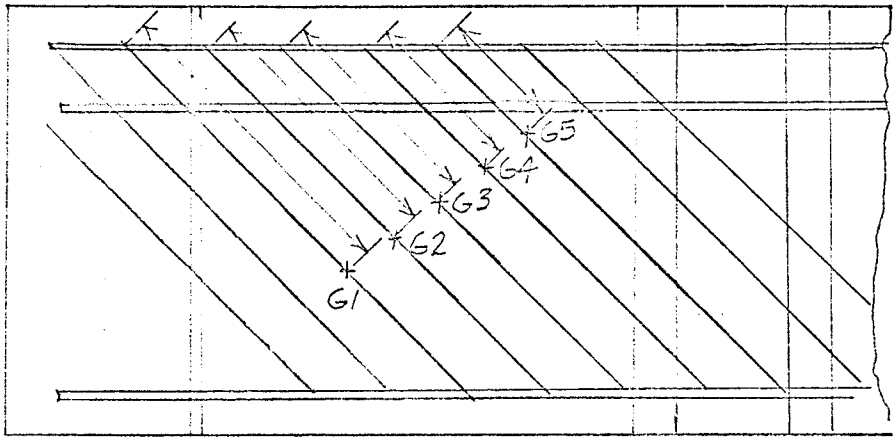

BEAM 2B

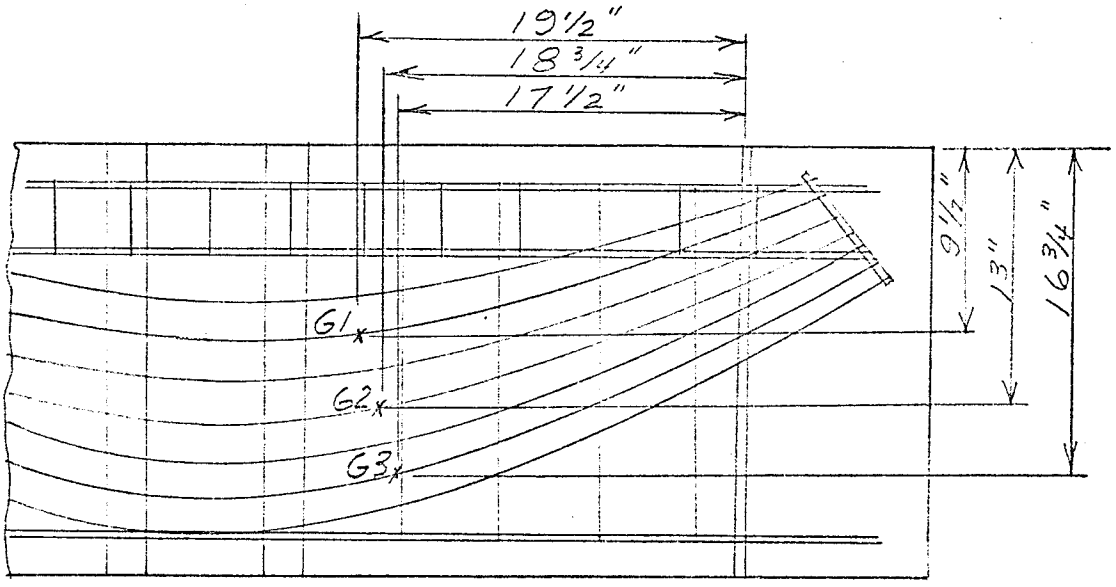

BEAM 3B

FIGURE 16

LOCATION OF STRAIN GUAGES

BEAM 2B AND BEAM 3B
scale: 1"=2"

with plastic tape. They were read using a "Datran Digital Strain Indicator" model A111D.

Beams 2B and 3B were loaded as beam 1B with an initial reading of 1 kip and all gauges and Demec points were given initial readings. Then the load was applied in 5 kip intervals until cracking.

At the ends of these increments the dial gauges and strain gauges were read. The times at which the Demec readings were taken were carefully selected due to the length of time required for reading. These times were selected by study of the test results of test series A.

For beam 1B the gauges were read at loads of 10 kips, 19 kips, 25 kips and 28 kips. At each set of Demec readings, which usually took from 2 to 5 hours, the drop off of load was found on the balance arm of the machine.

For beam 2B the grid was only read at 30 kips. The beam failed suddenly and unexpectedly before the second set of readings could be taken. More frequent rosette readings were taken once these values were felt to be more significant. Rosettes were read at loads of 20.7 kips, 30 kips, 40 kips and 45.6 kips and at 41.3 kips on the decreasing load-deformation curve. Again the load was read throughout the Demec readings and the electric resistance strain gauges were read during the Demec reading period.

For beam 3B the rosette readings were again given more attention since the time involved in taking these readings was only 30 to 45 minutes. The grid was read at loads of 30 and 72 kips. The rosettes were read at loads of 20 kips, 30 kips, 40 kips, 65 kips, 72 kips, 74.8 kips (crushing impending) and at 75.4 kips. Again during these Demec readings the load and strain gauges were read at various times.

2.6 Reduction of Experimental Data

The data from the experiments was collected, transferred to punch cards, and reduced by IBM 360 computer for tabulation and plotting.

a.) Calculations of Moments

The total moment at midspan is made up of the following:

$$M_p = \frac{PL}{4} - \frac{P\ell}{8} \qquad -(2.1)-$$

where: M_p = Moment due to applied load in kip-inches.

P =Applied load in kips.

L = Span length in inches.

ℓ = Length of load plate.

$$M_i = Pi \qquad -(2.2)-$$

where:

$$i = (G3+G5)-(G2+G4) \qquad -(2.3)-$$

M_i = increase in moment due to movement of supports.

P = applied load.
(See Figure 7 for gauge locations)

$G2$ = Reduced reading of gauge 2.

$G3$ = Reduced reading of gauge 3.

$G4$ = Reduced reading of gauge 4.

$G5$ = Reduced reading of gauge 5.

Therefore total moment = M_T

$$M_T = P\left(\frac{L+i}{4}\right) - \frac{P\ell}{8} \qquad -(2.4)-$$

b.) Calculations of End Rotations

Let G2 and G3 be the reduced readings of gauges 2 and 3 respectively. Then the total relative movement of points 2 and 3 is D_{32} where:

$$D_{32} = G3 - G2 \qquad -(2.5)-$$

If H is the vertical distance between points 2 and 3, then the rotation of this end of the beam is θ_1 where:

$$\tan\theta_1 = \frac{G3 - G2}{H} \qquad -(2.6)-$$

The same holds true for the gauges 4 and 5 and the other end of the beam. Therefore the rotation at the other end of the beam θ_2 is found by:

$$\tan\theta_2 = \frac{G5 - G4}{H} \qquad -(2.7)-$$

The total rotation θ_T is found by:

$$\theta_T = \theta_1 + \theta_2 \qquad -(2.8)-$$

c.) Strain Calculations

The Demec gauge measured the distance between two points on the concrete before and after the load. The reduced Demec reading multiplied by a factor of 2.48 x 10^{-5} is then average strain across the 2 inch gauge length. Therefore

i.) Deformations are

Strain x 2.

ii.) Total deformations are the sum of the deformations in each grid line.

iii.) Principal strains and their directions

Strains were measured with $\theta = 0°$, $\theta = 45°$ or $135°$, $\theta = 90°$

Therefore if the measured strains are

$$\epsilon_0 , \epsilon_{45}, \epsilon_{90}$$

Then $\epsilon_x = \epsilon_0$

$\epsilon_y = \epsilon_{90}$

and if $\epsilon_\theta = \epsilon_x \cos^2\theta + \gamma_{xy} \sin\theta\cos\theta + \epsilon_y \sin^2\theta$ -(2.9)-

$\theta = 45°$

$$\therefore \epsilon_{45} = \frac{\epsilon_x}{2} + \frac{\gamma_{xy}}{2} + \frac{\epsilon_y}{2} \quad \text{-(2.10)-}$$

$$\therefore \gamma_{xy} = 2\epsilon_{45} - \epsilon_x - \epsilon_y \quad \text{-(2.11)-}$$

if $\epsilon_0, \epsilon_{135}, \epsilon_{90}$

are measured

Then $$\epsilon_{135}° = \frac{\epsilon_x}{2} - \frac{\gamma_{xy}}{2} + \frac{\epsilon_y}{2} \quad \text{-(2.12)-}$$

$$\therefore \gamma_{xy} = \epsilon_x + \epsilon_y - 2\epsilon_{135} \quad \text{-(2.13)-}$$

Then the principal strains are:

$$\epsilon_{1,2} = \left(\frac{\epsilon_x + \epsilon_y}{2}\right) \pm \sqrt{\left(\frac{\epsilon_x - \epsilon_y}{2}\right)^2 + \left(\frac{\gamma_{xy}}{2}\right)^2} \quad \text{-(2.14)-}$$

and the direction is found by Mohr's circle and

$$\tan 2\theta = \frac{\gamma_{xy}/2}{\left(\frac{\epsilon_x - \epsilon_y}{2}\right)} \quad \text{-(2.15)-}$$

3. TEST RESULTS

3.1 INTRODUCTORY REMARKS

During the six tests performed in this study a large amount of information was gathered. In order to promote easier reading of these test results, the results have been tabulated, plotted or shown in diagrams. If further study of the original test results is required they may be found in the University of Manitoba Department of Civil Engineering Report ST-2-70, "A Report on the Testing of Six Reinforced Concrete Deep Beams."[29]

3.2 REINFORCING PATTERN #1

Beam 1A was cast on August 8, 1969 and tested on September 23, 1969. The load-deflection curve is shown in Figure 17 and moment-rotation curve is shown in Figure 18. Photographs of the test are shown in Figures 19 to 27.

Initial cracking took place at 12 kips at the place where the pilaster and panel meet. Cracks soon appeared in each face and the cracks moved towards the load. The load held well under large deflections until the main steel fractured just as the compression zone started cracking. There were few cracks in the panels however these cracks became very wide as the deflection increased through large values.

Beam 1B was cast on August 8, 1969 and tested on October 10, 1969. The load-deflection curve is shown in Figure 17 and the moment rotation curve is shown in Figure 18. Photographs of the test are shown in Figures 28 to 34. Demec readings reduced to average strains are shown in Figures 35 to 39. The measured total horizontal deformations are shown in Table 4 and the vertical deformations are shown in Table 5. These values represent the total deformation of 10, two inch Demec points or the deformation in a 20 inch section of the beam.

Beam 1B behaved as expected, in a manner quite similar to 1A. There was some more extensive cracking of the panel. The beam held load well over large deflections until failure of the main tensile bars. There was more indication of compression cracking on Beam 1B however, with the accompanying slight drop off of load.

3.3 REINFORCING PATTERN #2

Beam 2A was cast on August 20, 1969 and tested on October 9, 1969. The load-deflection curve is shown in Figure 40 and moment-rotation curve in Figure 41. Photographs of the test are found in Figures 42 to 48.

Initial cracking took place at 15 kips with cracks in the panels. As the load increased more cracks appeared across the panel faces. These cracks did not appear to open up and eventually the compression zone begun to crush with an accompanying drop off of load. Then the beam failed suddenly due to a fracture of a main tensile bar.

Beam 2B was cast on August 20, 1969 and tested on October 29, 1969. The load-deflection curve is shown in Figure 40 and the moment-rotation curve is shown in Figure 41. Photographs of the test are shown in Figures 49 to 58. The Demec readings for the grid are shown in Figure 59 in the form of average strains. The principal strains are shown for the compression zones in Figures 60 to 64. The strain gauge readings for the web reinforcing is shown in Figure 65. Total horizontal deformation measured by Demec gauges are shown in Table 6 and total vertical deformation is shown in Table 7.

Beam 2B behaved much the same as Beam 2A through most of the loading but failed suddenly due to a fracture of the tensile steel. This fracture came at 65% of the deflection attained in Beam 2A.

3.4 REINFORCING PATTERN #3

Beam 3A was cast on September 8, 1969 and tested on October 14, 1969. The load-deflection curve is shown in Figure 66 and the moment-rotation curve in Figure 67. The photographs of the test are shown in Figures 68 to 77.

The initial cracking took place at 18 kips and as the load increased very extensive cracking took place. The ultimate load was considerable larger than Beams 1A and 2A. The cracks climbed slowly to the compression zone with very little increase in crack width. Near ultimate load the compression zone began to crack and the load began to drop off rapidly. As the compression zone disintegrated showing buckled compressive reinforcing the load dropped to very low values at low deflections.

Beam 3B was cast on September 8, 1969 and tested on November 16, 1969. The load-deflection curve is shown in Figure 66 and moment-rotation curve is shown in Figure 67. The photographs of the tests are shown in Figures 78 to 86. Demec readings for the grid are shown in the form of average strains in Figures 87 and 88. The principal strains for the compression zone are shown in Figures 89 to 95. The total horizontal deformations for the grid are found in Table 8 and the vertical deformations are found in Table 9. The results of strain gauge readings on the web reinforcing is shown in Figure 96.

Beam 3B behaved much the same as Beam 3A. The panels were cracked extensively and failure was due to disintegration of the compression zone.

FIGURE 17
LOAD-DEFLECTION CURVES
FOR BEAMS 1A AND 1B

FIGURE 18

MOMENT-ROTATION CURVES

FOR BEAMS 1A AND 1B

FIGURE 19

LOAD = 20 K.
DEFL. = .067 in.

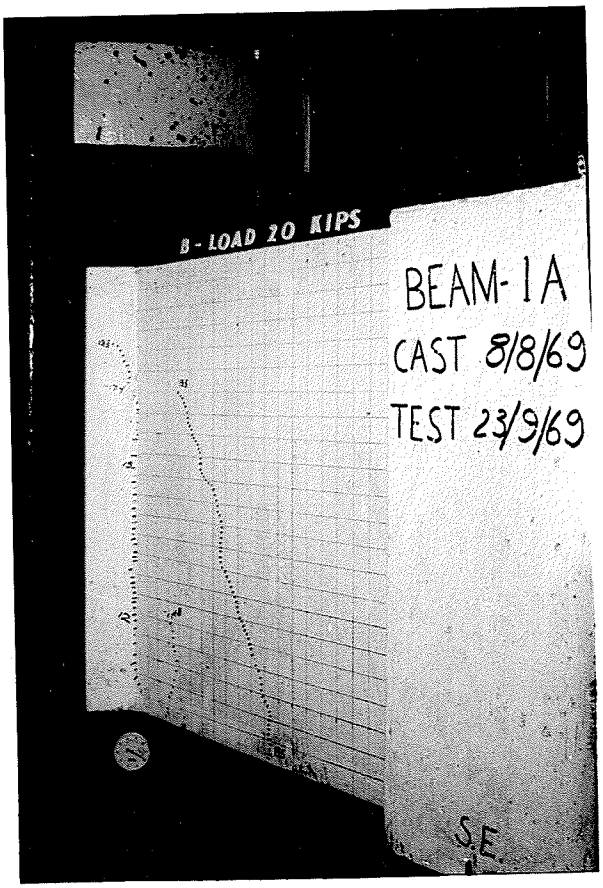

FIGURE 20

LOAD = 20 K.
DEFL. = .067 in.

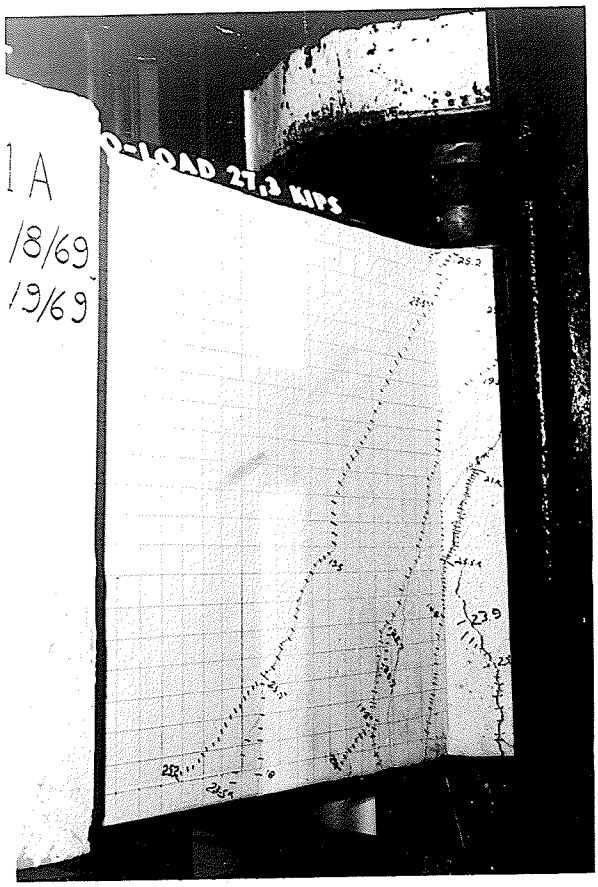

FIGURE 21

LOAD = 27.3 K.
DEFL. = .935 in.

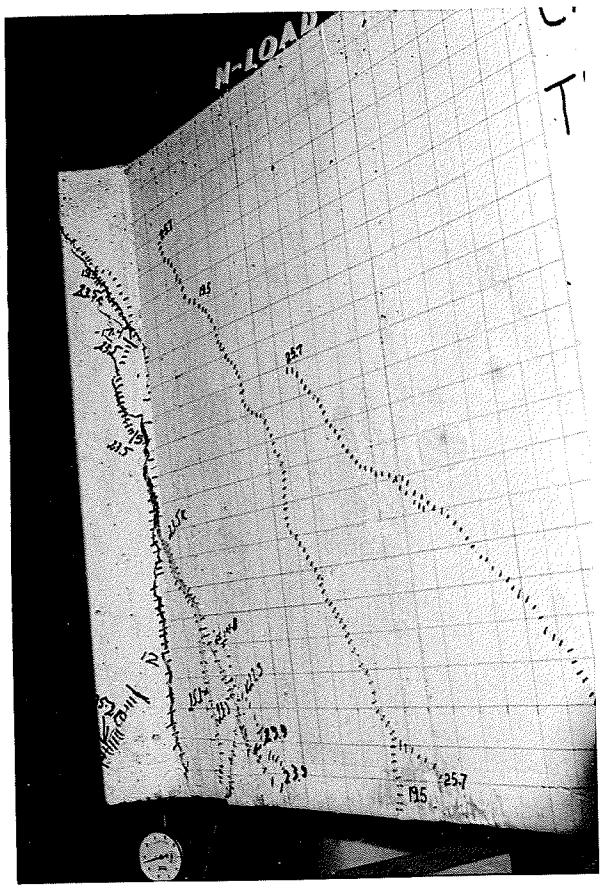

FIGURE 22

LOAD = 27.3 K.
DEFL. = .935 in.

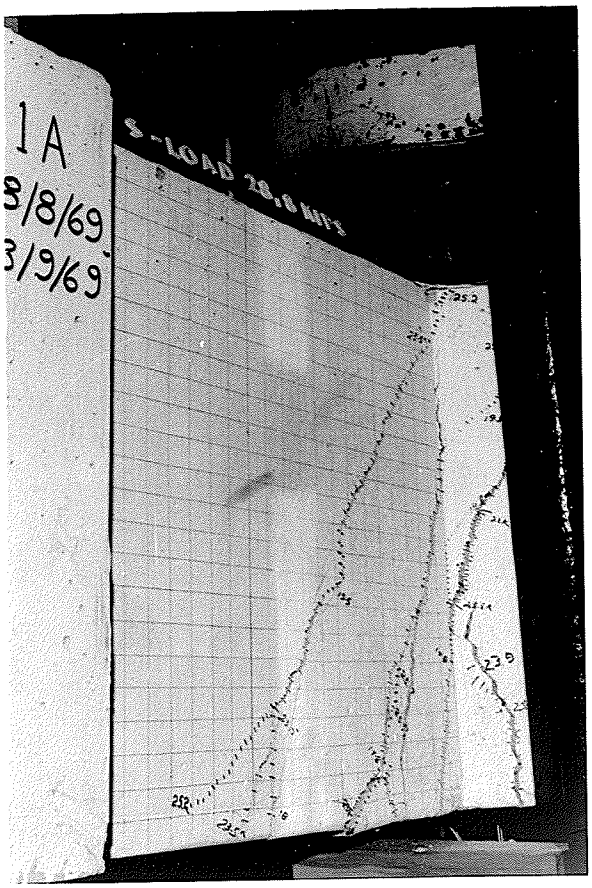

FIGURE 23

LOAD = 28.8 K.
DEFL. = 2.056 in.

FIGURE 24

FAILURE OF TENSILE REINFORCEMENT

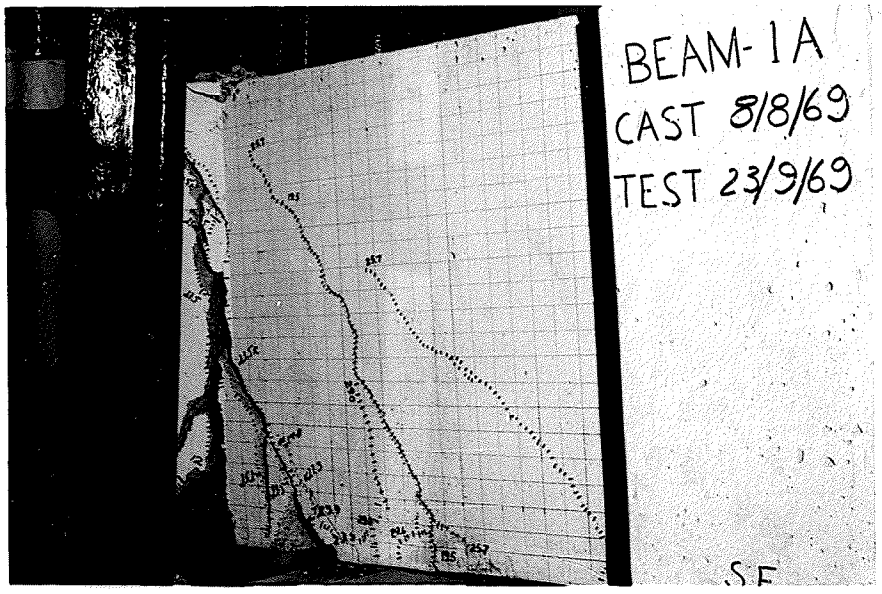

FIGURE 25

FAILURE

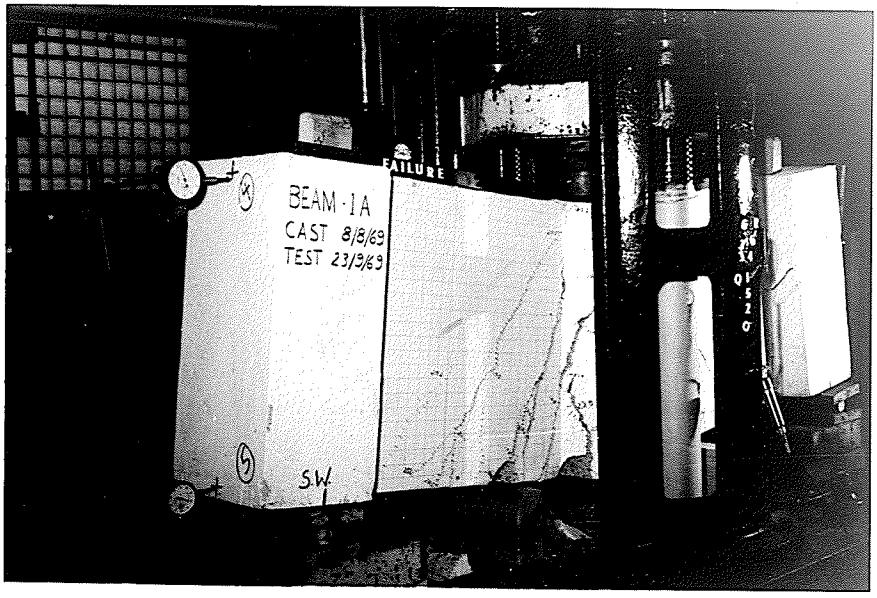

FIGURE 26

AFTER FAILURE

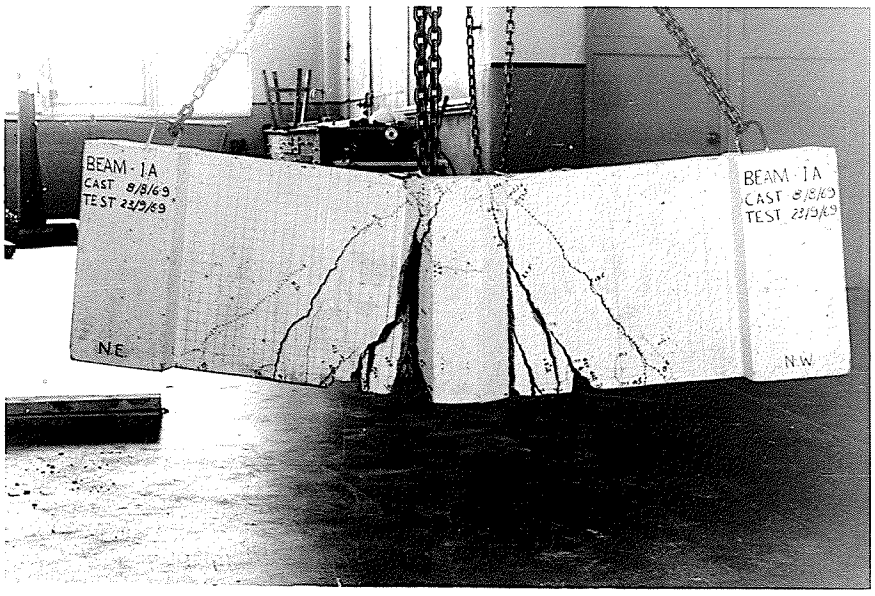

FIGURE 27

AFTER FAILURE

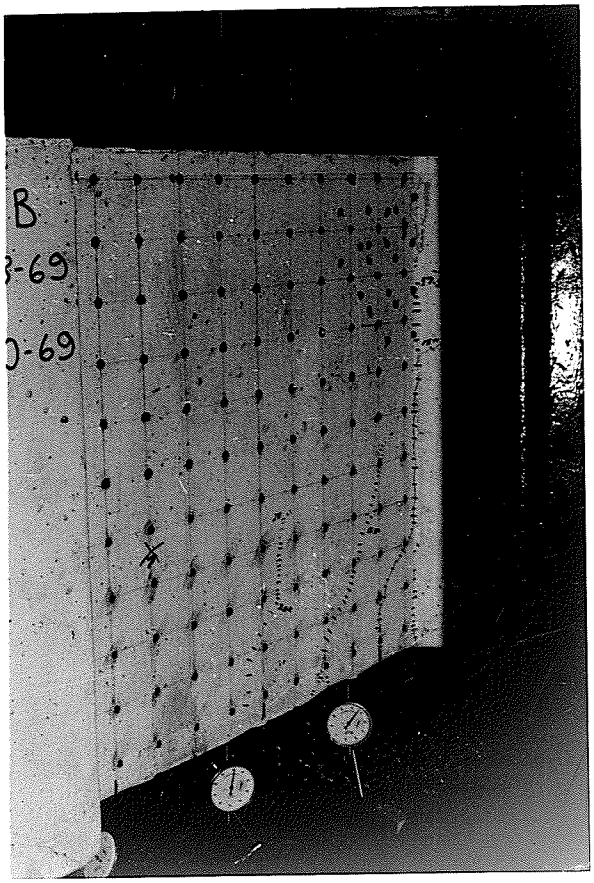

FIGURE 28

LOAD = 20 K.
DEFL. = .073 in.

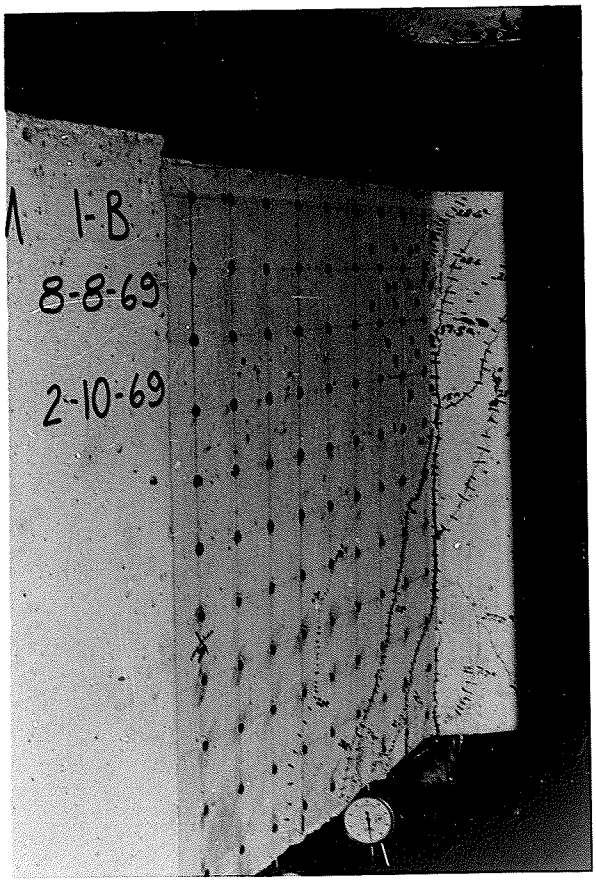

FIGURE 29

LOAD = 28.3 K.
DEFL. = 1.251 in.

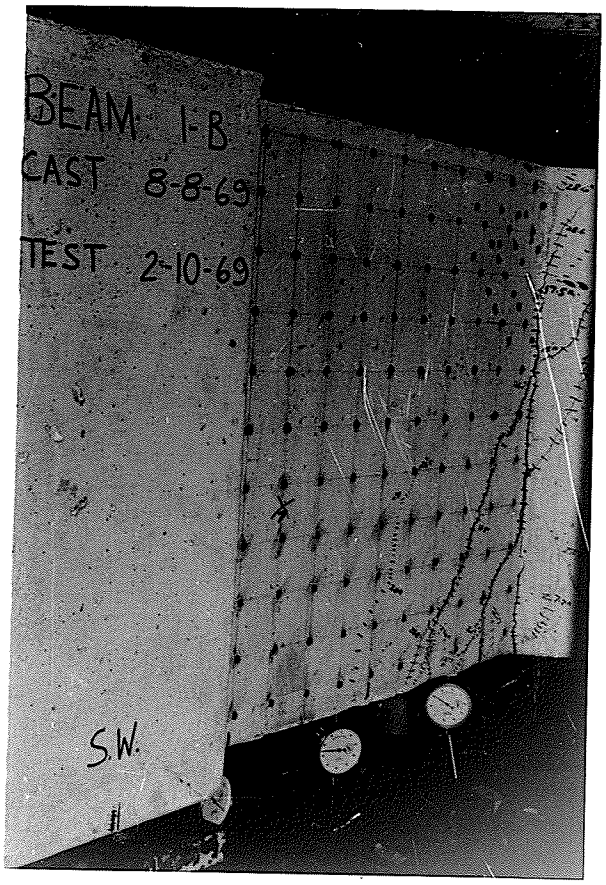

FIGURE 30.

LOAD = 28 K.
DEFL. = 1.460 in.

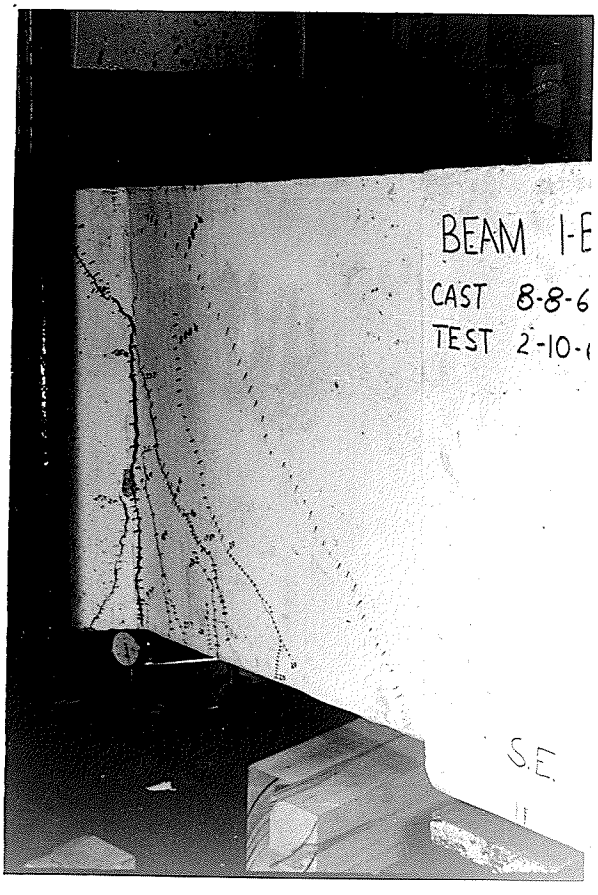

FIGURE 31

LOAD = 28 K.
DEFL. = 1.460 in.

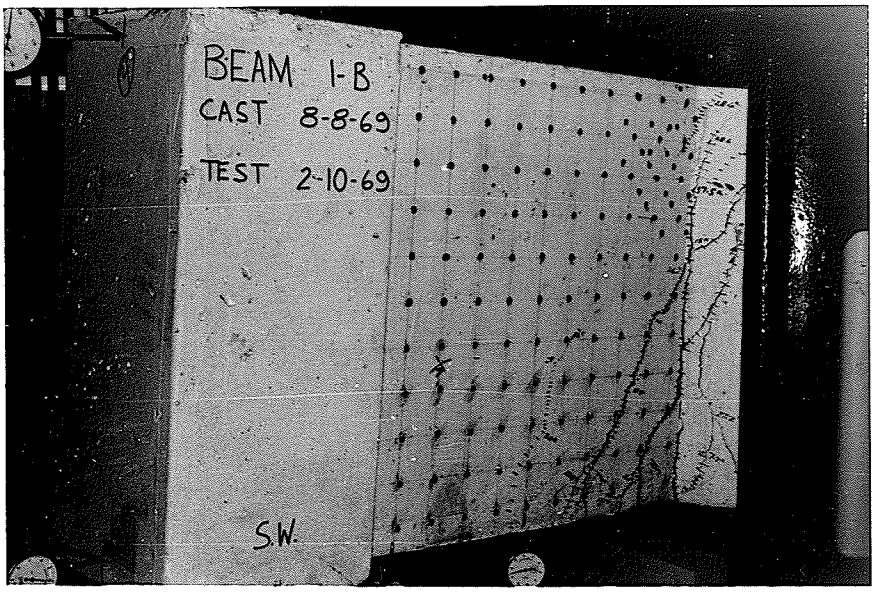

FIGURE 32

FAILURE

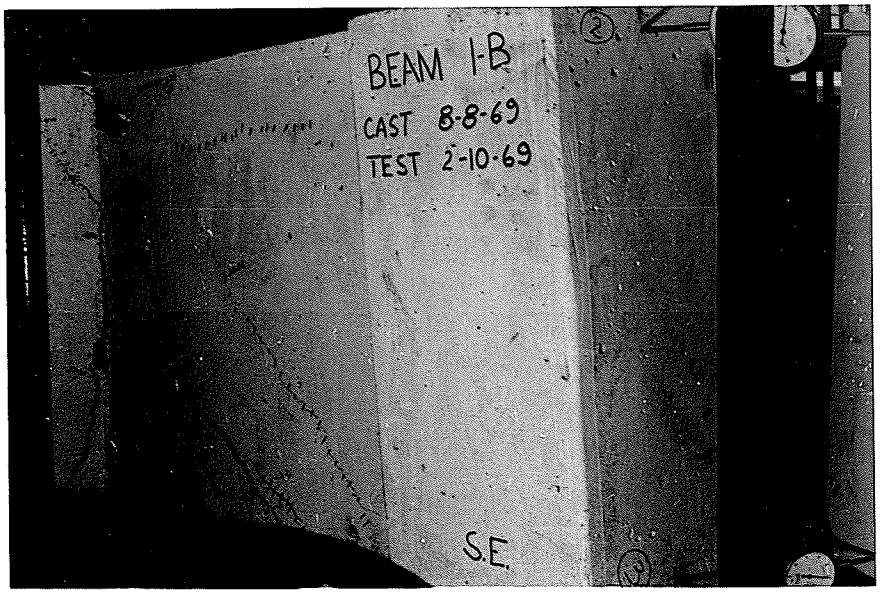

FIGURE 33

FAILURE

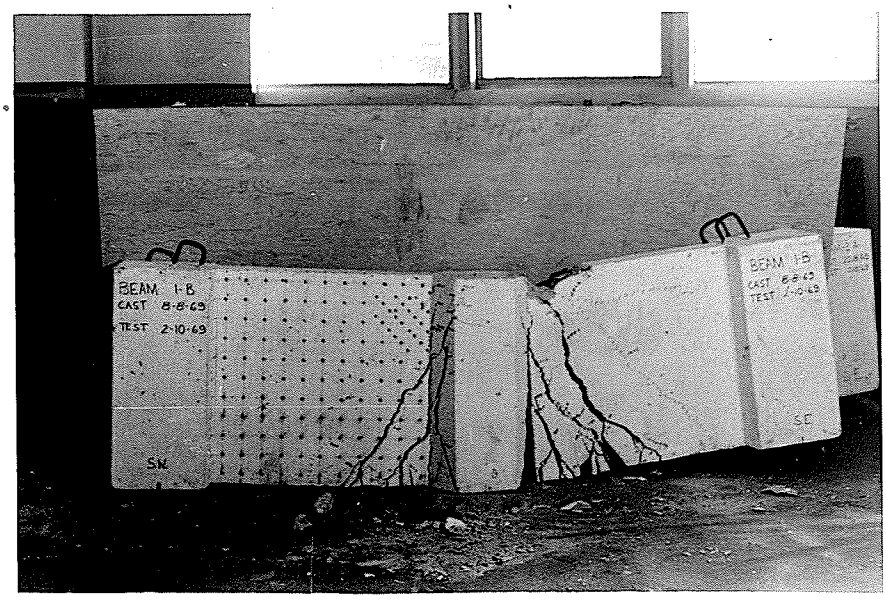

FIGURE 34

FAILURE

5" to load point

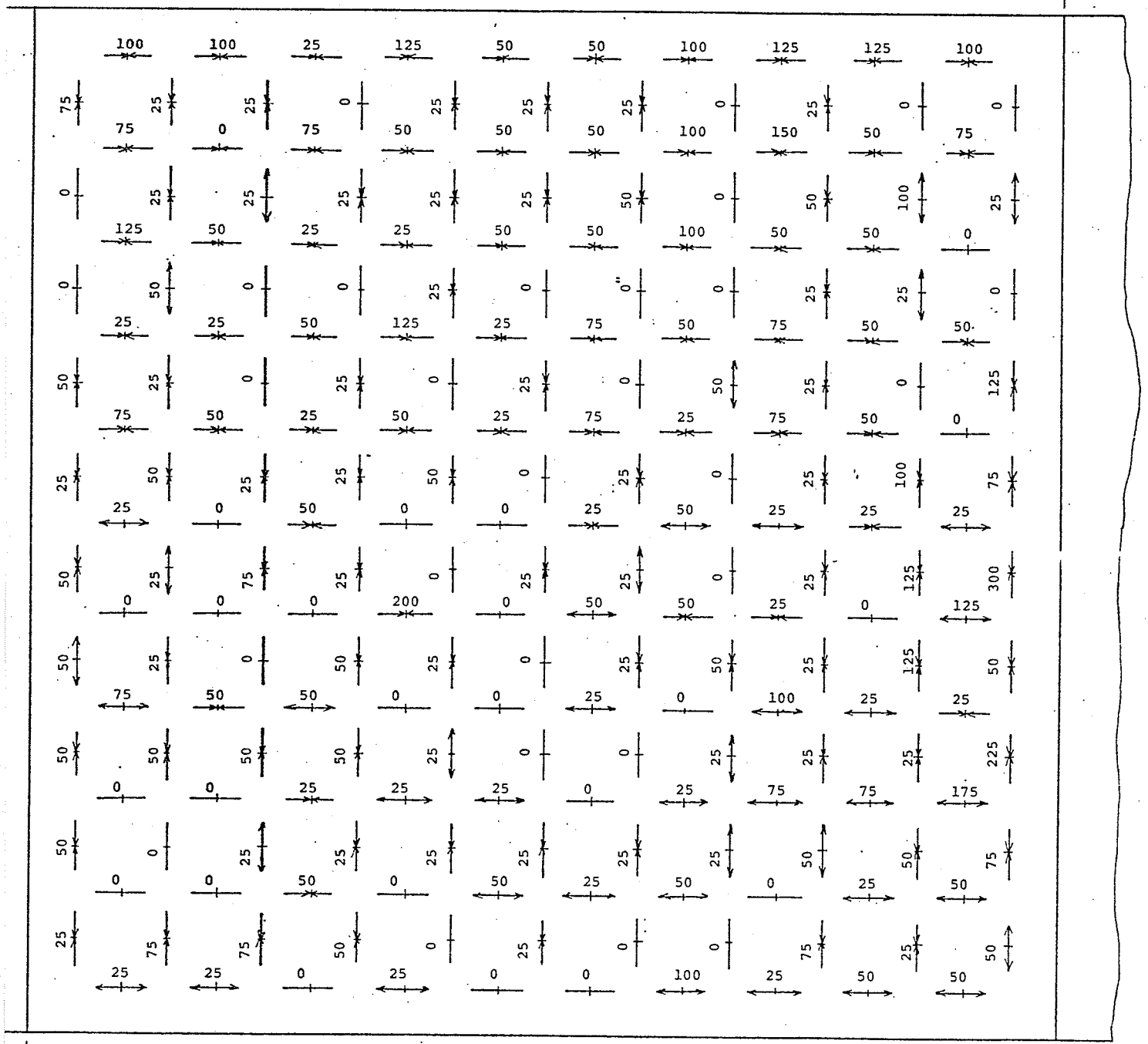

5" to reaction

FIGURE 35

AVERAGE STRAINS
(microinches per inch)

BEAM 1B LOAD= 10 kips

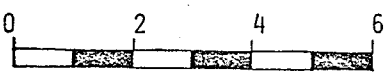

5" to load point →

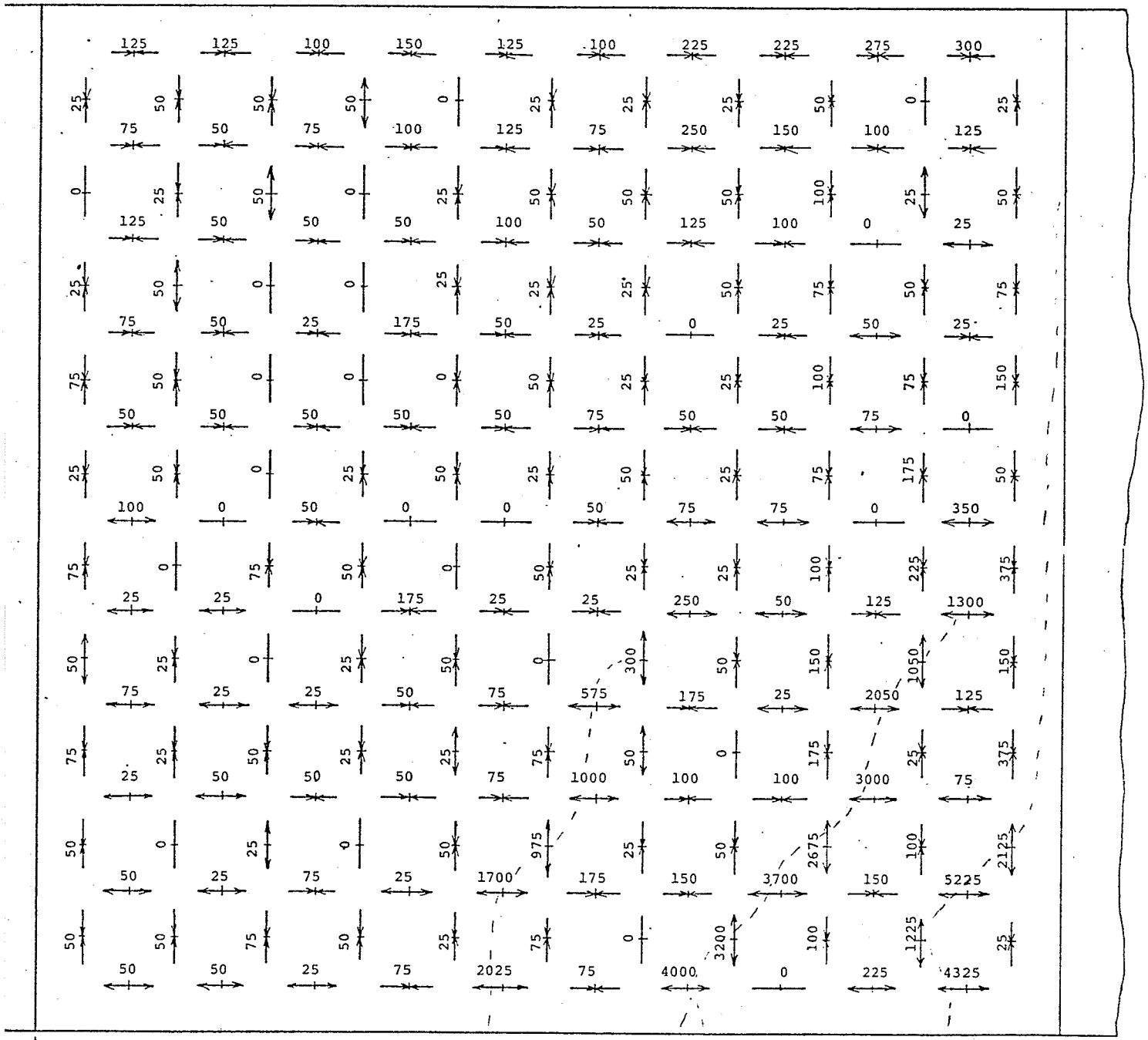

5" to reaction ←

FIGURE 36

AVERAGE STRAINS
(microinches per inch)

BEAM 1B LOAD = 19 kips

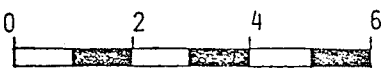

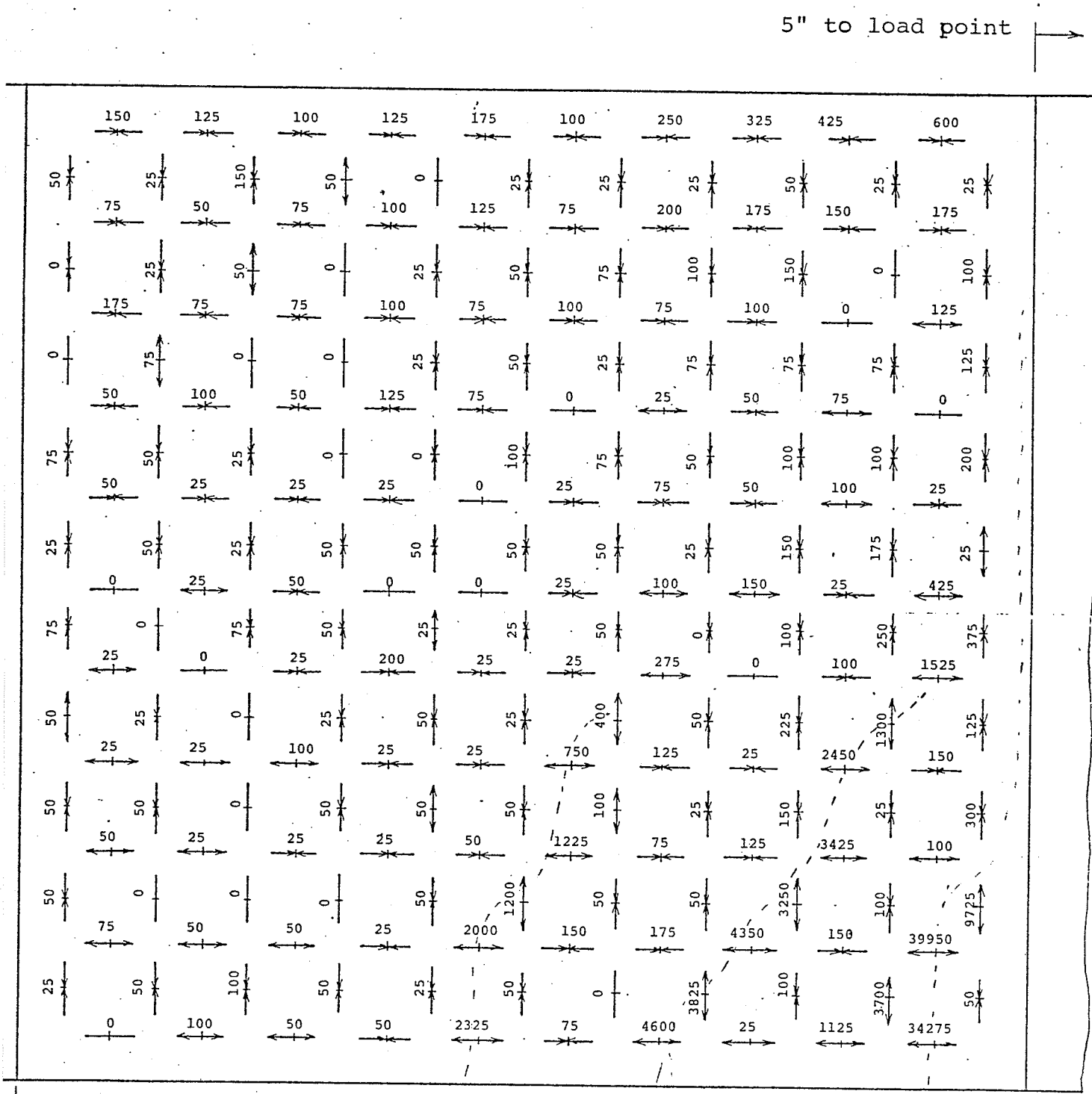

FIGURE 37

AVERAGE STRAINS
(microinches per inch)

BEAM 1B LOAD = 25 KIPS

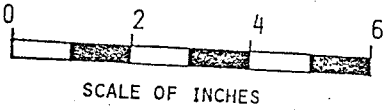

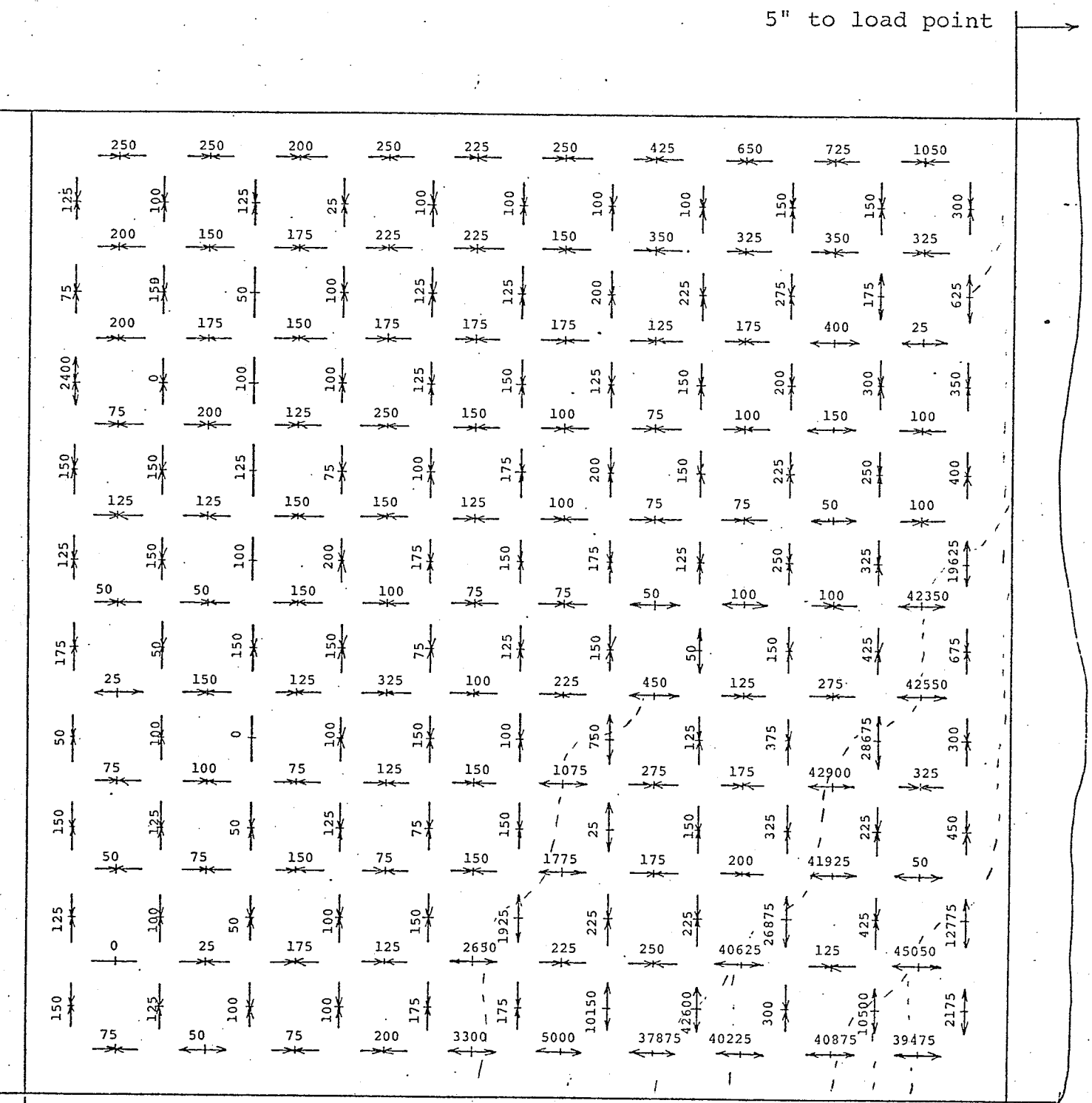

FIGURE 38

AVERAGE STRAINS
(microinches per inch)

BEAM 1B LOAD = 28 kips

5" to load point →

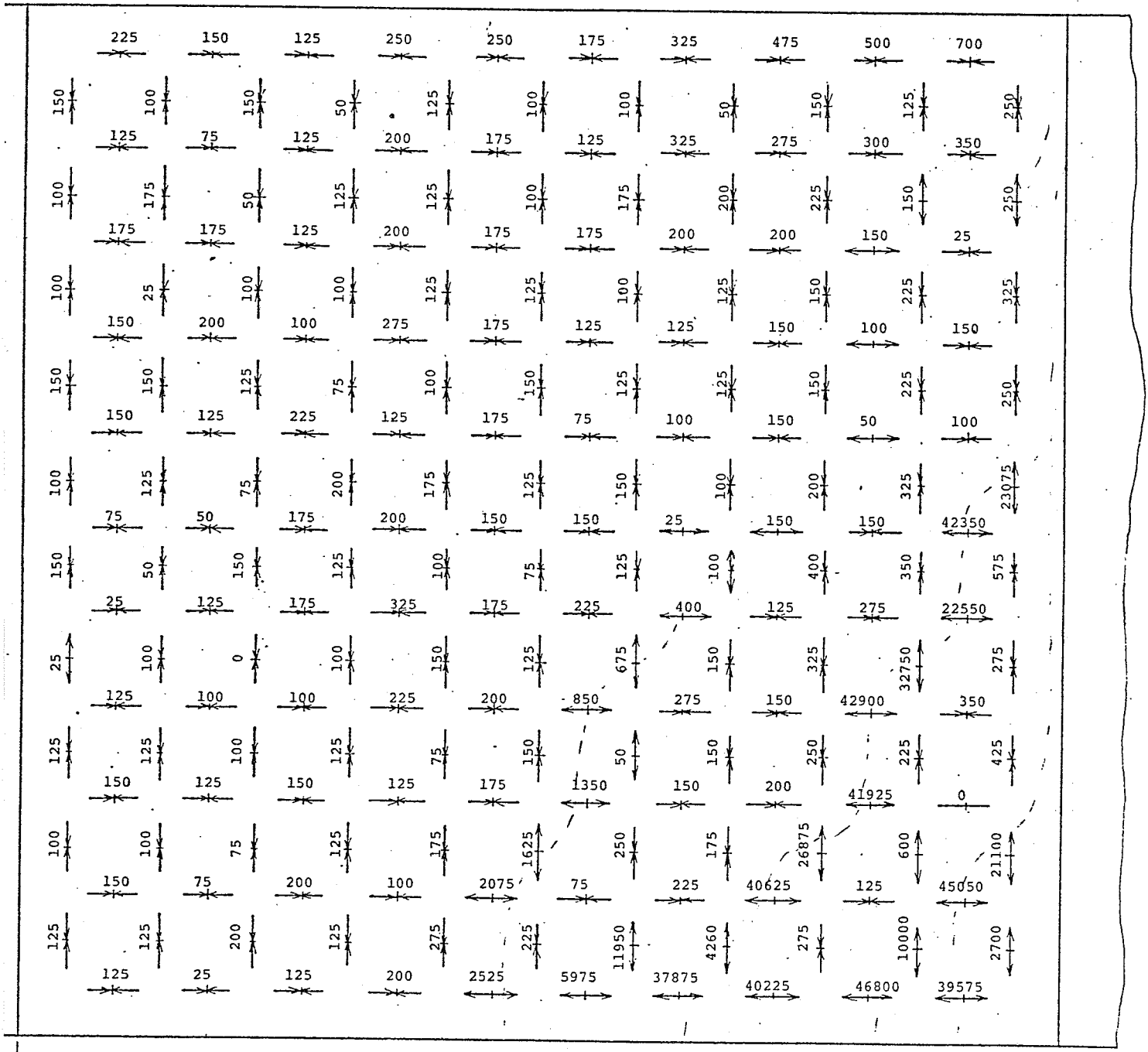

5" to reaction

FIGURE 37

AVERAGE STRAINS
(microinches per inch)

BEAM 1B LOAD = 0 kips

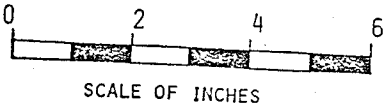

TABLE 4

TOTAL HORIZONTAL DEFORMATIONS

BEAM 1B

LOCATION	DISTANCE TO PANEL TOP (inches)	DEFORMATIONS (inches) 10 kips	19 kips	25 kips	28 kips	0 kips
L	1	-0.00180	-0.00350	-0.00475	-0.00875	-0.00635
M	3	-0.00135	-0.00225	-0.00240	-0.00495	-0.00415
N	5	-0.00105	-0.00125	-0.00130	-0.00185	-0.00260
O	7	-0.00110	-0.00080	-0.00070	-0.00205	-0.00270
P	9	-0.00090	-0.00070	-0.00040	-0.00195	-0.00235
Q	11	0.00005	0.00100	0.00120	0.08380	0.08315
R	13	-0.00020	0.00260	0.00290	0.08340	0.08300
S	15	0.00040	0.00470	0.00600	0.08535	0.08445
T	17	0.00075	0.00755	0.00905	0.08575	0.08440
U	19	0.00030	0.02035	0.09195	0.17480	0.17360
V	21	0.00060	0.02110	0.08475	0.33290	0.34480

TABLE 5

TOTAL VERTICAL DEFORMATIONS

BEAM 1B

LOCATION	DISTANCE TO LOAD POINT (inches)	DEFORMATIONS (inches) 10 kips	19 kips	25 kips	28 kips	0 kips
A	6	-0.00155	0.00170	0.01690	0.06545	0.09005
B	8	-0.00065	0.00330	0.00850	0.07450	0.08405
C	10	-0.00050	0.00350	0.00430	0.04925	0.05010
D	12	0.00010	0.00590	0.00685	0.08280	0.08325
E	14	-0.00025	0.00025	0.00030	0.01950	0.02330
F	16	-0.00030	0.00120	0.00155	0.00135	0.00090
G	18	-0.00030	-0.00040	-0.00030	-0.00250	-0.00285
H	20	-0.00055	-0.00025	-0.00035	-0.00215	-0.00230
I	22	-0.00040	-0.00035	-0.00065	-0.00170	-0.00205
J	24	-0.00040	-0.00045	-0.00040	-0.00210	-0.00215
K	26	-0.00055	-0.00070	-0.00060	0.00255	-0.00215

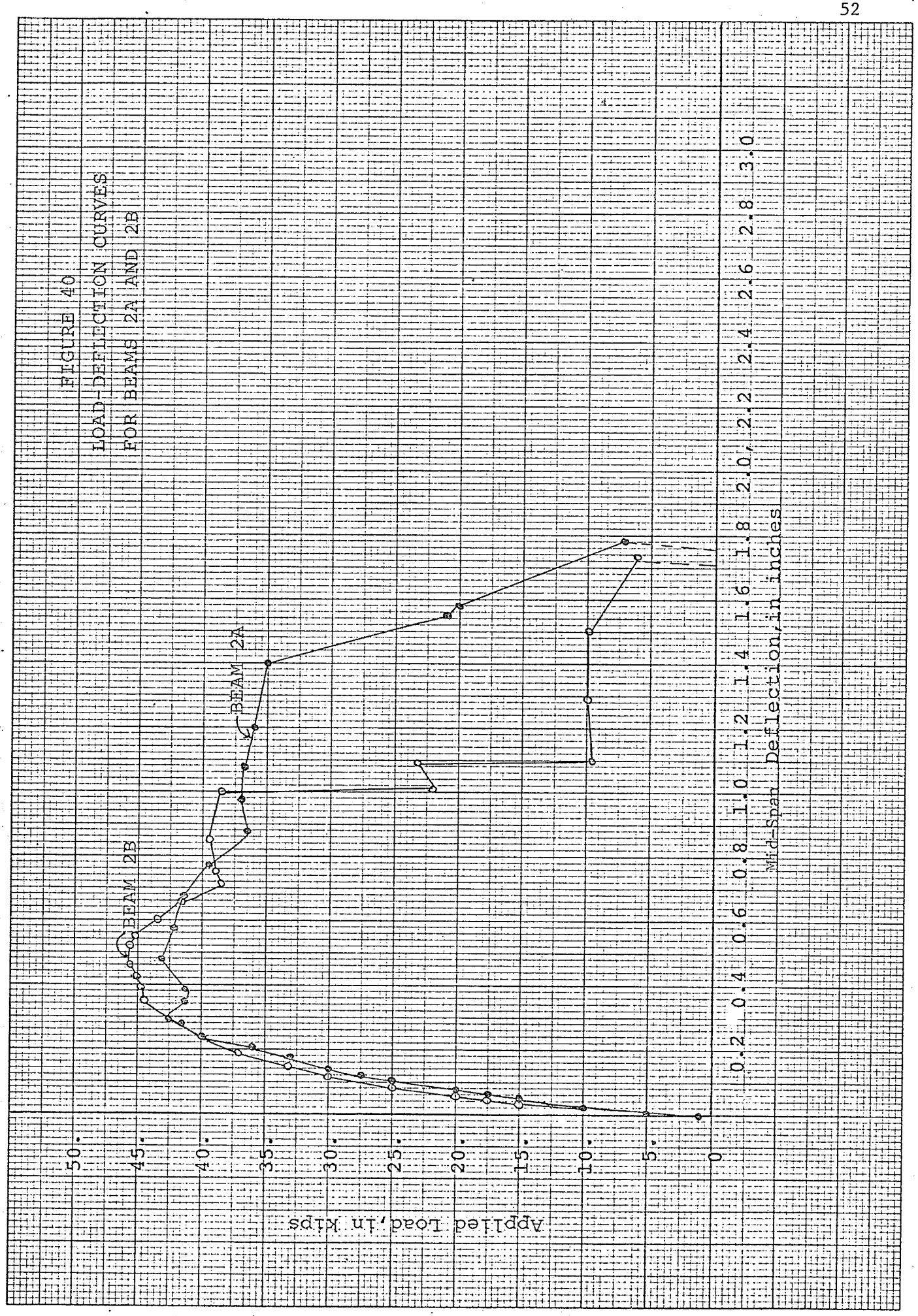

FIGURE 40
LOAD-DEFLECTION CURVES
FOR BEAMS 2A AND 2B

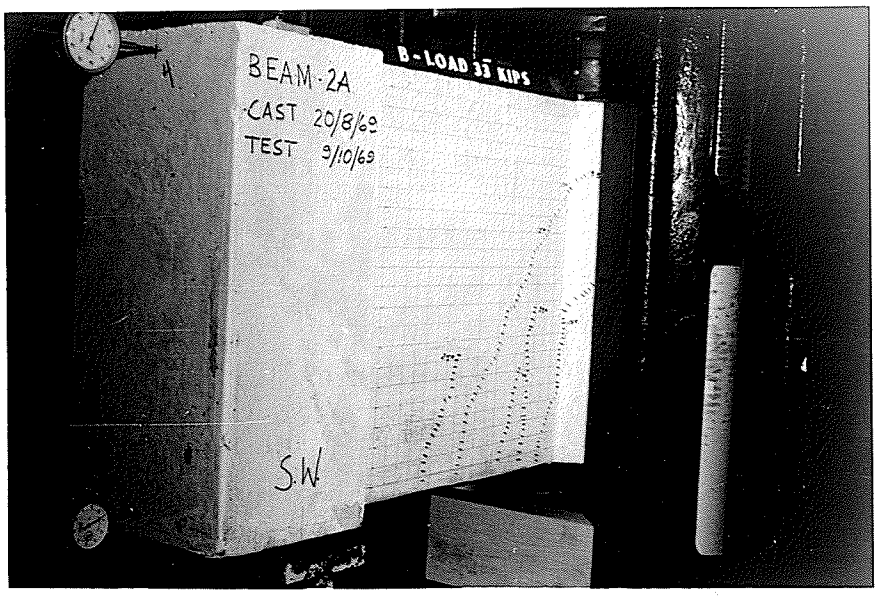

FIGURE 42

LOAD = 33 K.
DEFL. = .174 in.

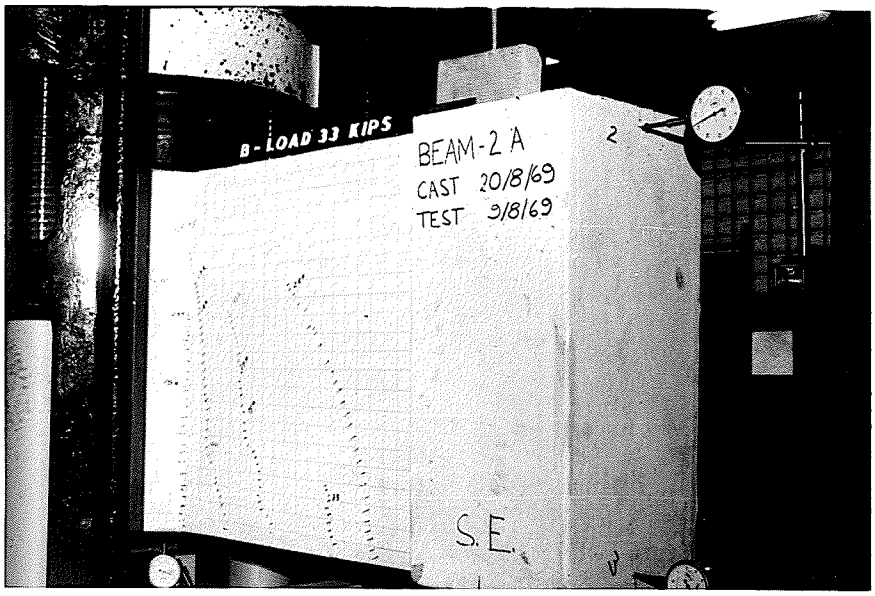

FIGURE 43

LOAD = 33 K.
DEFL. = .174 in.

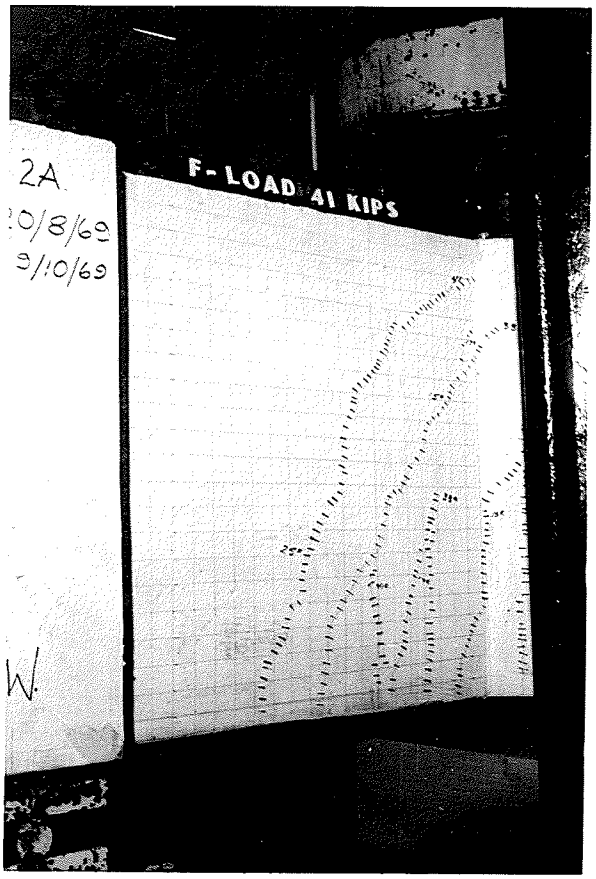

FIGURE 44

LOAD = 41 K.
DEFL. = .270 in.

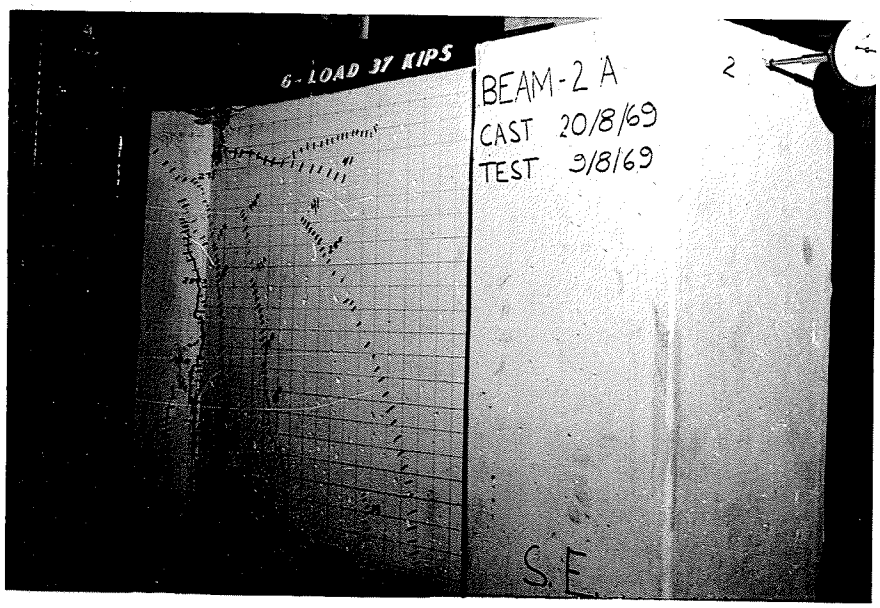

FIGURE 45

LOAD = 37 K.
DEFL. = .977 in.

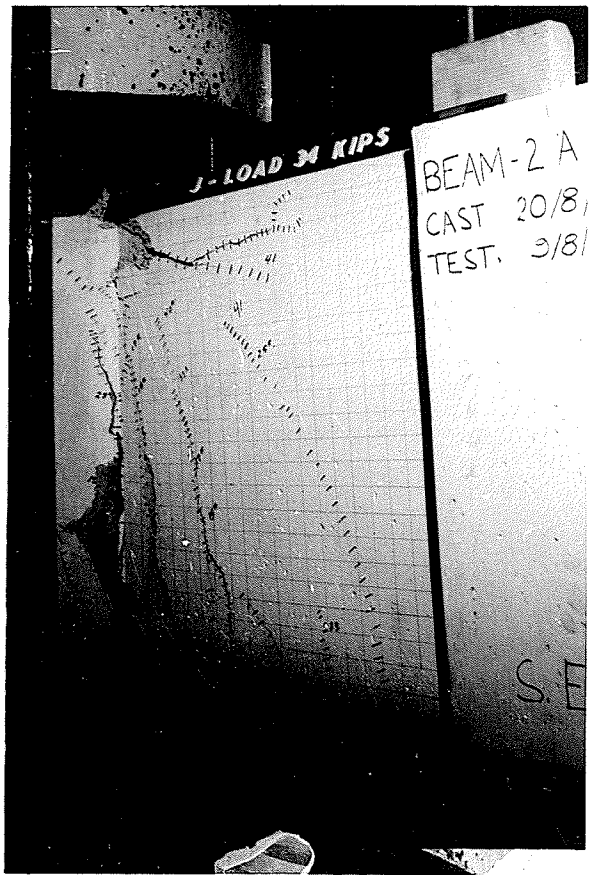

FIGURE 46

LOAD = 34 K.
DEFL. = 1.404 in.

FIGURE 47

CLOSE UP OF FRACTURE

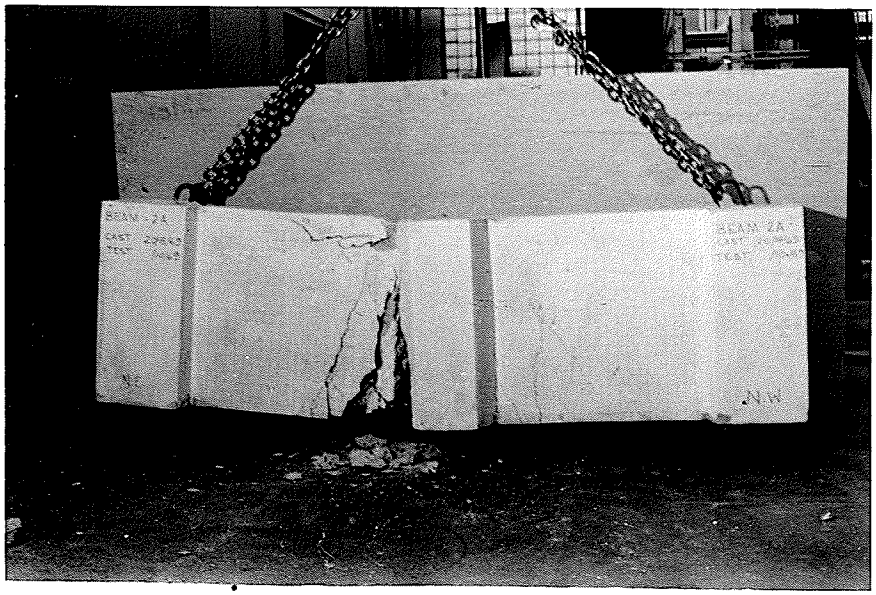

FIGURE 48

FAILURE

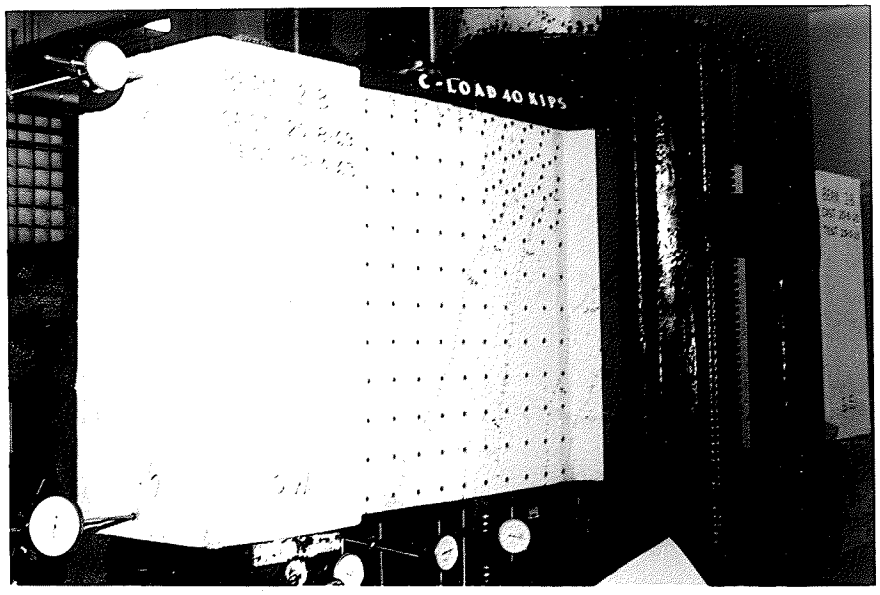

FIGURE 49

LOAD = 40 K.
DEFL. = .240 in.

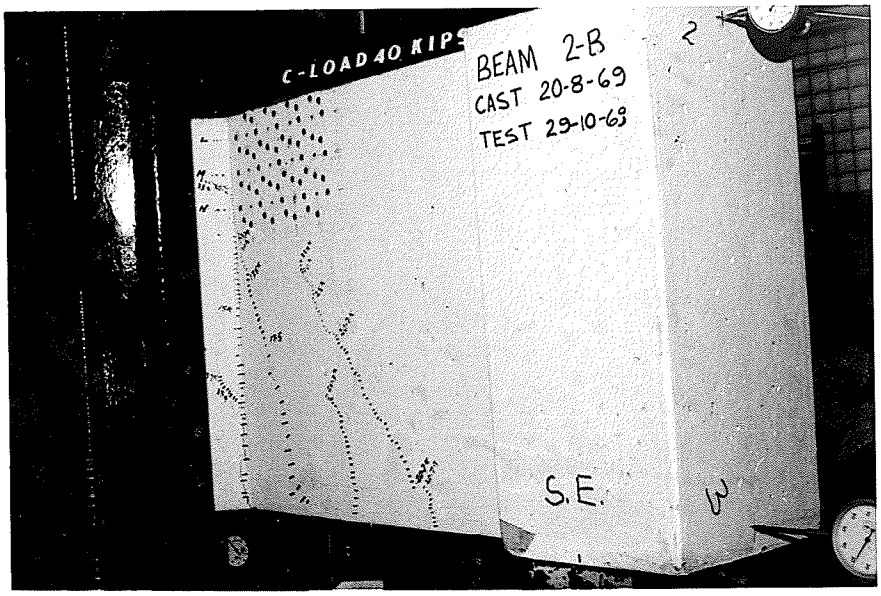

FIGURE 50

LOAD = 40 K.
DEFL. = .240 in.

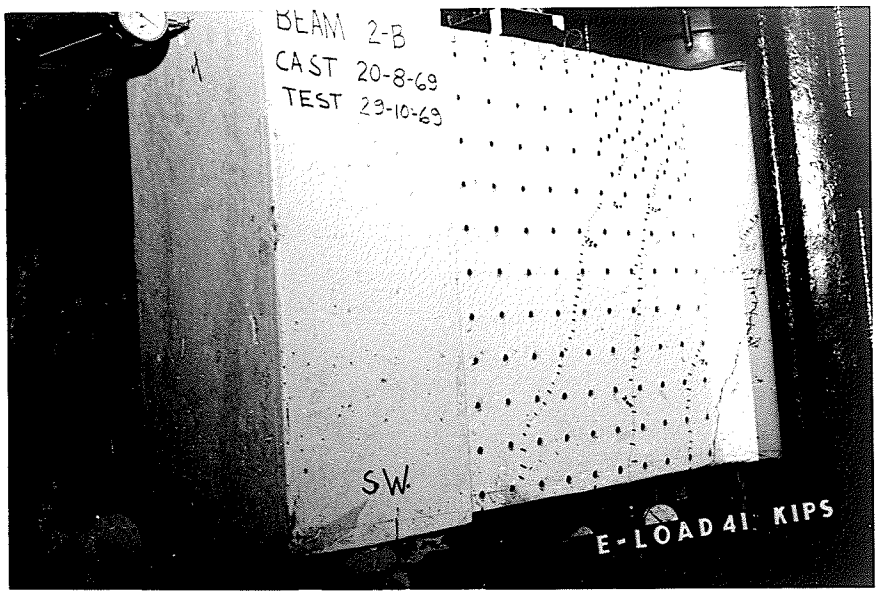

FIGURE 51

LOAD = 41.3 K.
DEFL. = .666 in.

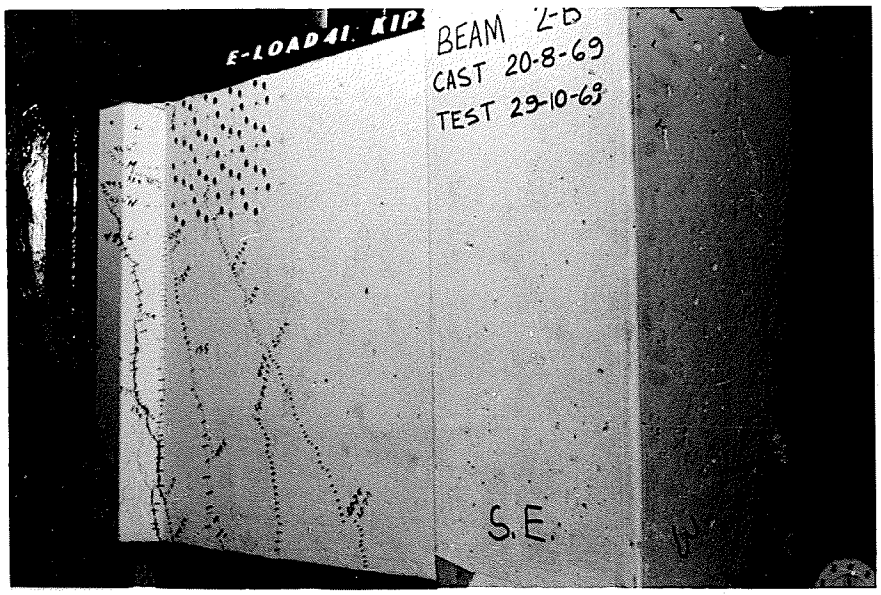

FIGURE 52

LOAD = 41.3 K.
DEFL. = .666 in.

FIGURE 53

DEMEC GUAGES
LOAD = 41.3 K.
DEFL. = .666in.

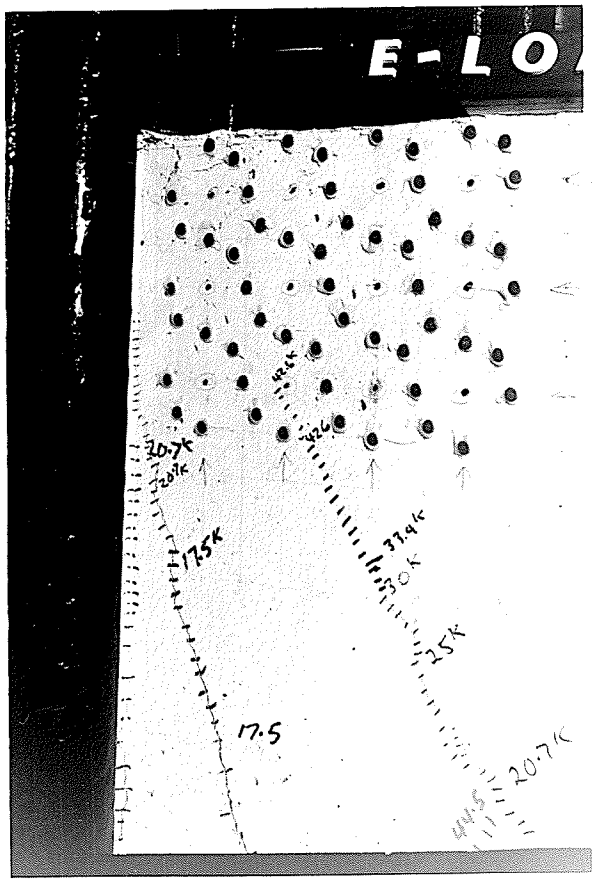

FIGURE 54

DEMEC GUAGES
LOAD = 41.3 K.
DEFL. = .666 in.

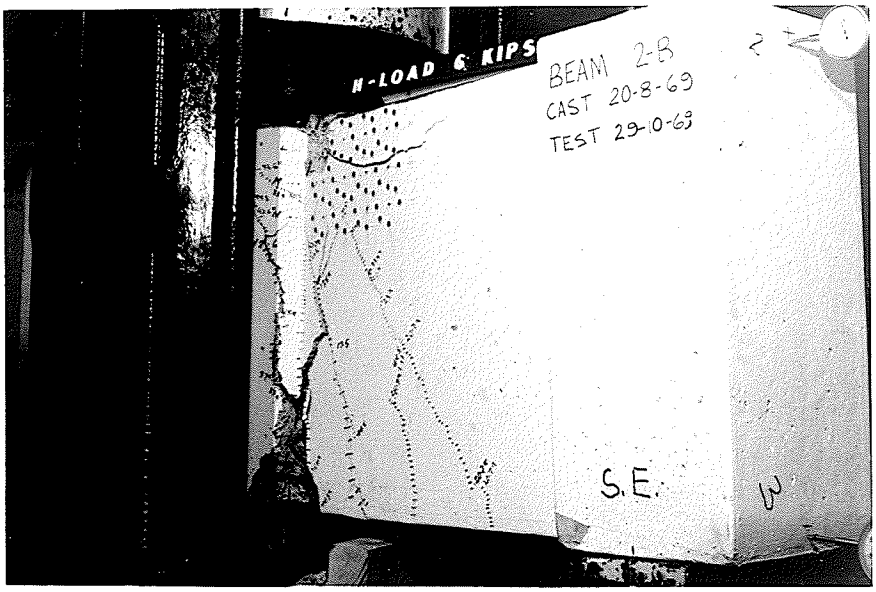

FIGURE 55

LOAD = 6 K.
DEFL. = 1.745 in.

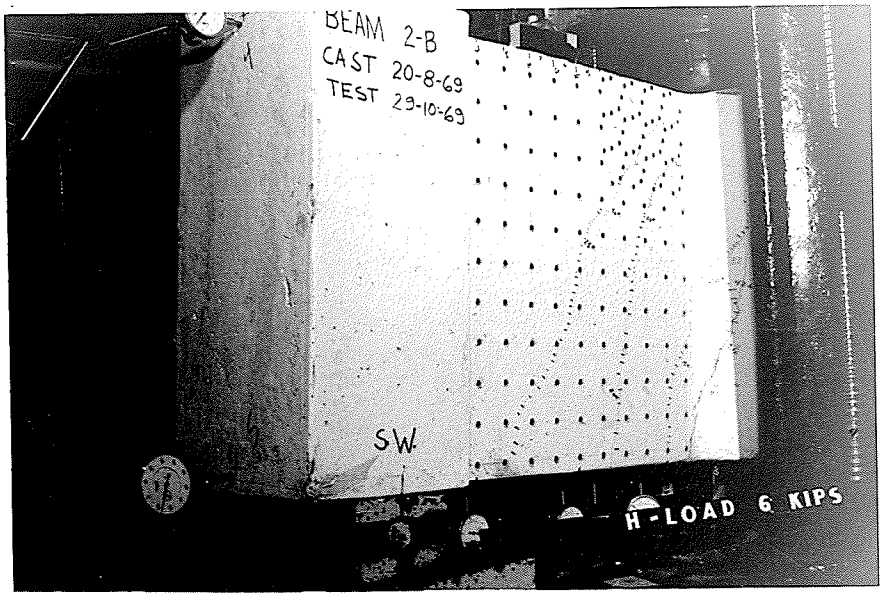

FIGURE 56

LOAD = 6 K.
DEFL. = 1.745 in.

FIGURE 57

FRACTURED TENSILE BAR

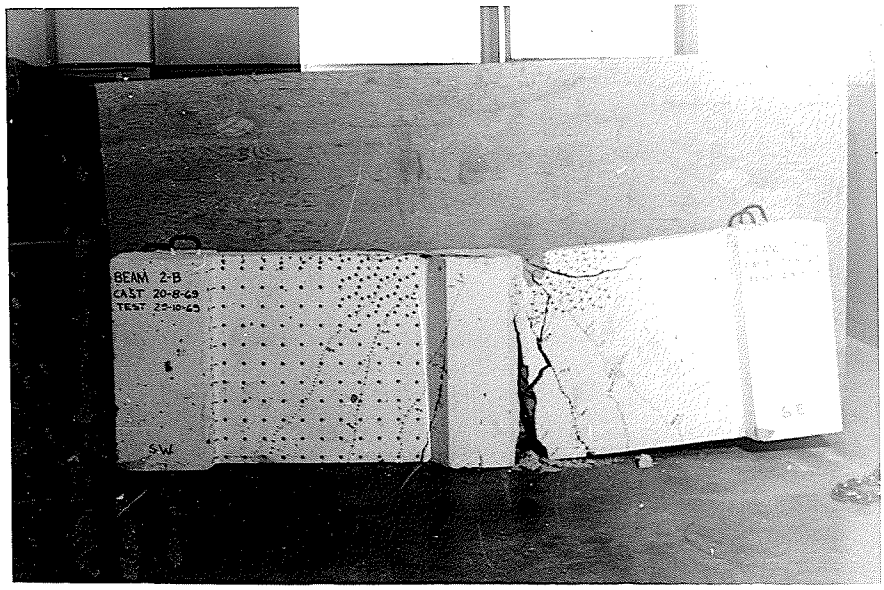

FIGURE 58

FAILURE

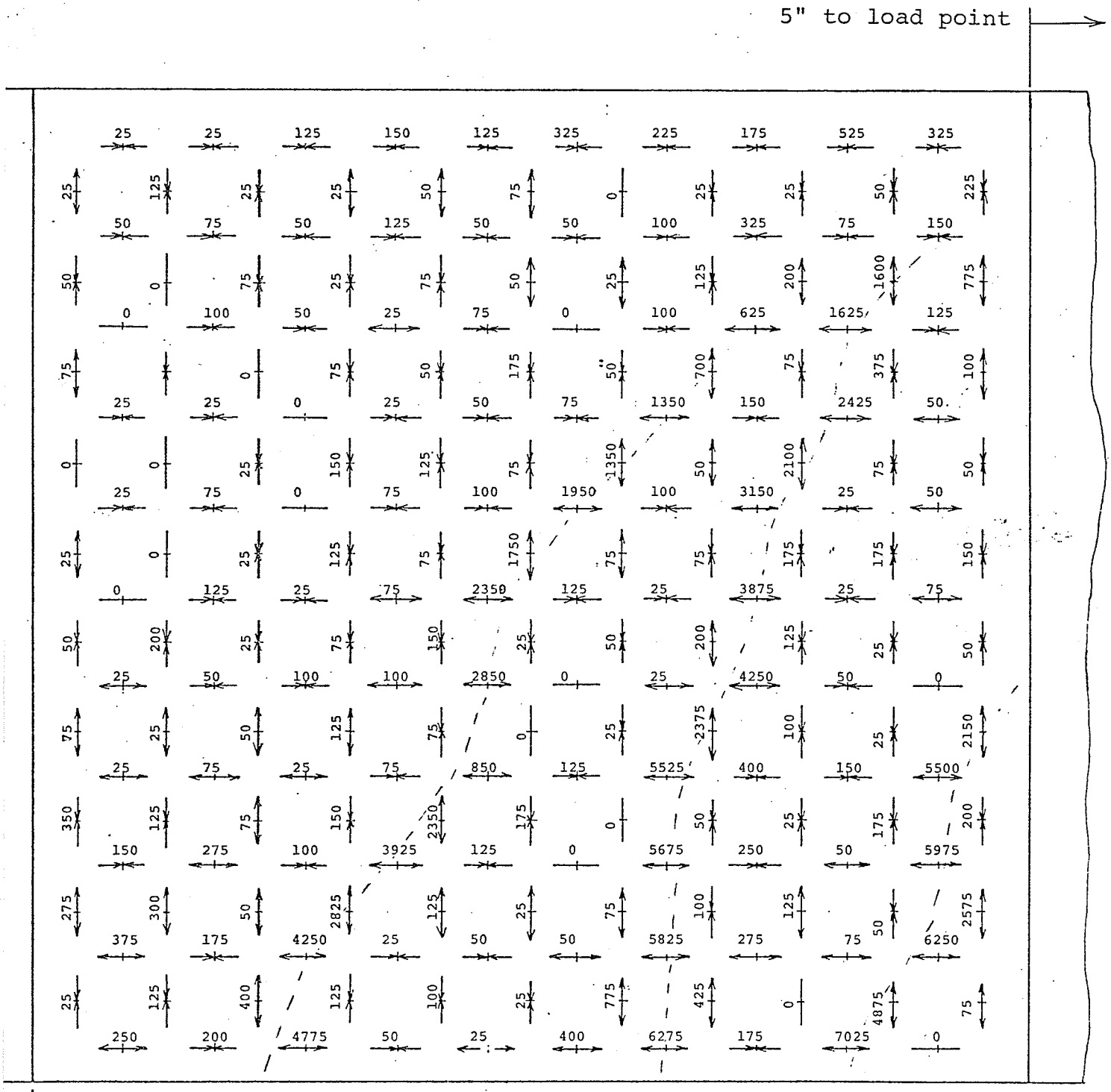

FIGURE 59

AVERAGE STRAINS
(microinches per inch)

BEAM 2B LOAD = 30 kips

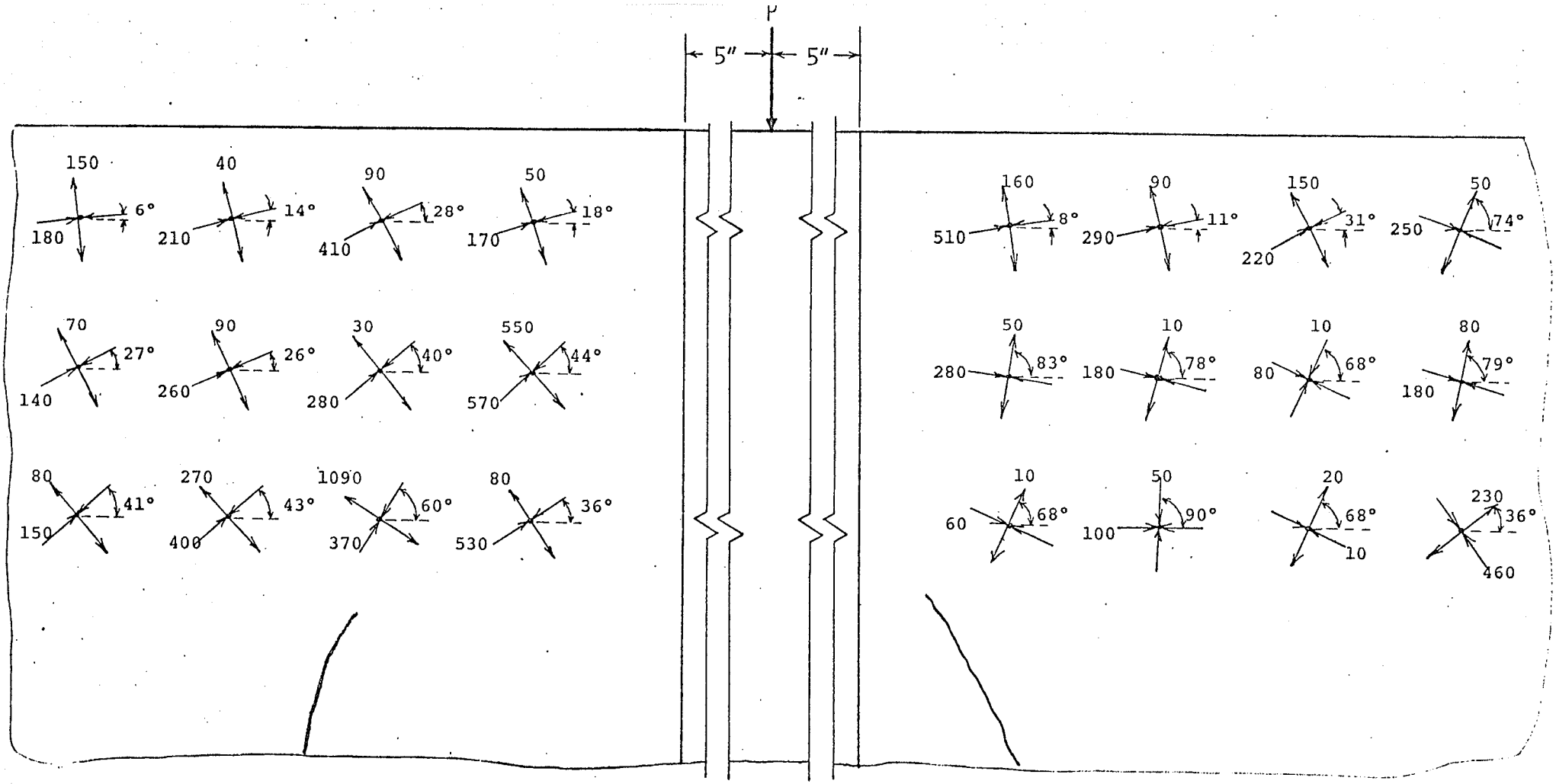

FIGURE 60

PRINCIPAL STRAINS
(microinches per inch)
scale: 1"=2"

BEAM 2B LOAD =20.7 kips

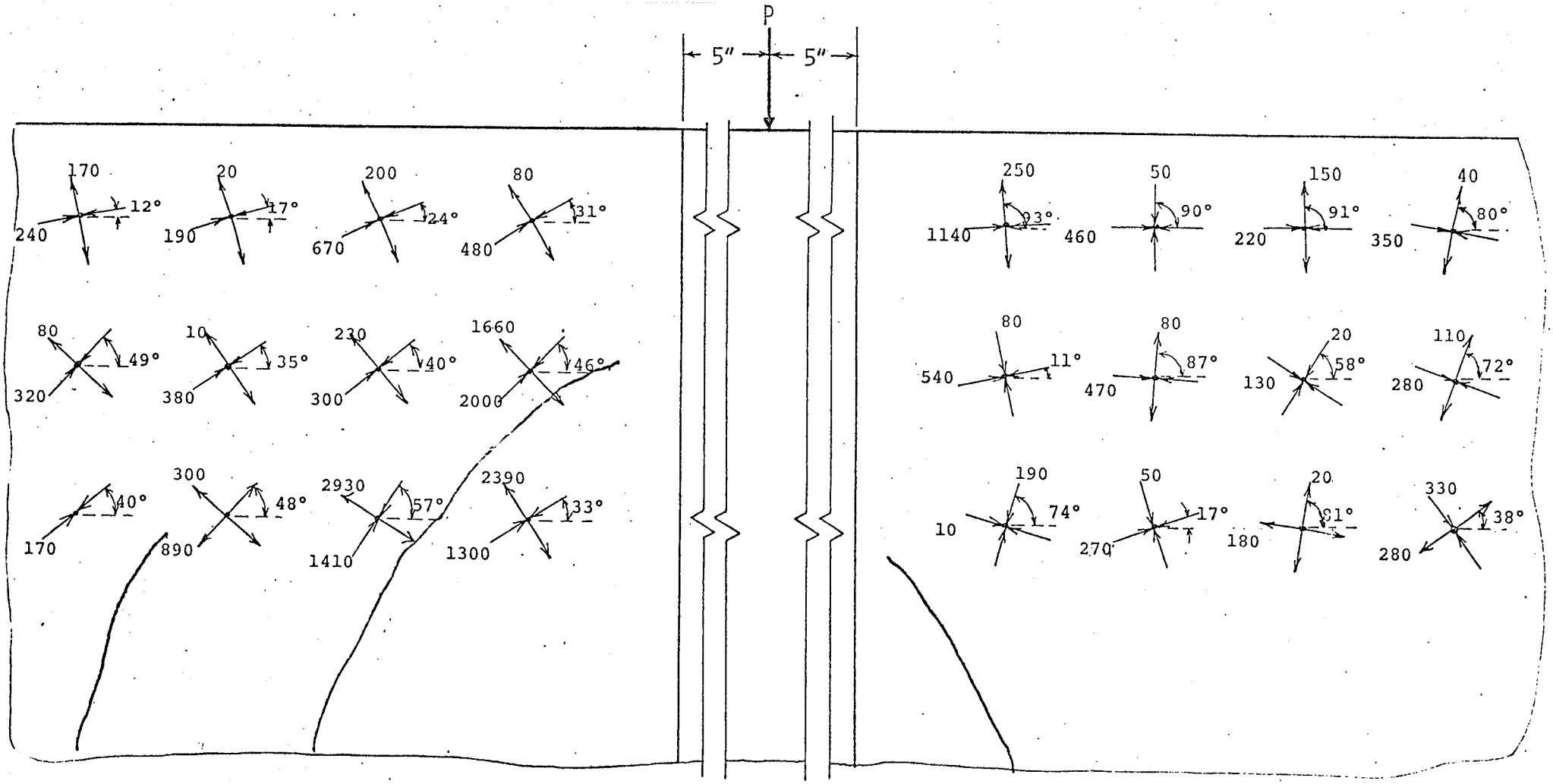

FIGURE 61

PRINCIPAL STRAINS
(microinches per inch)
scale: 1"=2"

BEAM 2B LOAD =30 kips

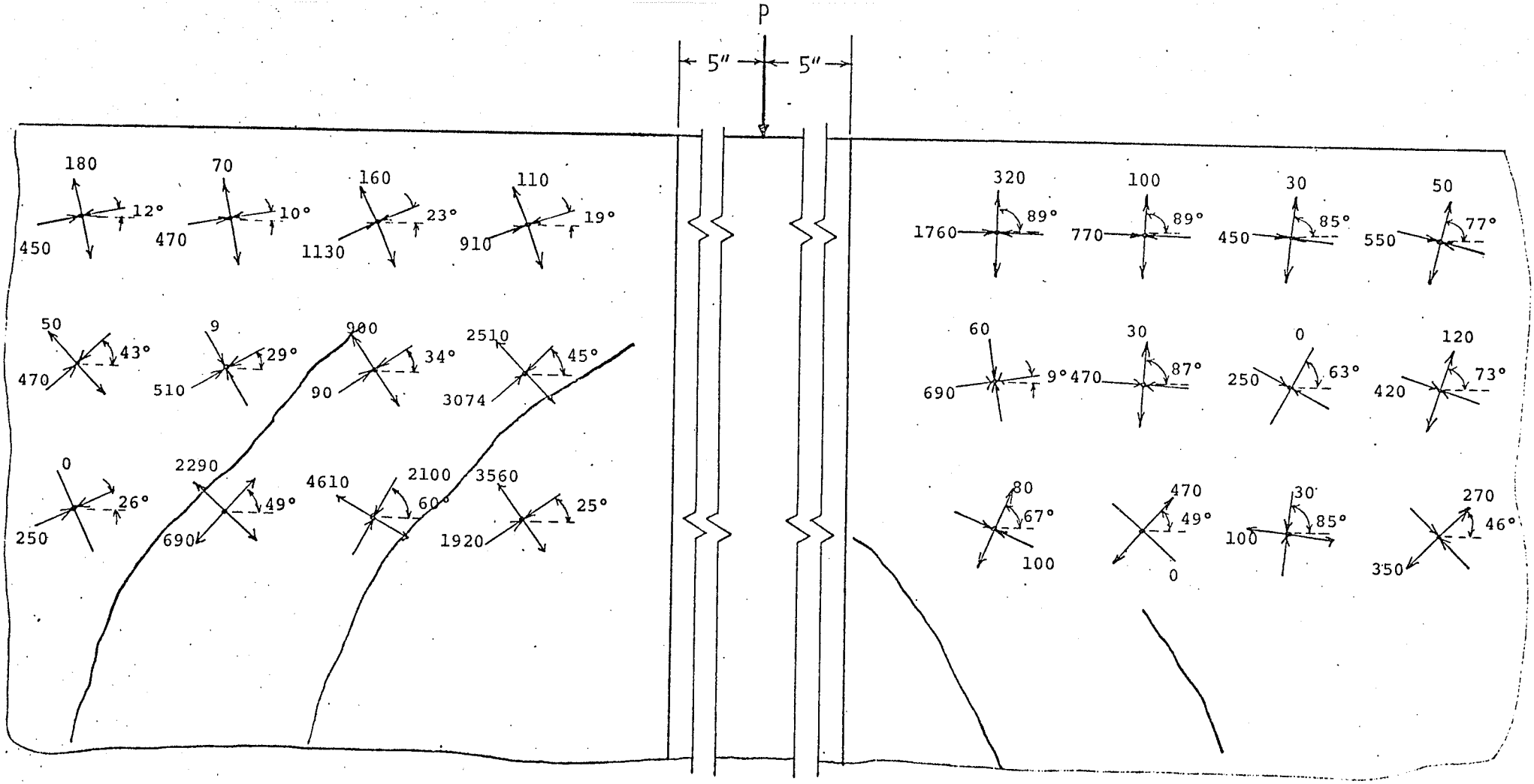

FIGURE 62

PRINCIPAL STRAINS
(microinches per inch)
scale: 1"=2"

BEAM 2B LOAD =40 kips

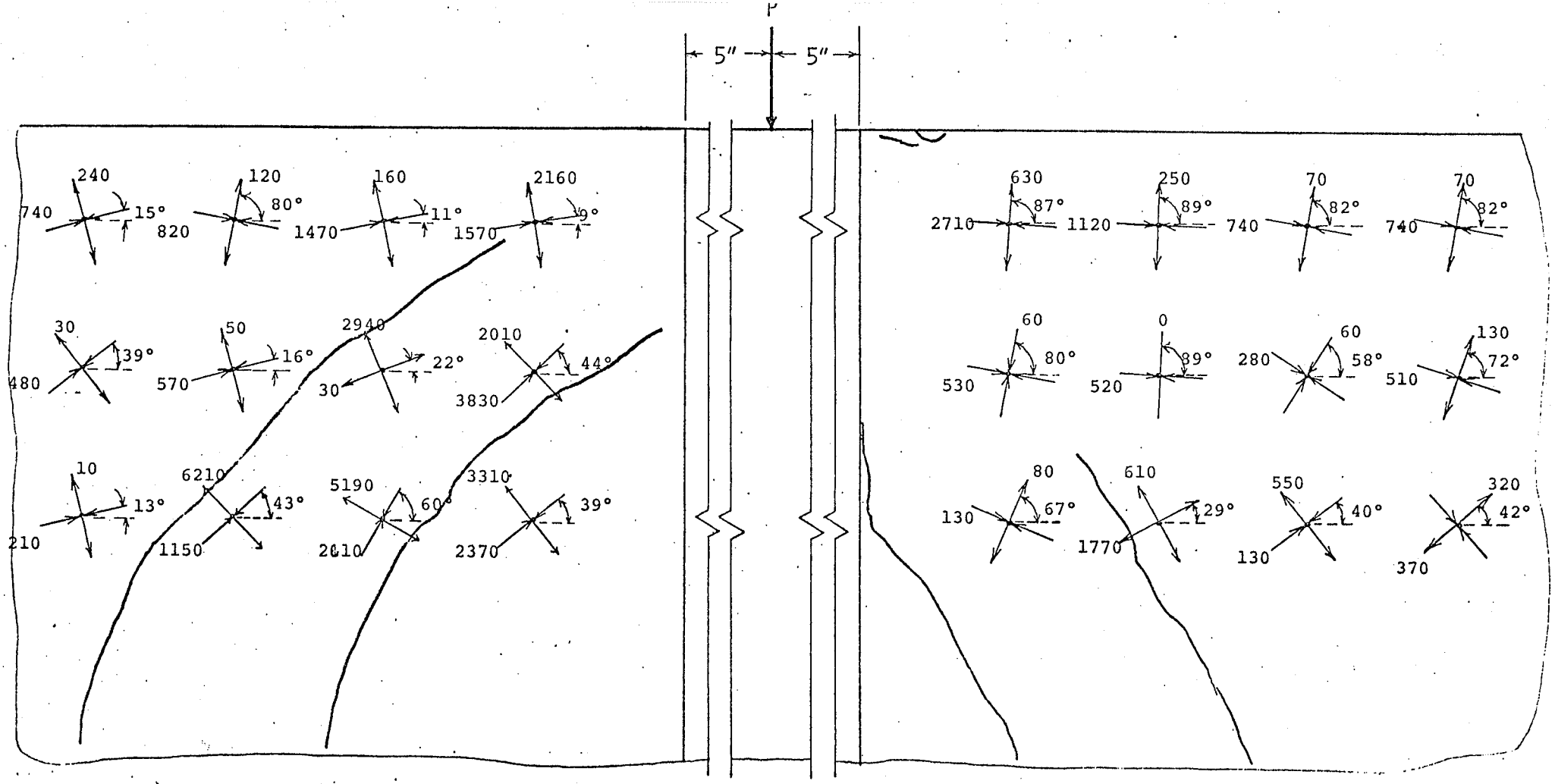

FIGURE 63

PRINCIPAL STRAINS
(microinches per inch)
scale: 1"=2"

BEAM 2B LOAD =45.6 kips

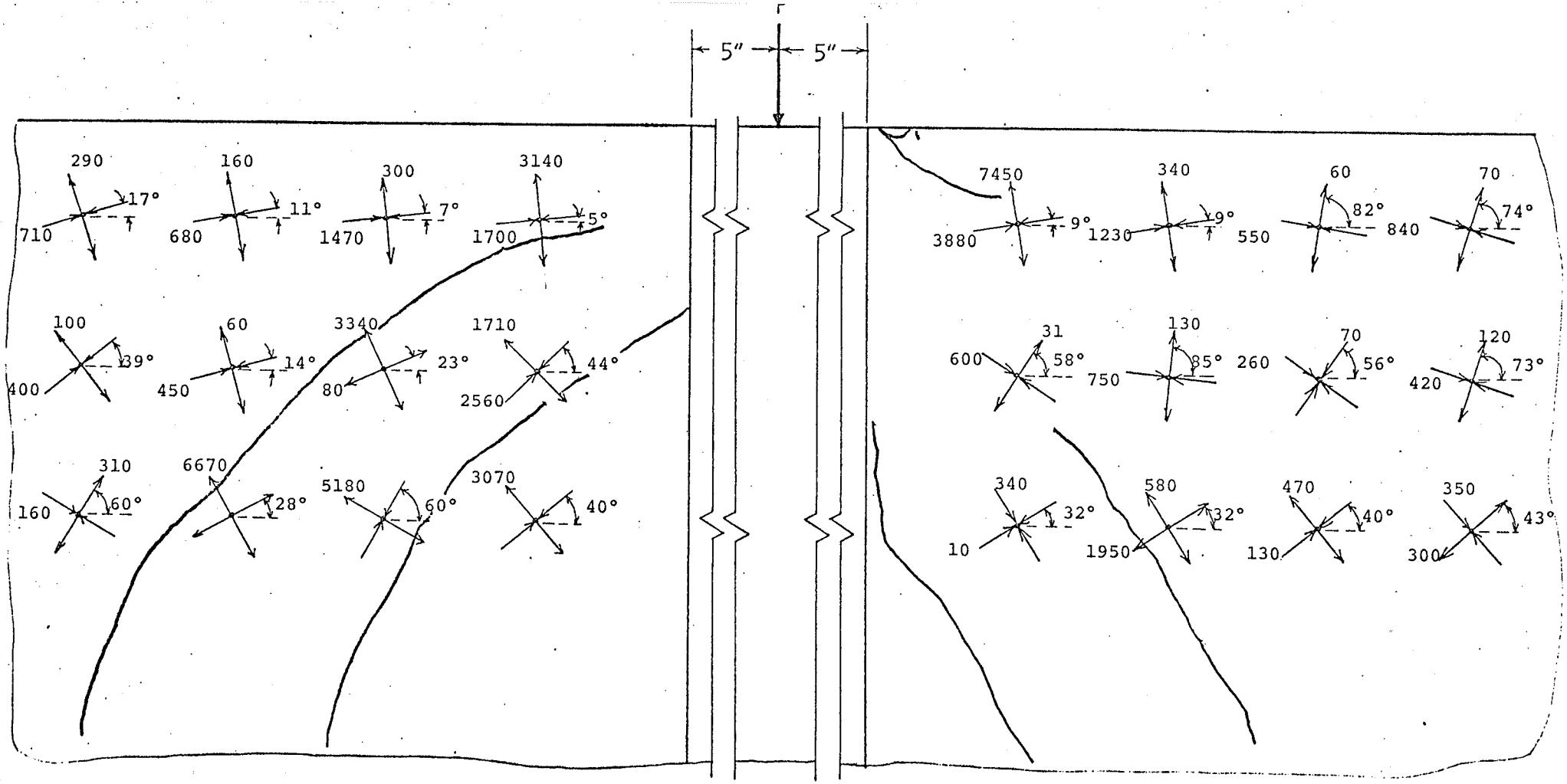

FIGURE 64

PRINCIPAL STRAINS
(microinches per inch)
scale: 1"=2"

BEAM 2B LOAD =41.3 kips
(decreasing)

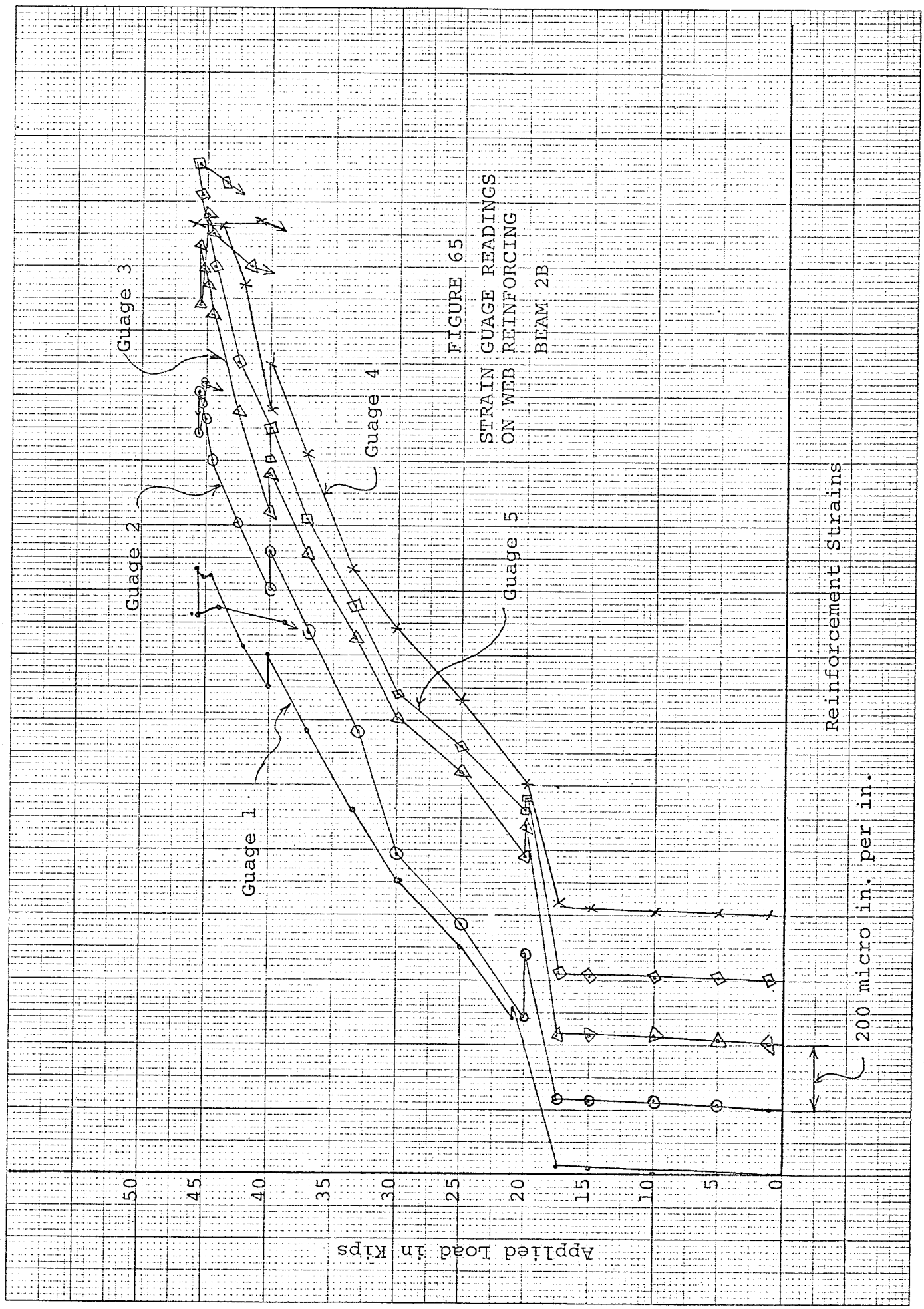

FIGURE 65
STRAIN GUAGE READINGS
ON WEB REINFORCING
BEAM 2B

TABLE 6

TOTAL HORIZONTAL DEFORMATIONS

BEAM 2B

LOCATION	DISTANCE TO PANEL TOP (inches)	DEFORMATIONS (inches) 30 kips
L	1	-0.00405
M	3	-0.00210
N	5	0.00365
O	7	0.00695
P	9	0.00950
Q	11	0.01210
R	13	0.01410
S	15	0.02250
T	17	0.03055
U	19	0.03370
V	21	0.03665

TABLE 7

TOTAL VERTICAL DEFORMATIONS

BEAM 2B

LOCATION	DISTANCE TO LOAD POINT (inches)	DEFORMATIONS (inches) 30 kips
A	6	0.01000
B	8	0.01105
C	10	0.00380
D	12	0.00675
E	14	0.00435
F	16	0.00285
G	18	0.00375
H	20	0.00450
I	22	0.00080
J	24	-0.00065
K	26	0.00000

FIGURE 66

LOAD-DEFLECTION CURVES

FOR BEAMS 3A AND 3B

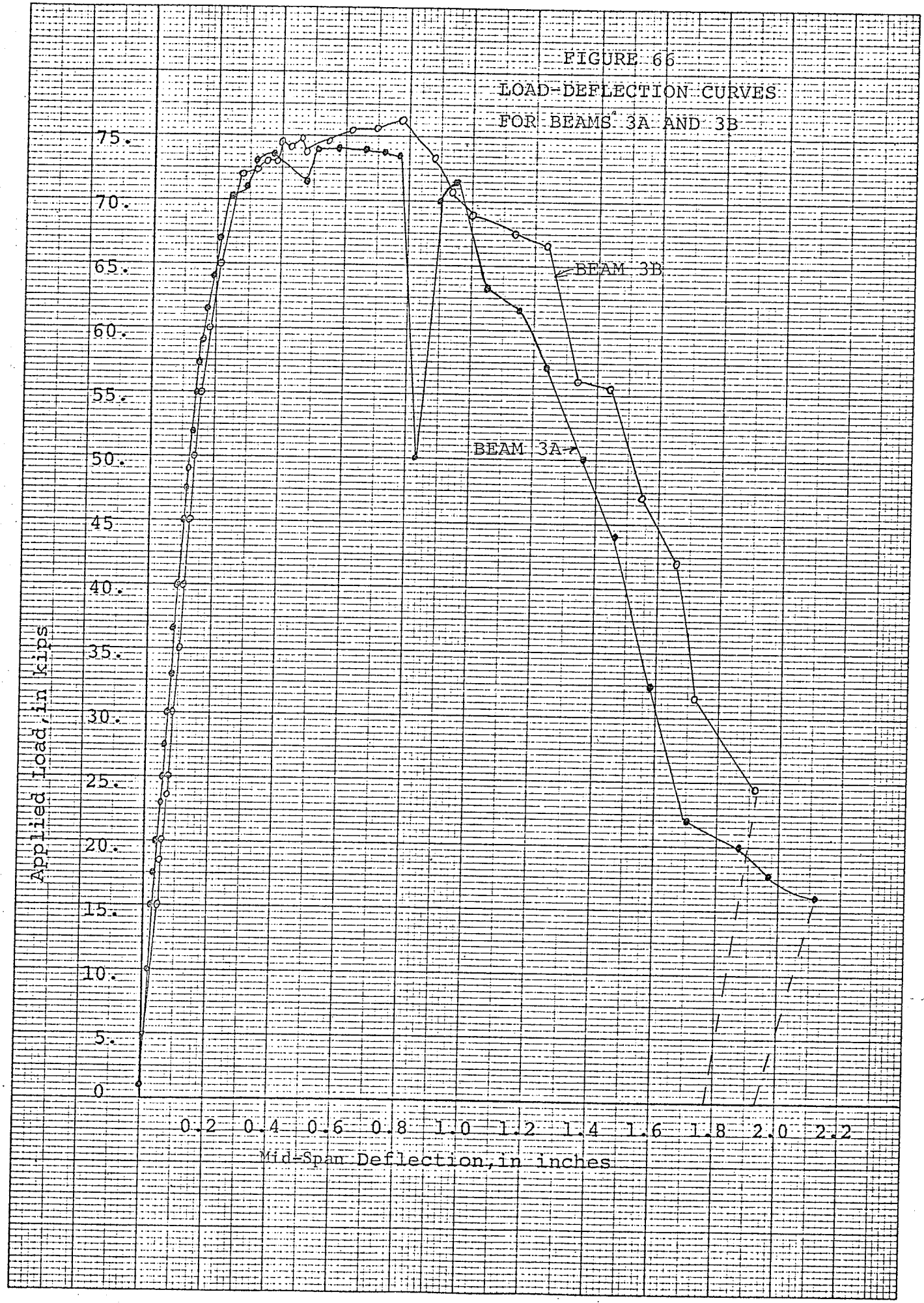

FIGURE 66
MOMENT-ROTATION CURVES
FOR BEAMS 3A AND 3B

Total Moment, in inch-kips

1200
1100
1000
900
800
700
600
500
400
300
200
100
0

.01 .02 .03 .04 .05 .06 .07 .08 .09 .10 .11 .12 .13 .14 .15

Sum of End Rotations, in radians

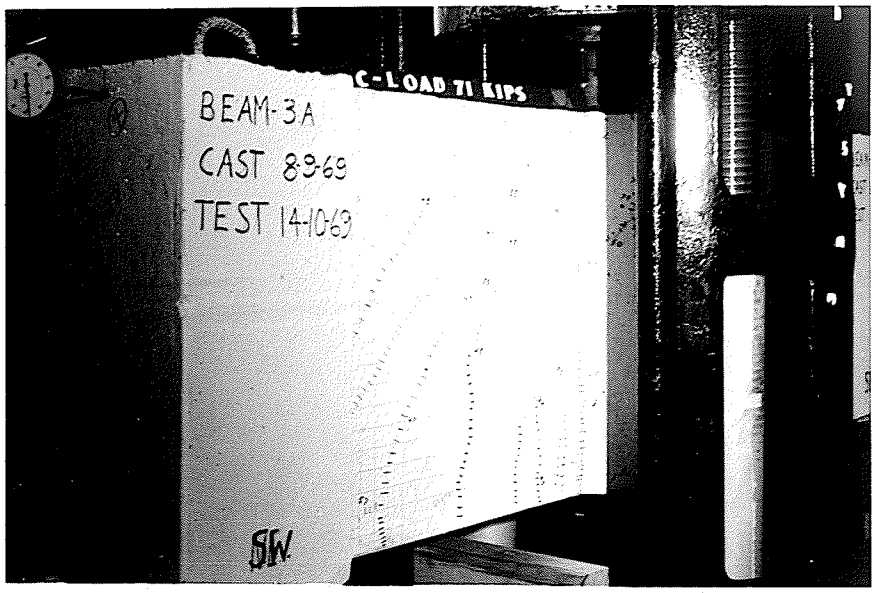

FIGURE 68

LOAD = 71 K.
DEFL. = .298 in.

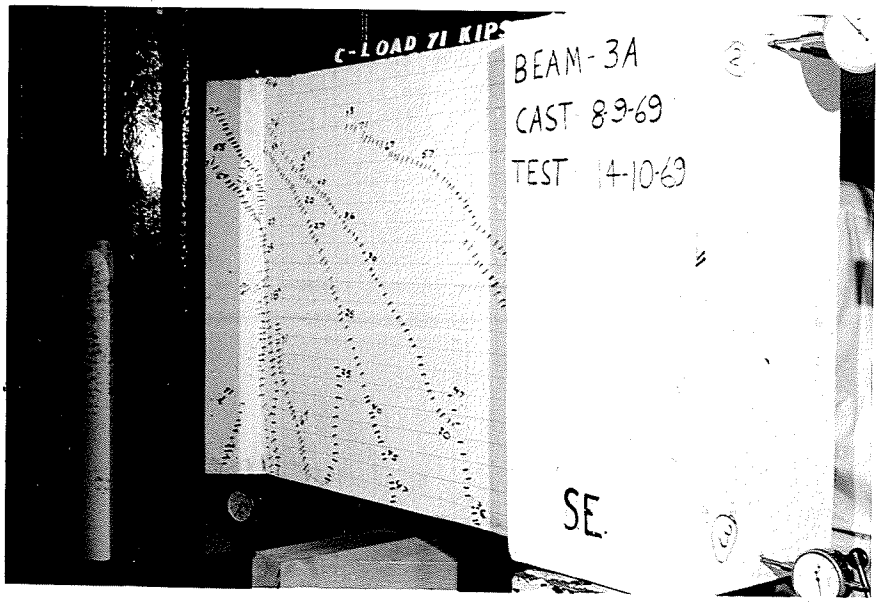

FIGURE 69

LOAD = 71 K.
DEFL. = .298 in.

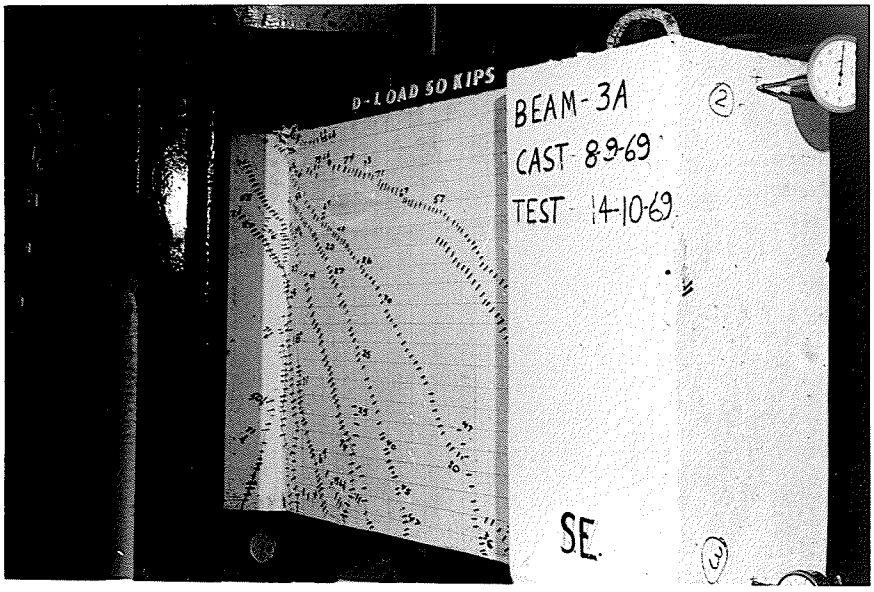

FIGURE 70

LOAD = 50 K.
DEFL. = .832 in.

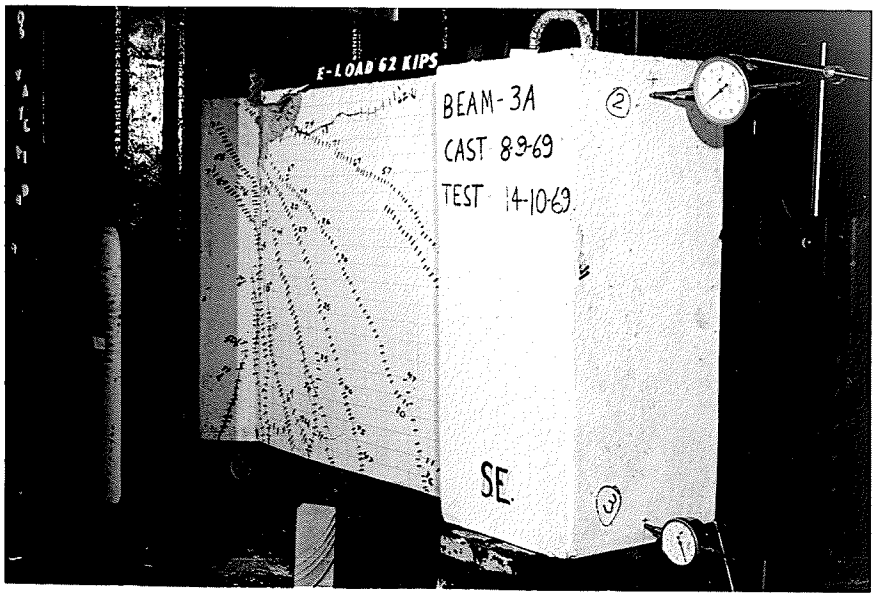

FIGURE 71

LOAD = 62 K.
DEFL. = 1.159 in.

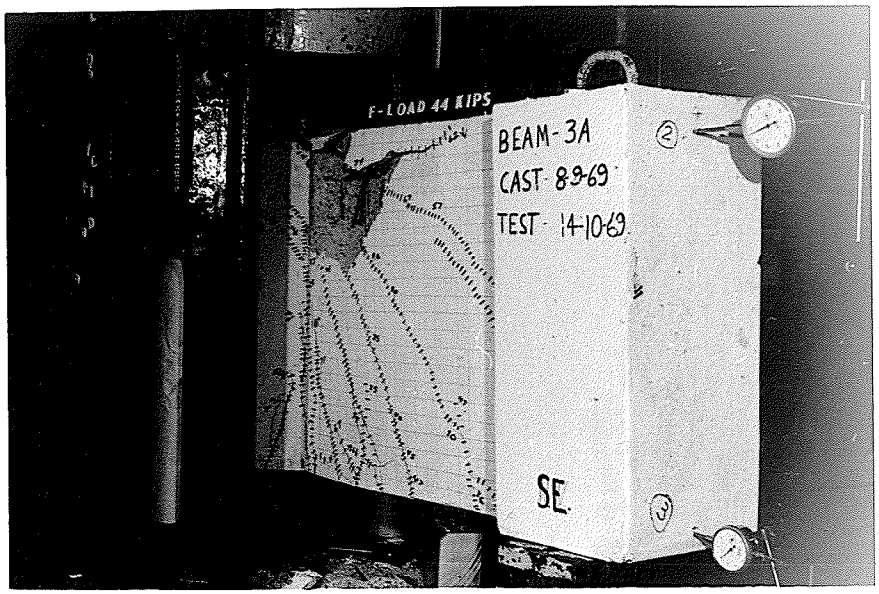

FIGURE 72

LOAD = 44 K.
DEFL. = 1.469 in.

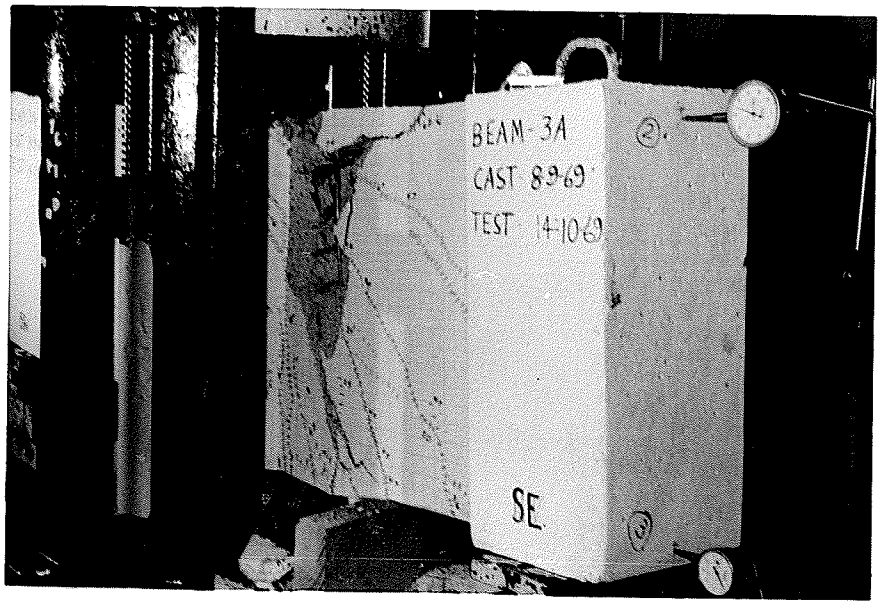

FIGURE 73

FAILURE

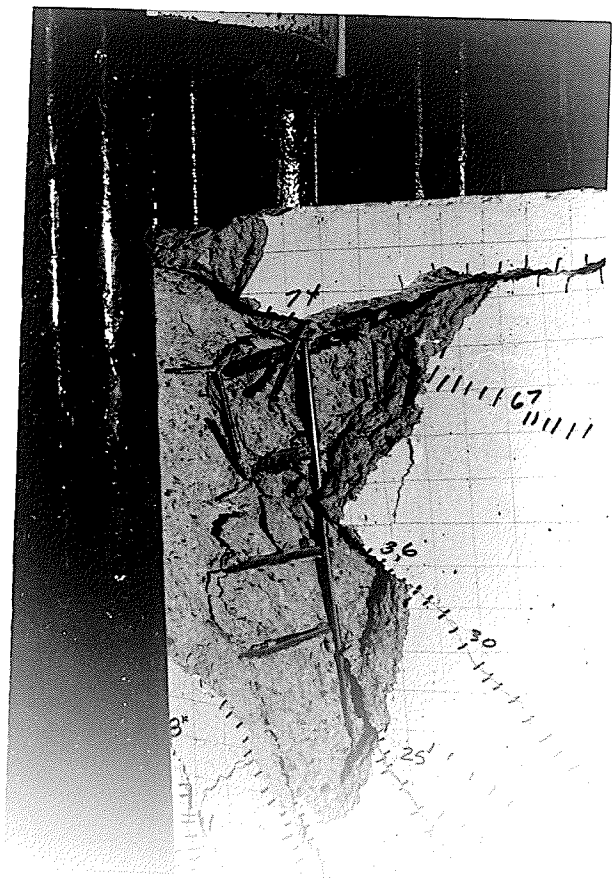

FIGURE 74

CLOSE UP OF BUCKLED COMPRESSIVE BARS

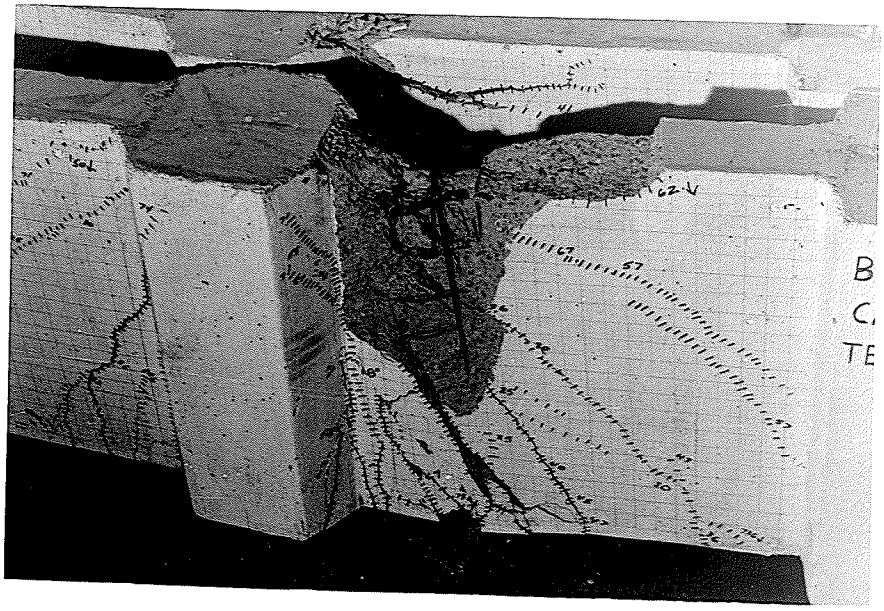

FIGURE 75

BEAM AFTER BROKEN CONCRETE REMOVED

FIGURE 76

FAILURE

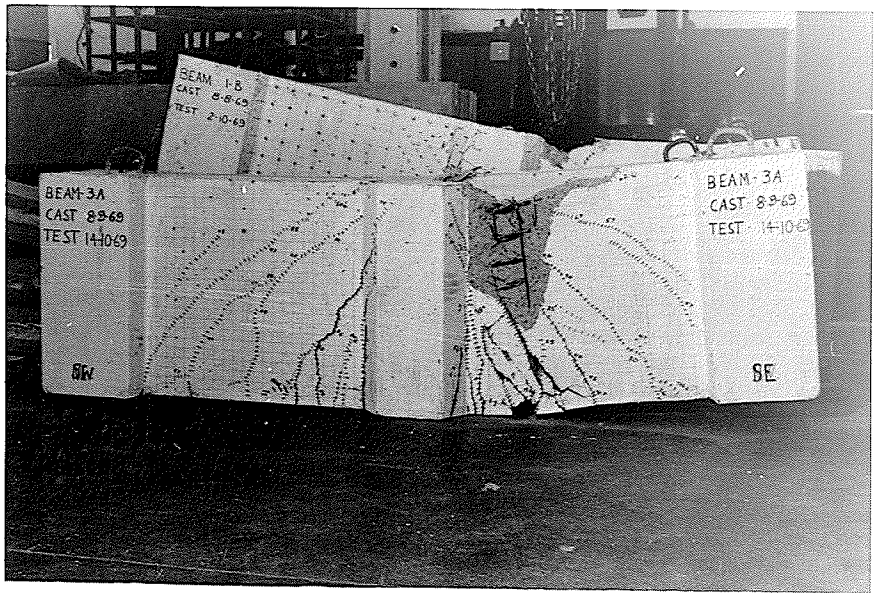

FIGURE 77

FAILURE

FIGURE 78

LOAD = 65 K.
DEFL. = .213 in.

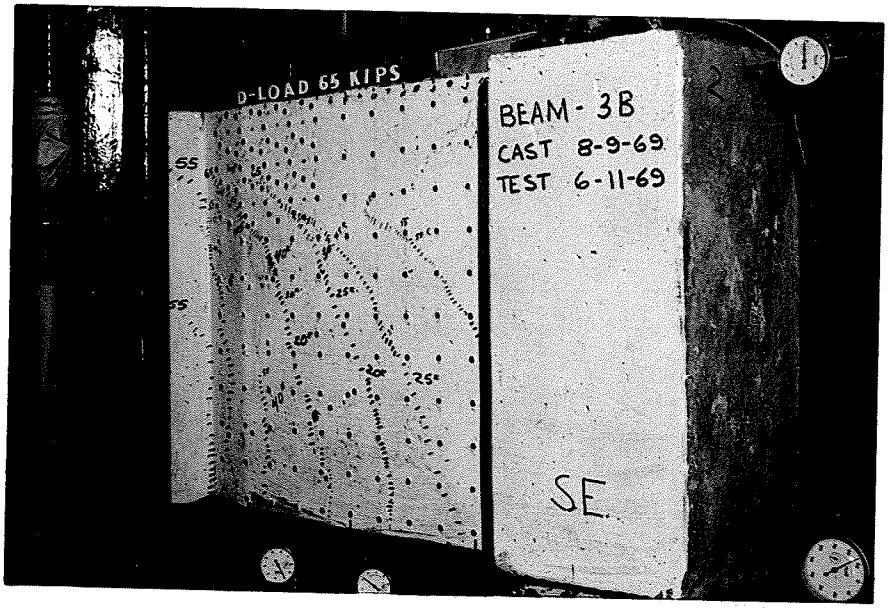

FIGURE 79

LOAD = 65 K.
DEFL. = .213 in.

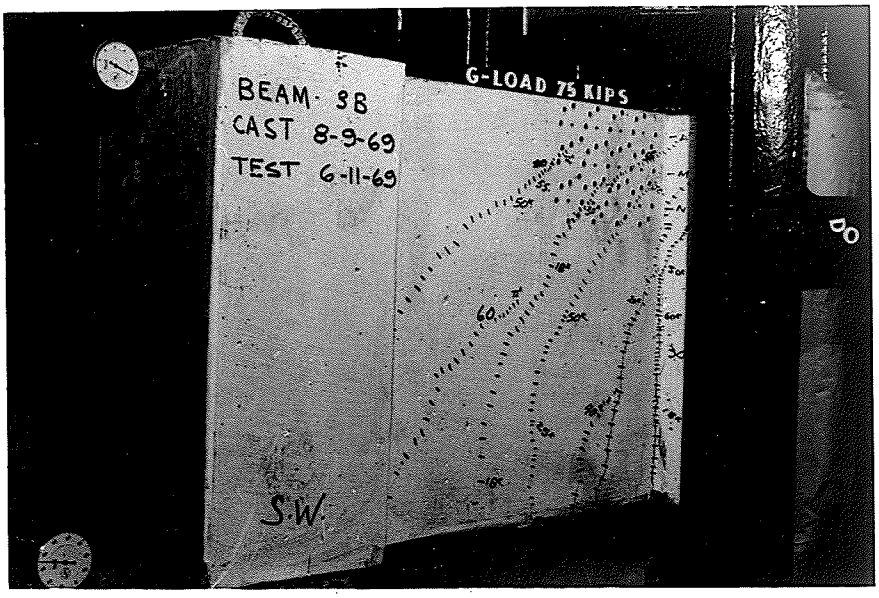

FIGURE 80

LOAD = 75.4 K.
DEFL. = .694 in.

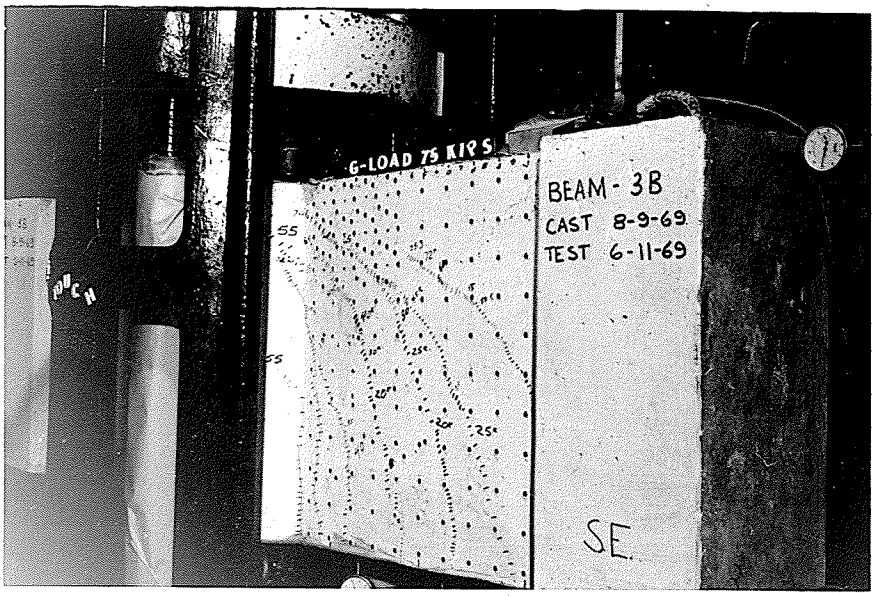

FIGURE 81

LOAD = 75.4 K.
DEFL. = .694 in.

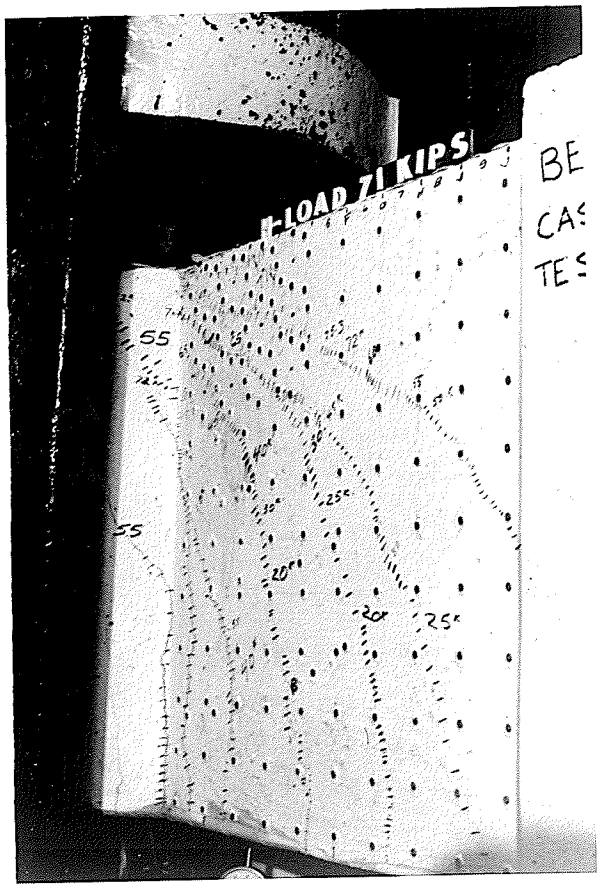

FIGURE 82

LOAD = 71 K.
DEFL. = .941 in.

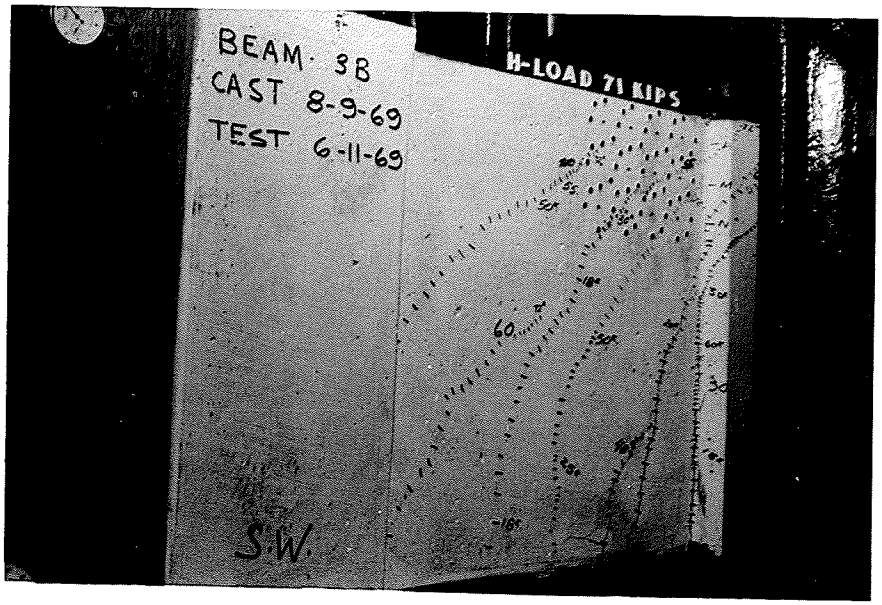

FIGURE 83

LOAD = 71 K.
DEFL. = .941 in.

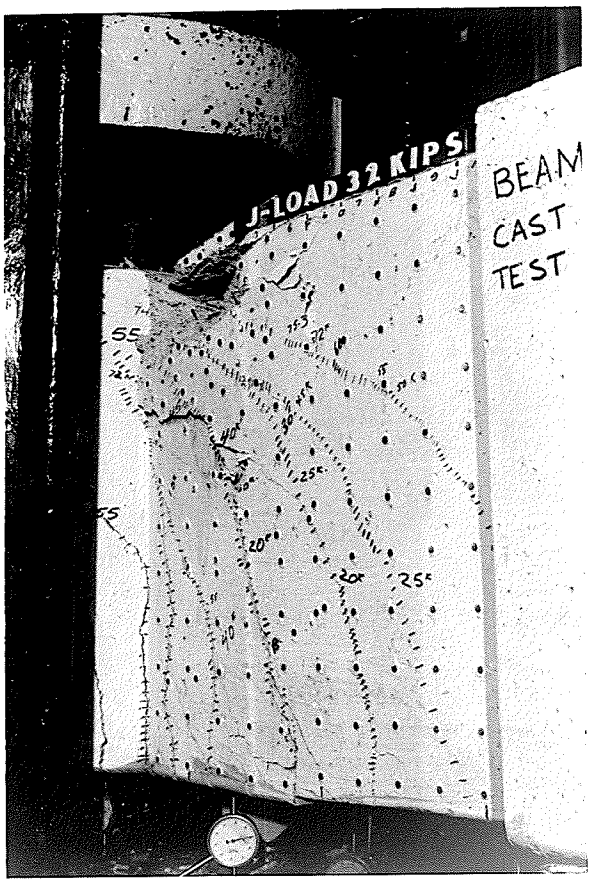

FIGURE 84

LOAD = 32 K.
DEFL. = 1.728 in.

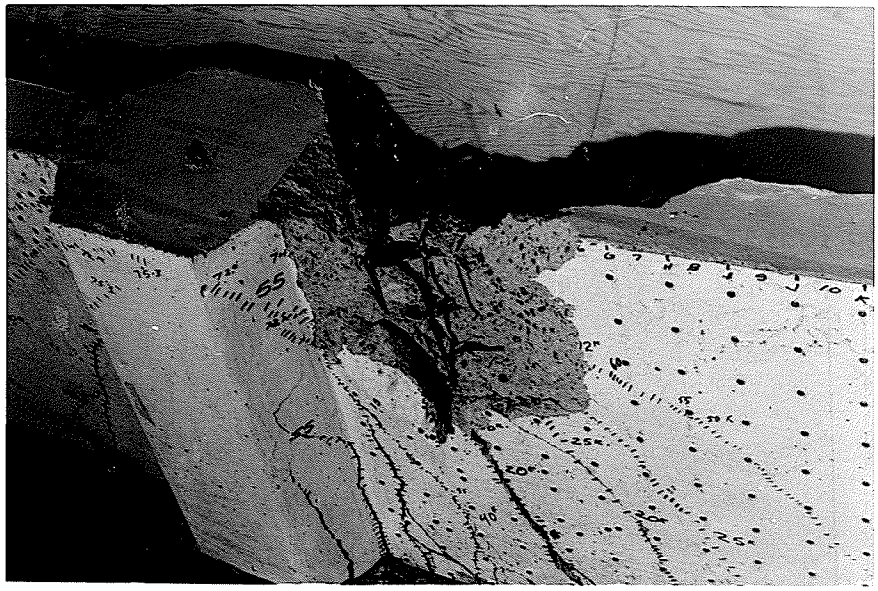

FIGURE 85

CLOSE UP OF BUCKLED COMPRESSIVE BARS

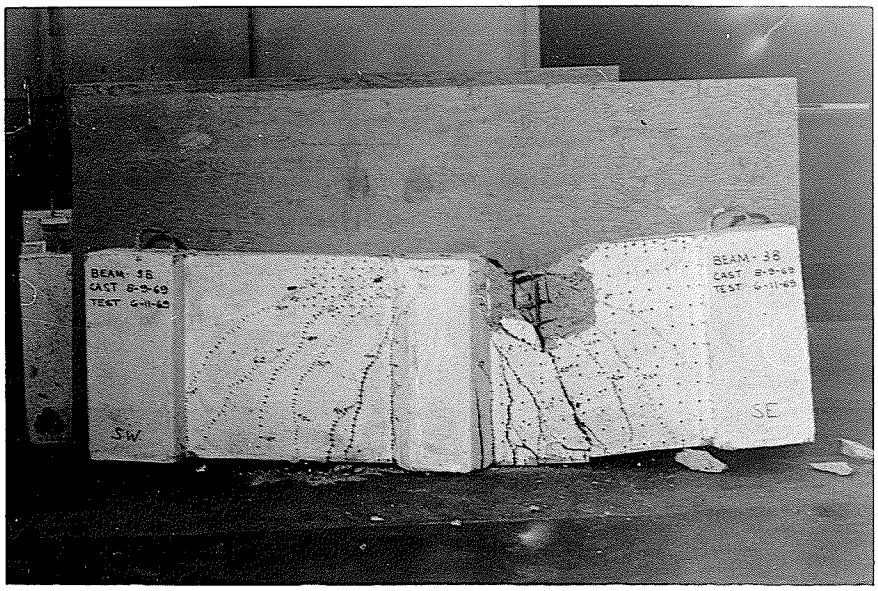

FIGURE 86

FAILURE

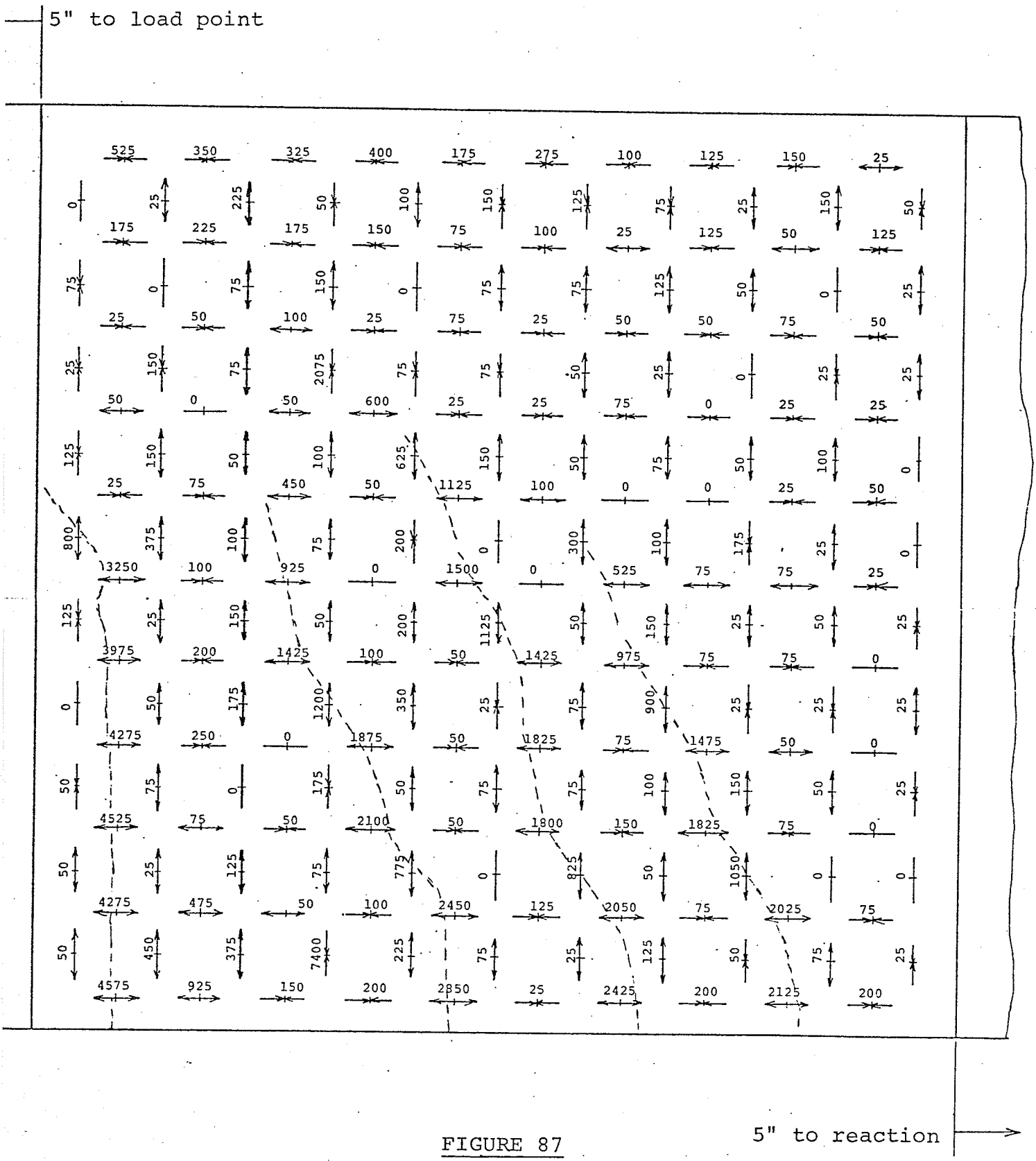

FIGURE 87

AVERAGE STRAINS
(microinches per inch)

BEAM 3B LOAD = 30 kips

5" to load point

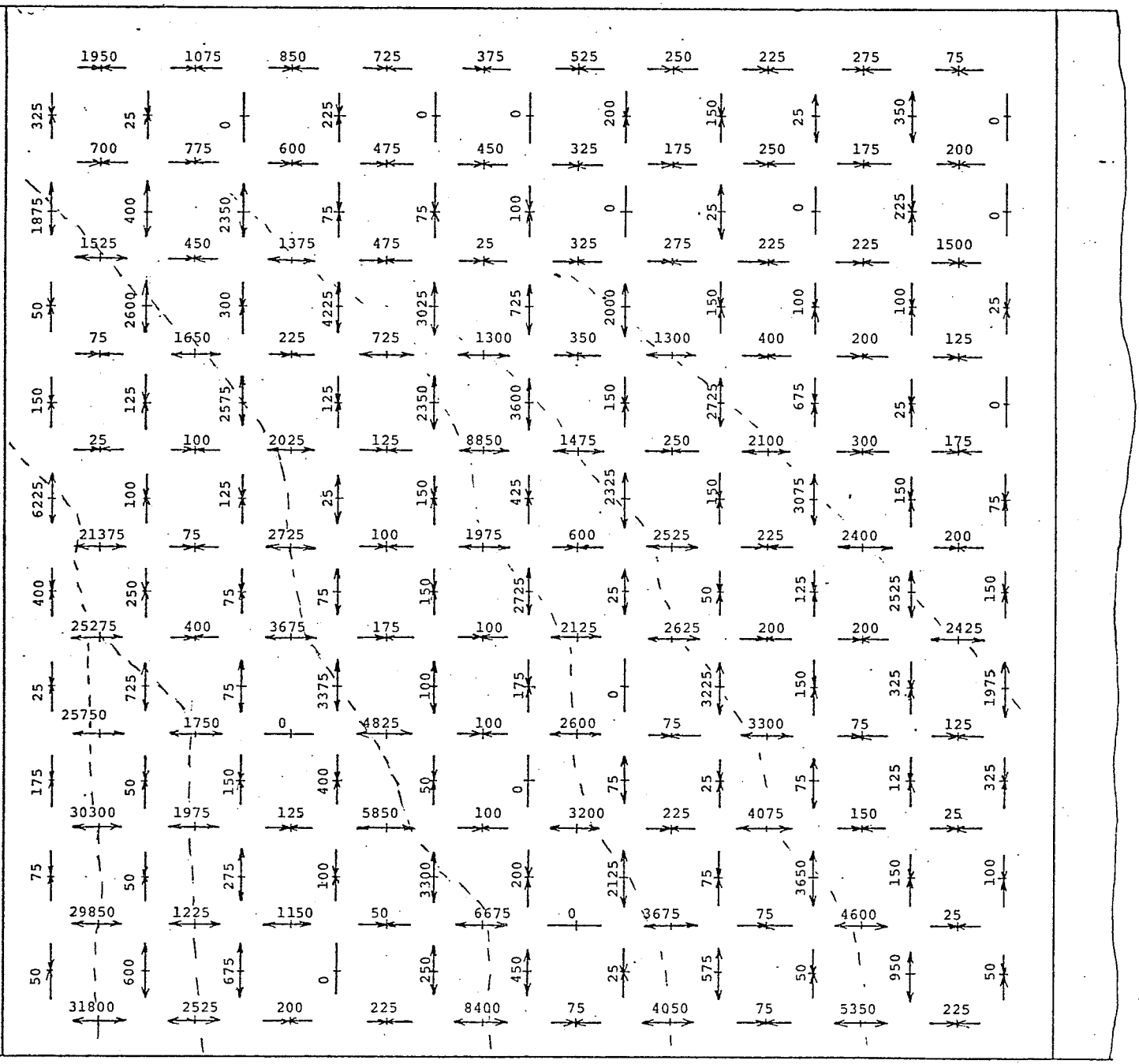

5" to reaction

FIGURE 88

AVERAGE STRAINS
(microinches per inch)
BEAM 3B LOAD = 72 kips

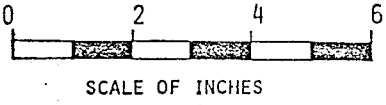

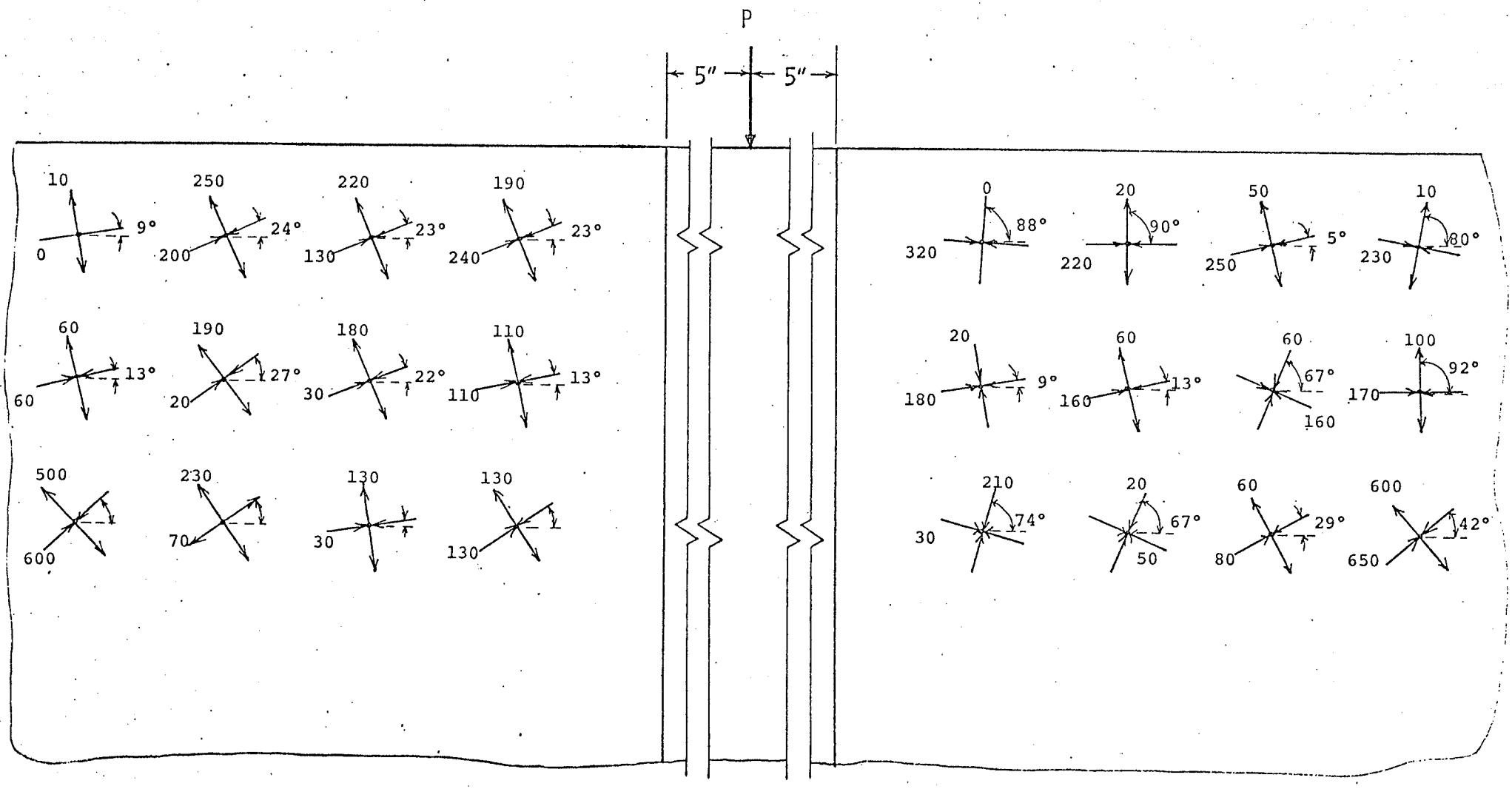

FIGURE 89

PRINCIPAL STRAINS
(microinches per inch)
scale: 1"=2"

BEAM 3B LOAD=20 kips

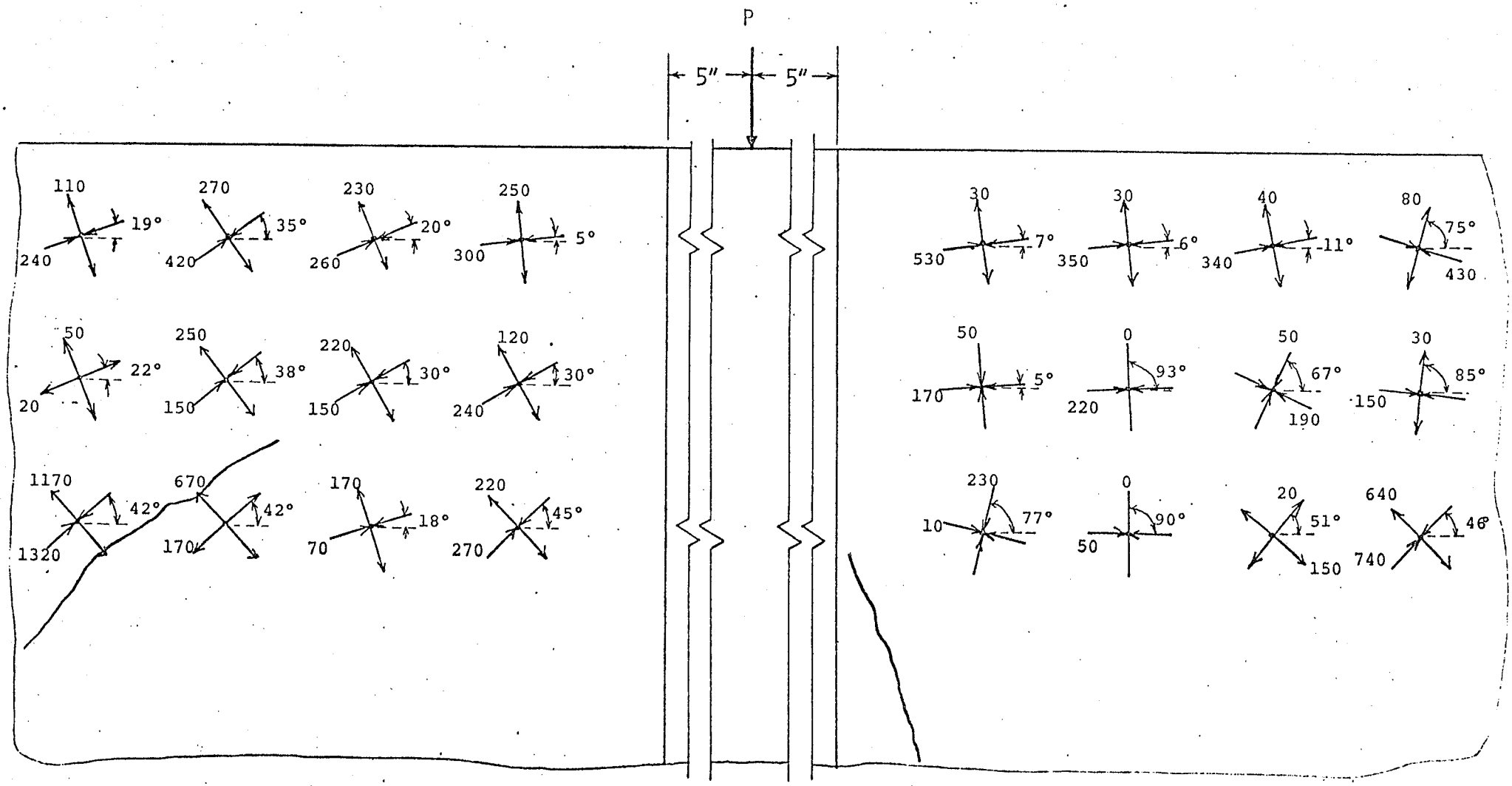

FIGURE 90

PRINCIPAL STRAINS
(microinches per inch)
scale: i"=2"

BEAM 3B LOAD =30 kips

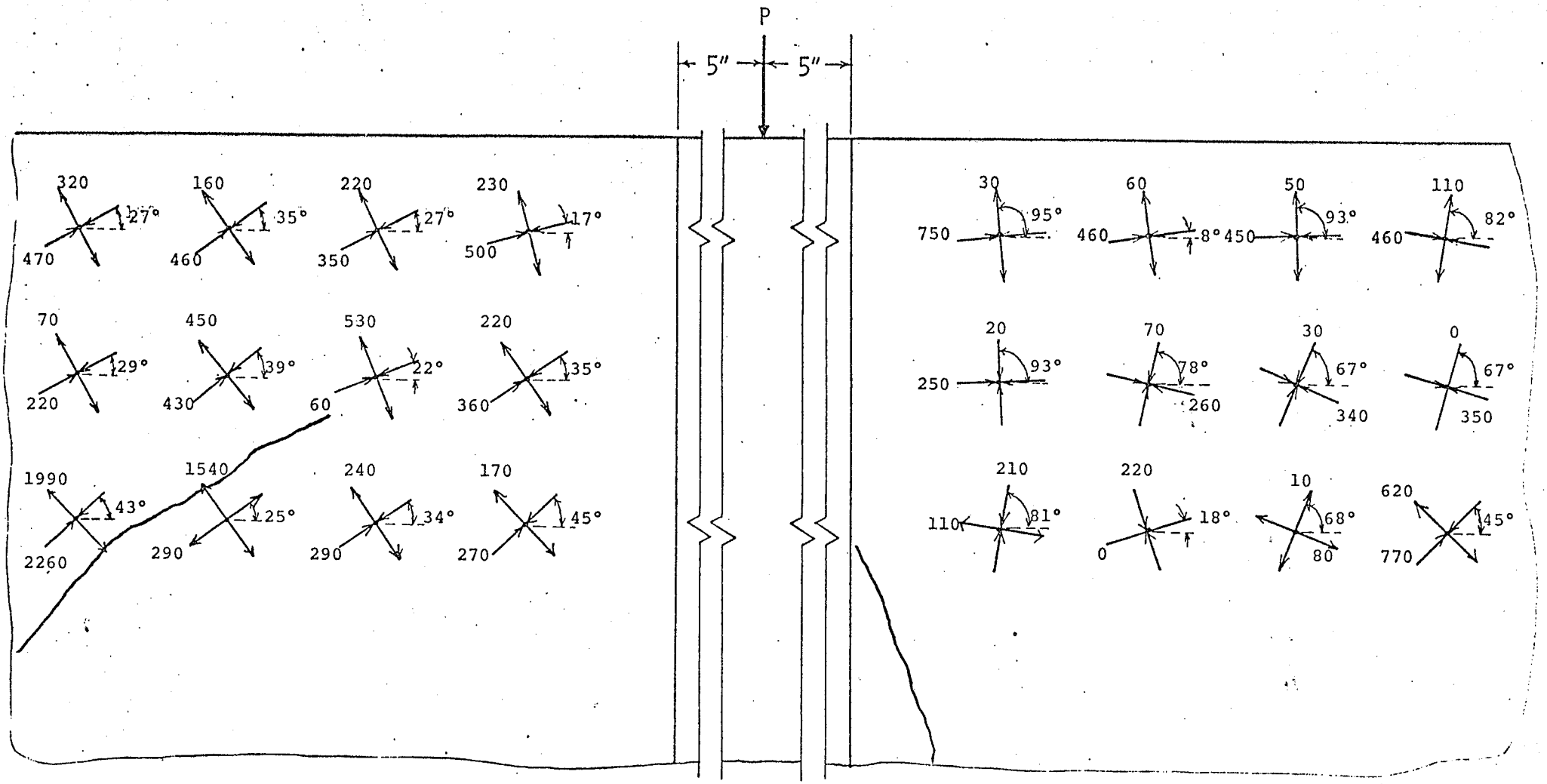

FIGURE 91

PRINCIPAL STRAINS
(microinches per inch)
scale: 1"=2"

BEAM 3B LOAD=40 kips

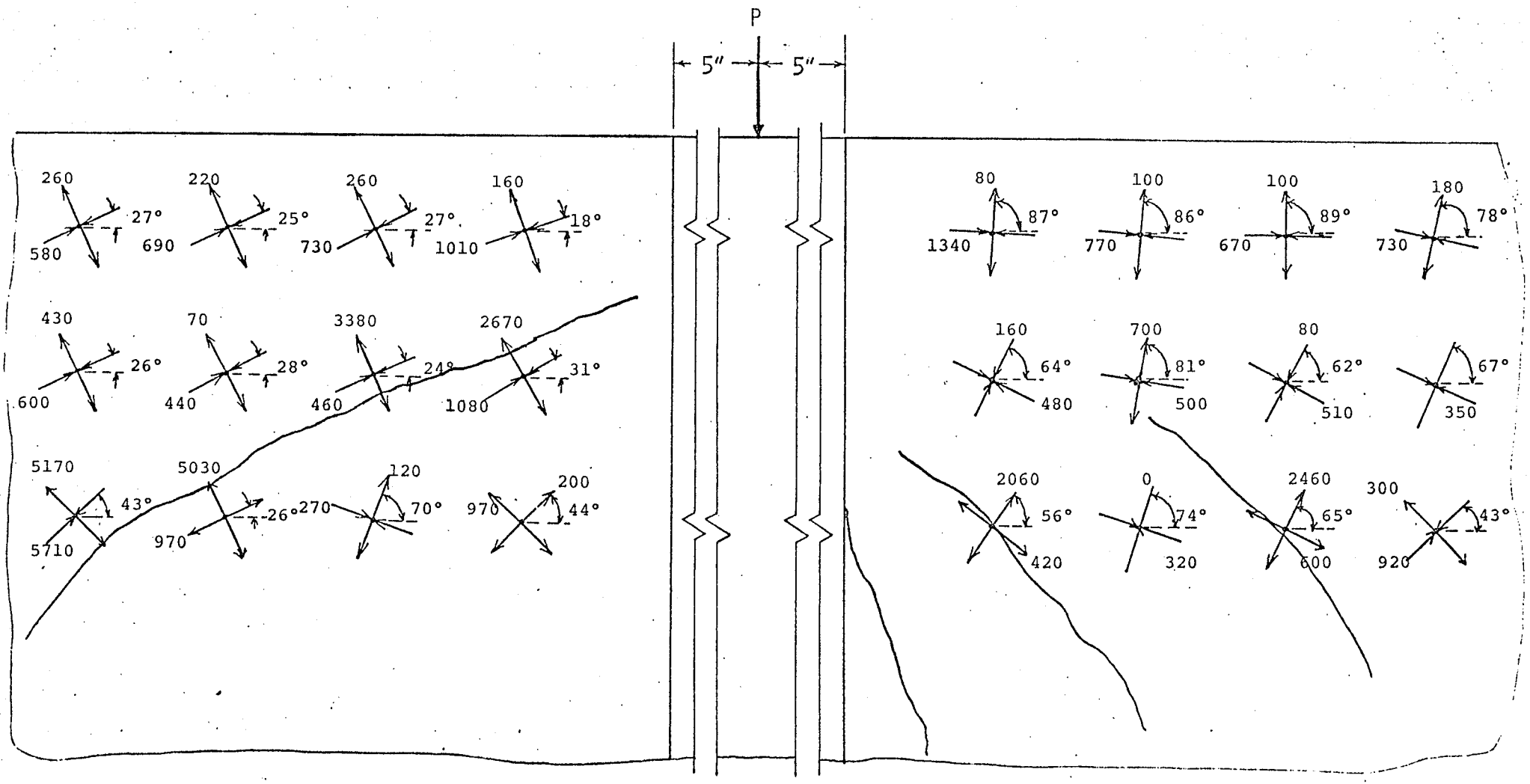

FIGURE 92

PRINCIPAL STRAINS
(microinches per inch)
scale: 1"=2"

BEAM 3B LOAD =65 kips

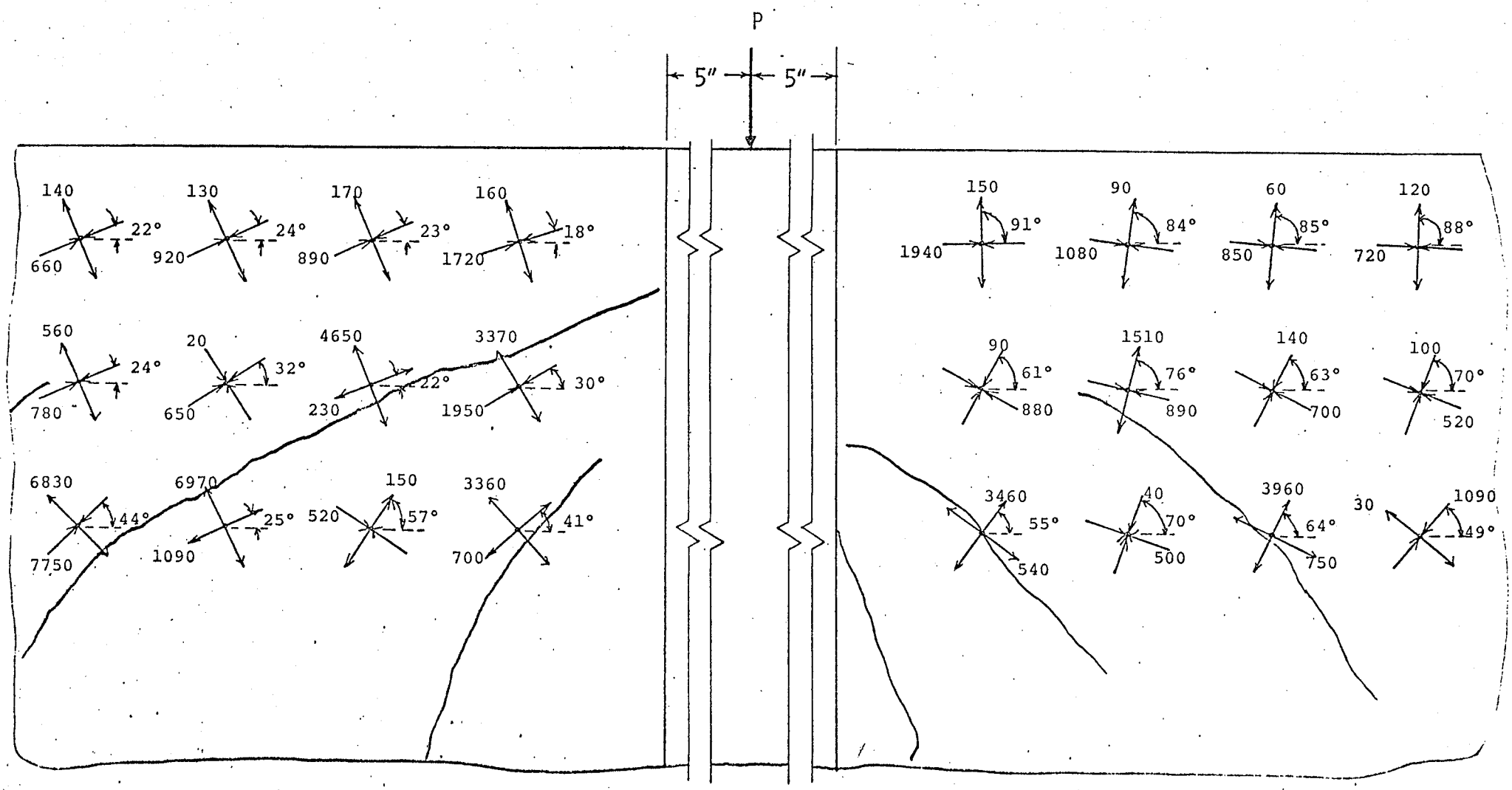

FIGURE 93

PRINCIPAL STRAINS
(microinches per inch)
scale: 1"=2"

BEAM 3B LOAD =72 kips

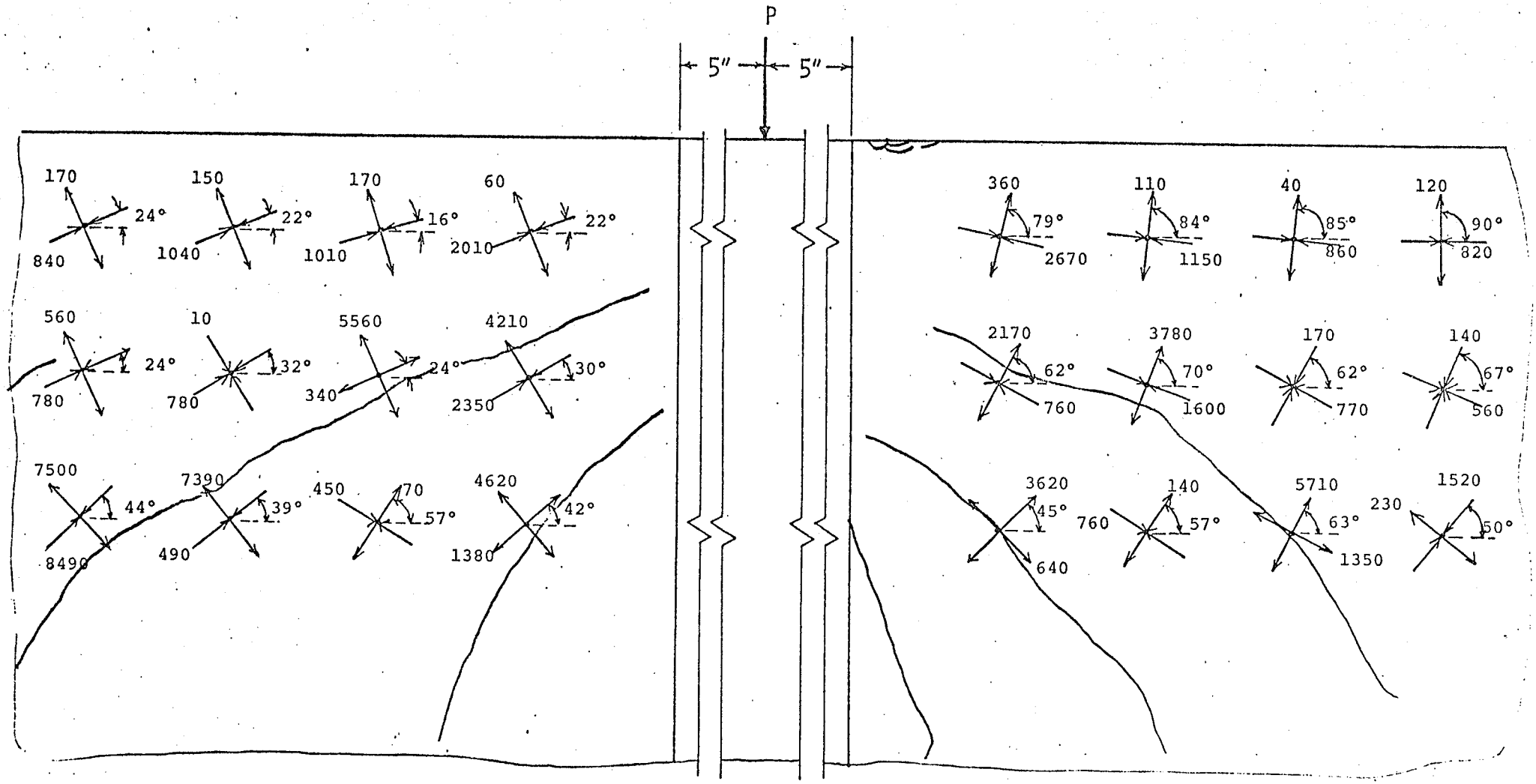

FIGURE 94

PRINCIPAL STAINS
(microinches per inch)
scale: 1"=2"

BEAM 3B LOAD=74.8 kips

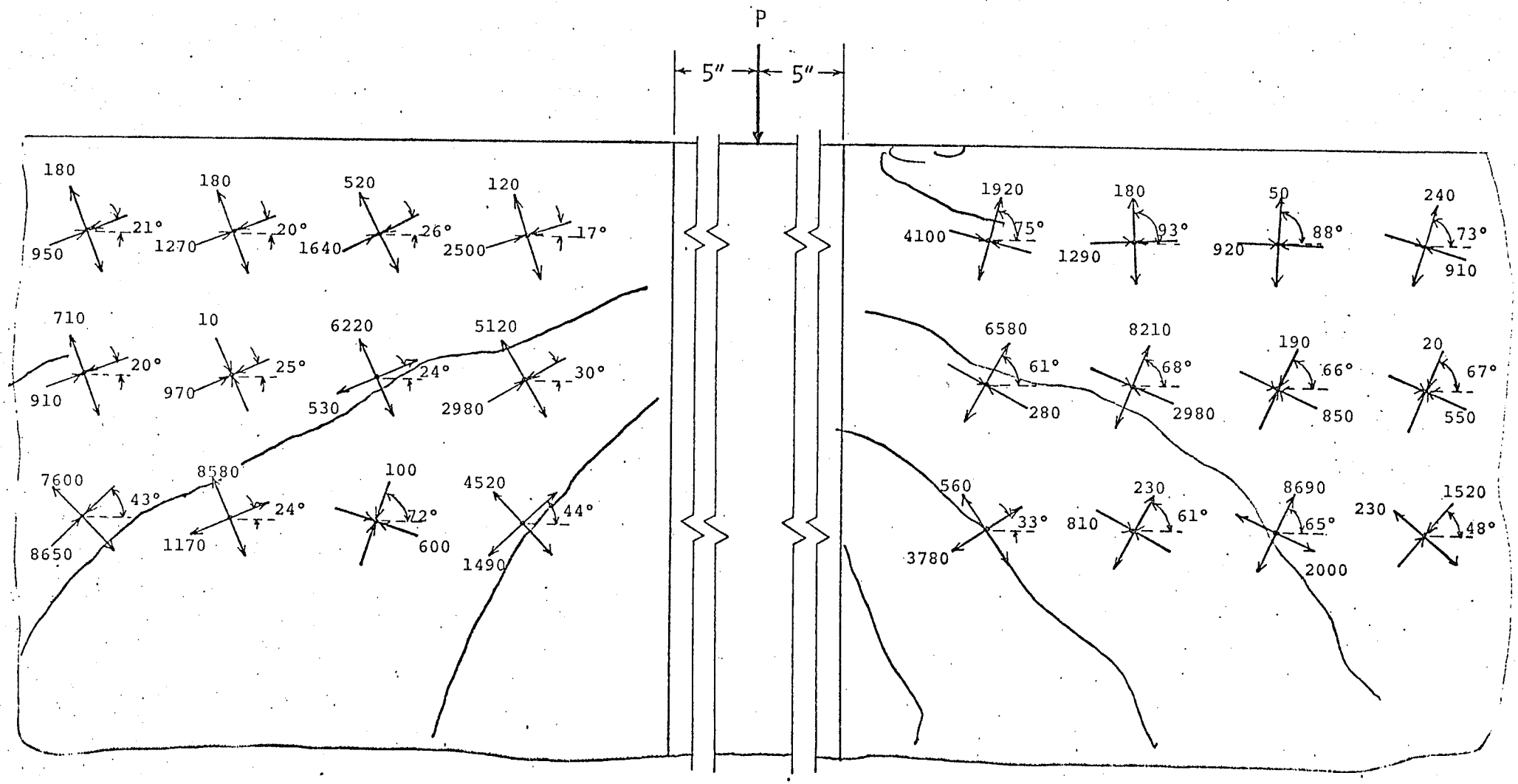

FIGURE 95

PRINCIPAL STRAINS
(microinches per inch)
scale: 1"=2"

BEAM 3B LOAD =75.4 kips

TABLE 8

TOTAL HORIZONTAL DEFORMATIONS

BEAM 3B

LOCATION	DISTANCE TO PANEL TOP (inches)	DEFORMATIONS (inches) 30 kips	72 kips
L	1	-0.00480	-0.01265
M	3	-0.00215	-0.00825
N	5	-0.00065	0.00140
O	7	0.00105	0.00705
P	9	0.00290	0.02695
Q	11	0.01245	0.05960
R	13	0.01460	0.07010
S	15	0.01825	0.07570
T	17	0.02000	0.08955
U	19	0.02170	0.09405
V	21	0.02425	0.10265

TABLE 9

TOTAL VERTICAL DEFORMATIONS

BEAM 3B

LOCATION	DISTANCE TO LOAD POINT (inches)	DEFORMATIONS (inches) 30 kips	72 kips
A	6	0.00100	0.01370
B	8	0.00205	0.00745
C	10	0.00270	0.01060
D	12	-0.01610	0.01355
E	14	0.00410	0.01720
F	16	0.00250	0.01320
G	18	0.00280	0.01235
H	20	0.00315	0.01190
I	22	0.00220	0.01145
J	24	0.00080	0.00545
K	26	-0.00010	0.00250

FIGURE 96

STRAIN GUAGE READINGS
ON WEB REINFORCING
BEAM 3B

4. DISCUSSION OF TEST RESULTS

4.1 DEMEC READINGS

In a report on anchor block stresses by Zielinski and Rowe[27], Demec gauges were used to study stress patterns. A statistical study for the accuracy of the 2 inch Demec gauges showed an accuracy of 9.3×10^{-6} strain. A short study of accuracy of the Demec gauges showed this value to be reasonable. For all strains shown the expected accuracy with the $\pm 10 \times 10^{6}$ strain.

Very early in the test of Beam 1B it became obvious that with this accuracy the strains in the tensile zone would be hard to read before cracking. The gauges did give a useful picture of the movement patterns of the panel.

After the test of Beam 1B the attention of the study was focussed on the compressive zone close to the load. At this point more reliable strain readings could be obtained in a shorter time. The compression zone was also the centre of attention since past studies had shown that the failure is often initiated by the cracks entering the compressive zone.

The reading of the Demec points was slow and tedious, often taking 2 to 5 hours. The load dropped during this period as shown in Figure 97. The load regained its value as soon as loading was resumed and since the test machine used was very rigid this period of time had little effect on the outcome of the test.

In spite of the problems of the Demec gauges discussed in this section, the Demec gauge proved to be quite versatile. Even after cracking had taken place, information could be gathered.

4.2 DISCUSSION OF RESULTS OF DEMEC READINGS

While the results obtained from the grid of Demec points are not as analytically useful as a rosette of Demec points, interesting information is

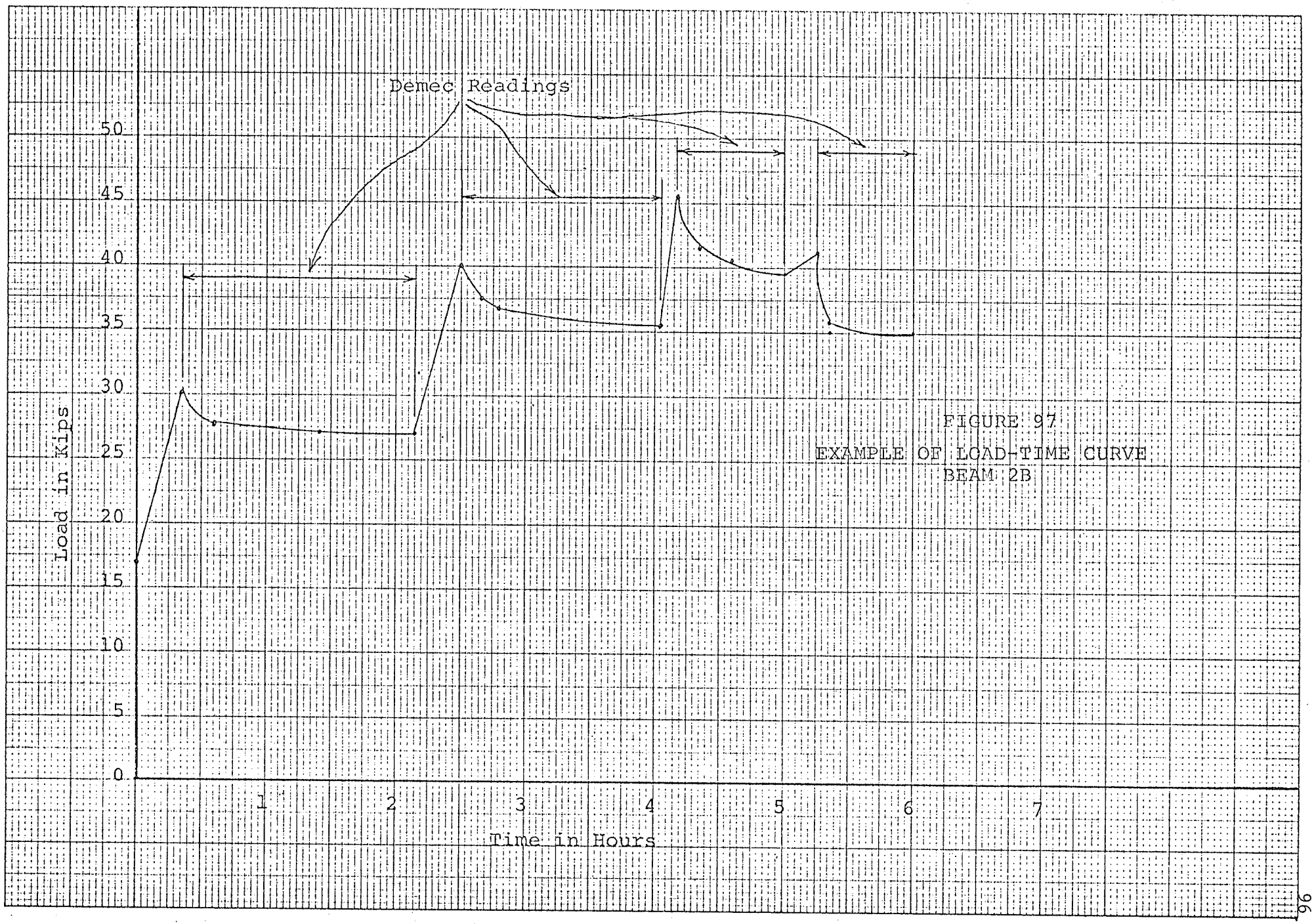

FIGURE 97
EXAMPLE OF LOAD-TIME CURVE
BEAM 2B

brought to light by these readings. Since the Demec gives change of length over 2 inches of the concrete, both average strains and deformation information can be gathered.

For Beam 1B the results were quite valuable. Strain distribution across the depth of the beam is hard to plot as the accuracy of the readings at low loads does not allow this. At higher loads the cross section is cracked causing large, inconsistent values.

Once the cross section had cracked however, the rate at which the cracks open can often be measured by using Demec gauges to measure deformation. These readings, in particular the total deformations of 10 gauge lengths, give insight into the panel movement. For Beam 1A the horizontal deformations of the compressive zone became very large. A close study of the deformations in this zone shows that the tensile steel is deforming over most of its length. At the same time there is little movement in the upper corner of the panel which is furthest away from the load.

In Beams 2B and 3B large deformations do not appear to take place, although not enough information was gathered on Beam 2B due to the sudden failure. The first set of readings showed very little deformation over the extent of the panel. At the same time the readings of 3B tend to show some compression in a line from the load to the reaction which tends to support the tied-arch analogy.

The results of the rosette readings, when principal strains are calculated and plotted, are of great value. In general, except where influenced by cracking, the principal compressive strains are inclined to the horizontal, often by as much as 30° to 45°. This fact tends to be consistent with the tied-arch analogy. There is also a tendency for cracks and principal strains to take the same line of action. These will be discussed later in Chapter 5.

There was a tendency, however, to a lack of symmetry on either side of the loading head. This could be due to a lack of precision in placing the beam in the test bed. The load may not have been exactly centered in the pilaster in spite of the care taken. The failure was then concentrated on one panel. In general, the side that had a more inclined principal strain was the side more affected by inclined cracking. The other side of the load then became the centre for crushing and compressive failure.

Another discrepancy in these results was the principle strains found at location N4 of Beam 3B. Here there was a tensile strain at an angle of 42° to 50° in the direction of the load and a high compressive strain at right angles. This is contrary to what is expected by tied-arch analogy and other readings found in the test. A check of readings showed no obvious error involved in reading or reducing the readings. The best explanation is that a parabolic reinforcing bar near this point is in compression and influencing the concrete strain at this point, causing compression in the direction of the bar.

4.3 STRAIN GAUGE READINGS

The main purpose for placing electric resistance strain gauges on the web reinforcing was for qualitative study of the effectiveness of this reinforcing. A great deal of care was required to ensure that the gauges were not damaged by the water or aggregate during the placing of concrete. As a result of this care 8 out of 10 of the gauges worked properly. Unfortunately, the only two gauges that failed were placed 8 to 10 inches from existing gauges in an attempt to show strain differentials in the same bar, or the effect of bond on these web reinforcing bars.

In Beam 2B the reinforcing showed little increase in strain as the load increased in the uncracked state. As soon as the first crack appeared there was a sudden increase in strain (approximately 10 to 30 times the value

just before cracking). The reinforcing strains then increased as the load but did not reach their yield points. The conclusion drawn is the position of the reinforcing is effective for the purpose intended. The reinforcing became too effective in holding the panel together and does not allow general deformation of the tensile steel, possibly due to too high a percentage of web reinforcing.

In the case of Beam 3B the reinforcing did not show a definite strain increase at cracking but a general increase over the loading of the beam. The reinforcing did reach yield values even before the ultimate load. This type of reinforcing appears to have too much influence on the tensile capacity of the beam, as the parabolas are affected as much by bending as by crack progression.

4.4 DISCUSSION OF REINFORCING PATTERNS

a). REINFORCING PATTERN #1

Since the reinforcing of Beams 1A and 1B are used only standard vertical stirrups these beams were expected to fail in shear. Using the 2 #3 bars for main steel as Malus did[5], the beams were extremly under-reinforced. The ultimate moment capacity was thus reached before the "diagonal tension" capacity, hence a tensile failure occured.

One interesting point that follows from the results of the test of Beam 1B, was the large deformation of the panels in the plastic range. The large cracks formed throughout the central area of the beam afforded the optimum use of the full length of the tensile reinforcement. Thus a large amount of energy was absorbed. The ultimate load was quite small for a beam this size yet a type of "plastic hinge" was formed.

b). REINFORCING PATTERN #2

When compared with reinforcing #1 it becomes obvious that not only does the inclined reinforcing prevent the shear cracks from opening it also increases the tensile capacity of the beam. The ultimate load was increased by 15 kips, however the final deflection was reduced to half that of Beam #1. There was a start of a compression failure followed by a sudden unexpected tensile failure.

This sudden tensile failure can be attributed to the web reinforcing being so effective that a local failure of the main steel was forced. The Beam 2B however, may have failed due to a local deficiency in the steel as there was very little necking of the bar which broke.

c). REINFORCING PATTERN #3

The parabolic web reinforcing carried almost 90% more load than even the 45° web reinforcing which testifies to the utility of the parabolas not only as "shear" reinforcing but as moment reinforcing.

The strength of this type of reinforcing led however to a compressive type of failure with the accompanying rapid fall of load and vast destruction of the compressive zone. Such a failure is no more desirable than a shear failure. This failure did provide the opportunity to study a compressive failure quite closely.

5. SUMMARY AND CONCLUSIONS

5.1 COMPARISON OF TEST RESULTS TO PAST RESEARCH

As discussed in the Introduction, the past research has mainly involved prediction of cracking and ultimate loads. These studies have produced further understanding of the behavior of deep reinforced concrete beams. At the same time a number of thought provoking theories on the failure mechanisms have been introduced.

One of the most interesting developments in the attempt to understand the failure mechanism is the formation of the tied-arch analogy. This analogy has often been used to explain shear behavior or deep beam behavior. This analogy was often referred to in the series of tests at the University of Illinois[16, 17, 18]. Although Kani was mainly dealing with shear behavior, he used the tied-arch analogy in an enlightening discussion on shear mechanism[22].

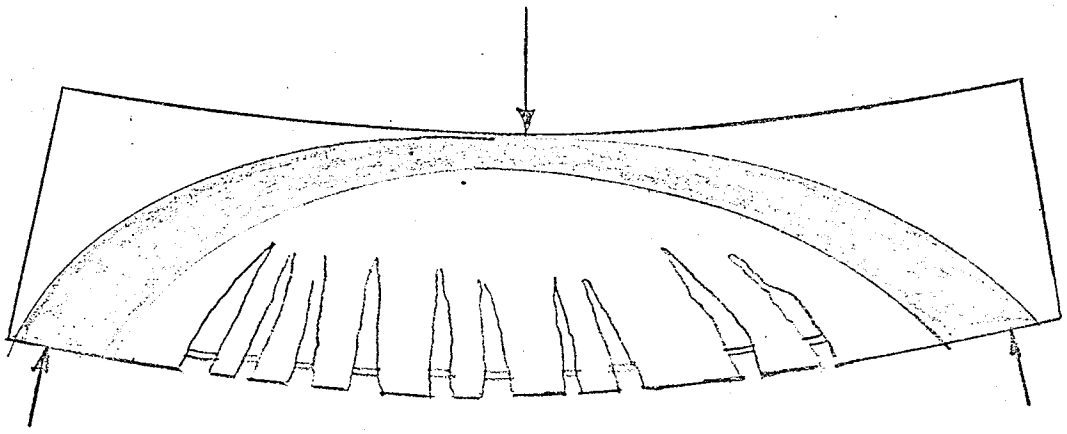

FIGURE 98

TIED-ARCH ANALOGY

Briefly, Kani suggests after initial cracking the beam can be considered to act as a tied-arch as shown in Figure 98. The remaining uncracked concrete carries the compression as if it were an arch. In this state the load carrying capacity of the beam is not impaired by the cracking.

The load carrying capacity of the remaining arch can be reduced in the following ways. If the tie reaches the point when it can no longer carry load, that is the tensile steel yields, the beam deflects in a ductile manner until a fracture of one or more of the tensile bars. Often before the tensile capacity of the bars are reached the arch may fail. This failure of the arch may take the form of a splitting caused by a progression of the cracks across the arch, or a shear failure. If these cracks are not allowed to split the compressive zone, it is possible the compressive forces can increase until a cracking of the arch takes place, with loss of load carrying capacity.

At present, at least with beams of normal depth, the action of the tensile and crushing type of failures are fairly well understood. The shear mechanism has not been fully discovered as yet. The results of the test performed in this study tend to confirm the arch analogy. The compressive trajectories shown for Beams 2B and 3B tend to follow the line of this arch. Unfortunately the extent of the zone studied was not enough to draw firm conclusions. Future studies should include beams with the possible line of the arch instrumented in an attempt to confirm the presence of high compressive strains and the direction of the compressive trajectories.

In the same paper Kani attempts to examine the diagonal tension cracking mechanism[22]. He suggests the diagonal cracks line up with the compressive trajectories. In studying the results of Beams 2B and 3B one can see a definite tendency for the principal compressive strains and the cracks to follow the same direction. Further study of this phenomenon is warranted.

5.2 DISCUSSION OF THE DUCTILE BEHAVIOR OF REINFORCING PATTERN #1

Although Beams 1A and 1B failed at a relatively low ultimate load, they failed in an extremely ductile manner. These beams contained a very low percentage of tensile steel, and their behavior is quite consistent with the results of DePaiva[18] who found that deep beams with a low percentage of tensile reinforcing failed in a ductile manner. Those beams with larger amounts of reinforcing failed in shear. The placing of web reinforcing to prevent the shear failure will often lead to such an increase in moment capacity that the beam then fails in compression.

5.3 RECOMMENDATIONS AND CONCLUSIONS

At present little can be suggested for practical use in design of deep beams. If a ductile beam is desired then the reinforcing percentage should be kept low even at a reduction of ultimate load. Since the cracking load does not vary appreciably with the amount of tensile reinforcing the working load range of the structure will not be adversly affected. Unfortunately, there is a lack of conclusive knowledge of what percentage of reinforcing will insure a ductile behavior of a deep beam. DePaiva used varying percentages of reinforcing in his tests and his results can be helpful. To follow this idea, a number of tests on different sizes of beams, and different amounts of reinforcing would be required. At the same time analytical approaches would be desired.

To increase the ultimate load a number of lines of investigation can be followed. The first could involve intensive tests of a conventionally reinforced concrete deep beam with enough main tensile reinforcing to cause a shear failure. The experiments could involve beams instrumented with Demec points or even electrical resistance strain gauges. Such a procedure could hopefully give more insight into the mechanism in a shear failure of a deep

reinforced concrete beam.

This test series could be coupled to an extensive analytical study involving the finite element technique. With the help of some knowledge of fracture mechanics of concrete a series of analyses could be carried out involving concrete deep beams with different stages of cracking. Coupled with the experimental test series a great deal of insight could be gained in the failure mechanism for a deep beam.

As suggested in section 5.1, the ultimate load of the ductile beam could be increased by increasing the strength of the remaining arch. At the same time the tie must be allowed to be effective over its length. One possible method of accomplishing this would be to allow the initial cracks to move to the neutral axes to allow the tensile reinforcing to be effective. These axis must not be allowed to enter the compressive zone. At the same time the compressive zone must be prevented from cracking.

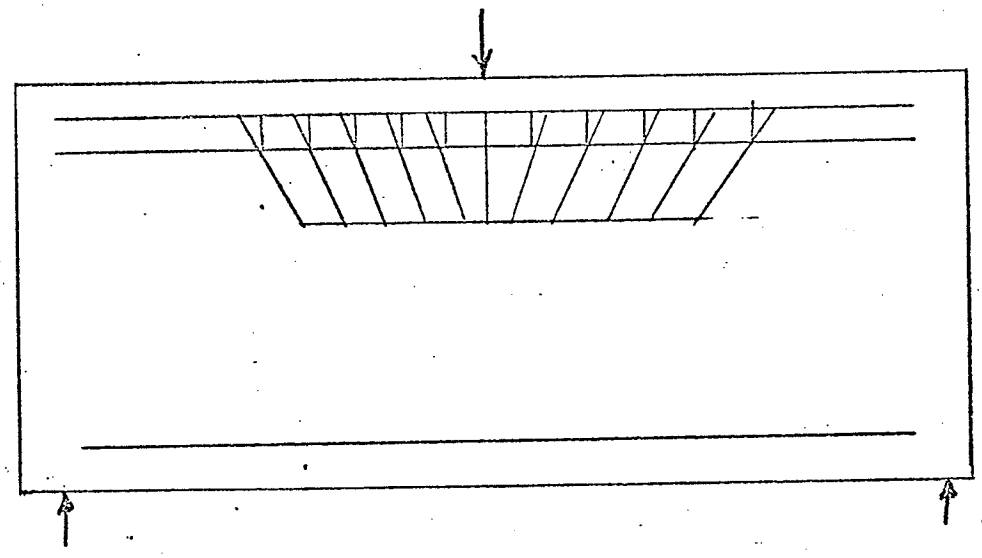

FIGURE 99

SUGGESTED PATTERN OF REINFORCEMENT

The results of the experiments presented herein have shown the effects of different reinforcement patterns on the behavior of a deep reinforced concrete beam. While the basic tensile reinforcing has been kept constant, changes in web reinforcing have brought about differences not only in ultimate load but mode of failure.

The beams containing reinforcement pattern #1 failed at low load but in a ductile manner. When changes were made to this basic pattern such as found in patterns #2 and #3, the ultimate load increased but a ductile mode was not established. The reinforcement patterns, while proving effective in retarding or preventing a shear type of failure, proved to be detrimental to other aspects of the beam's behavior.

These results point out that in considering possible patterns of web reinforcing for deep beams all aspects of deep beam behavior must be considered.

One possible pattern of web reinforcing is shown in Figure 105. A horizontal bar is placed near the neutral axis to prevent or slow cracking from entering the compressive zone. The compressive is tied heavily as a column and then tied again at 30^{o} to meet stress tragectories. While tests involving this web reinforcing would be interesting, the answer to the problem likely lies in the solution of the failure mechanisms.

BIBLIOGRAPHY

1. Committee of Structural Steel Producers of America Iron and Steel Institute, The Agadir, Morocco Earthquake, February 29, 1960, New York: American Iron and Steel Institute, 1962.

2. Kawasumi, Hirosi, General Report on The Niigata Earthquake of 1964, Tokyo, Japan: Tokyo Electrical Engineering College Press, 1968.

3. David, R. E., Earthquake, A Report on the Caracas Earthquake of July 29, 1967, Montreal: Canadian Institute of Steel Construction, 1968.

4. Ministry of Housing and Local Government, Report of The Inquiry into the Collapse of Flats at Ronan Point, Canning Town, London: Her Majesty's Stationery Office, 1968.

5. Malus, J. G., An Experimental Investigation of a Reinforcement Pattern for Deep Reinforced Concrete Beams Providing Ductility to Collapse, Thesis submitted to University of Manitoba for The Degree of M.Sc., April 1968.

6. Geer, Elihu, Stresses in Deep Beams, Journal of The American Concrete Institute, Proceedings v. 56, No. 7, January 1960, pp. 651-660.

7. Austin, W. J., Egger, W., Untrauer, R. E., and Winemuller, J.R., An Investigation of the Behavior of Deep Members of Reinforced Concrete and Steel, Structural Research Series No. 187, Civil Engineering Studies, Department of Civil Engineering, University of Illinois, Urbana, Illinois, January, 1960.

8. Dischinger, F.. "Contributions to the Theory of the Half-Plate and Wall-Type Beams", Publications, International Association for Bridge and Structural Engineering, Zurich, Vol. 1, 1932, pp. 69-93.

9. "Design of Deep Girders", Concrete Information No. St-66, Portland Cement Association, Chicago.

10. Coker, E.G. and Filon, L.N.G., A Treatise on Photo-Elasticity, Cambridge: The University Press, Cambridge, 1957.

11. Kaar, P.H., "Stresses in Centrally Loaded Deep Beams", Proceedings, Society for Experimental Stress Analysis, Vol. 15, No. 1, pp. 77-84, 1957.

12. Saad, S., and Hendry, A.W.. "Stresses in a Deep Beam With a Central Concentrated Load", Experimental Mechanics, Vol. 1, No. 6, June 1961, pp. 192-8.

13. Klingroth, H., "Tests of Reinforced Concrete Load Bearing Walls and Their Evaluation", Beton and Eisen, 1942, No. 9.

14. Nylander, H., and Holst, H., "Some Investigations Concerning Panels and Deep Beams of Reinforced Concrete", Transactions, Royal Technical University, Stockholm, Sweden, No. 2, 1946.

15. Benjamin, J.R., and Williams, H.A., "Behaviour of Reinforced Concrete Shear Walls", ASCE Transactions, Paper No. 2998, Vol. 124, 1959, pp. 669-708.

16. Untrauer, R.E., "Strength and Behavior in Flexure of Deep Reinforced Concrete Beams Under Static and Dynamic Loading," Thesis Presented to the University of Illinois, at Urbana, Illinois, in 1961, in partial fulfilment of the requirements for the Degree of Doctor of Philosophy.

17. Dell, A.F., "Strength and Behavior of Restrained Deep Reinforced Concrete Beams under Static Loading." Thesis presented to the University of Illinois at Urbana, Illinois, in 1964, in partial fulfilment of the requirements for the Degree of Doctor of Philosophy.

18. DePaiva, H.A., "Strength and Behavior in Shear of Reinforced Concrete Deep Beams Under Static and Dynamic Loading," Thesis presented to the University of Illinois, at Urbana, Illinois, in 1961, in partial fulfilment of the requirements for the Degree of Doctor of Philosophy.

19. Crist, R.A., "Shear Behavior of Deep Reinforced Concrete Beams", Proceedings, Symposium on the Effects of Repeated Loading of Materials and Structural Elements, V. IV. RILEM, Paris; Mexico City: Instituto Mexicano del Cemento y del Concreto, 1966.

20. Rama Brishnan, V. and Ananthanarayana, Y. "Ultimate Strength of Deep Beams in Shear." Journal of the American Concrete Institute, Proceedings. V. 65, No. 7, February, 1968, pp. 87-98.

21. "Proposed Revision of ACI 318-63 Building Code Requirements for Reinforced Concrete". Journal of the American Concrete Institute, Proceedings., V. 67, No. 8, February, 1970, pp. 77-186.

22. Kani, C.N.J. "The Riddle of Shear Failure and Its Solution". Journal of the American Concrete Institute, Proceedings. V. 61, No. 4, April, 1964, pp. 441-467.

23. . "Basic Facts Concerning Shear Failure." The Journal of the American Concrete Institute, Proceedings. V. 63, No. 4, June 1966, pp. 675-692.

24. . "How Safe Are Our Targe Reinforced Concrete Beams?". The Journal of The American Concrete Institute Proceedings. V. 64, No. 3, March 1967, pp. 128-141.

25. Wood, B.R.. "Study of the Behavior of a Deep Reinforced Concrete Beam in Failure", Thesis submitted to University of Manitoba for the degree of B. Sc. (C.E.), April 1967.

26. "Building Code Requirements for Reinforced Concrete, (ACI 318-63)". Detroit: American Concrete Institute, 1963.

27. "Compressive Strength of Molded Concrete Cylinders", 1965 Book of ASTM Standards with Related Material, Part 10, Concrete and Mineral Aggregates, (Philadelphia: American Society for Testing and Materials, 1965) C 39-64, pp. 25-27.

28. "Splitting Tensile Strength of Molded Concrete Cylinders", 1965 Book of ASTM Standards with Related Material, Part 10, Concrete and Mineral Aggregates, (Philadelphia: American Society of Testing and Materials, 1965) C 496-64T, pp. 357-360.

29. Wood, B.R.. "A Report on the Testing of Six Reinforced Concrete Deep Beams". University of Manitoba Department of Civil Engineering Report ST-2-70, September, 1970.

30. Zelinski, J. and Rowe, R.E.. "An Investigation of the Stress Distribution in the Anchorage Zones of Post-Tensioned Concrete Members". Cement and Concrete Association, Research Report No. 9, September 1960.